Fig. 5.10

Rate of aurocyanide desorption for carbons initially loaded to 10mg Au/g eluted with 0,30 M aqueous ammonia

Temperature = 83°C

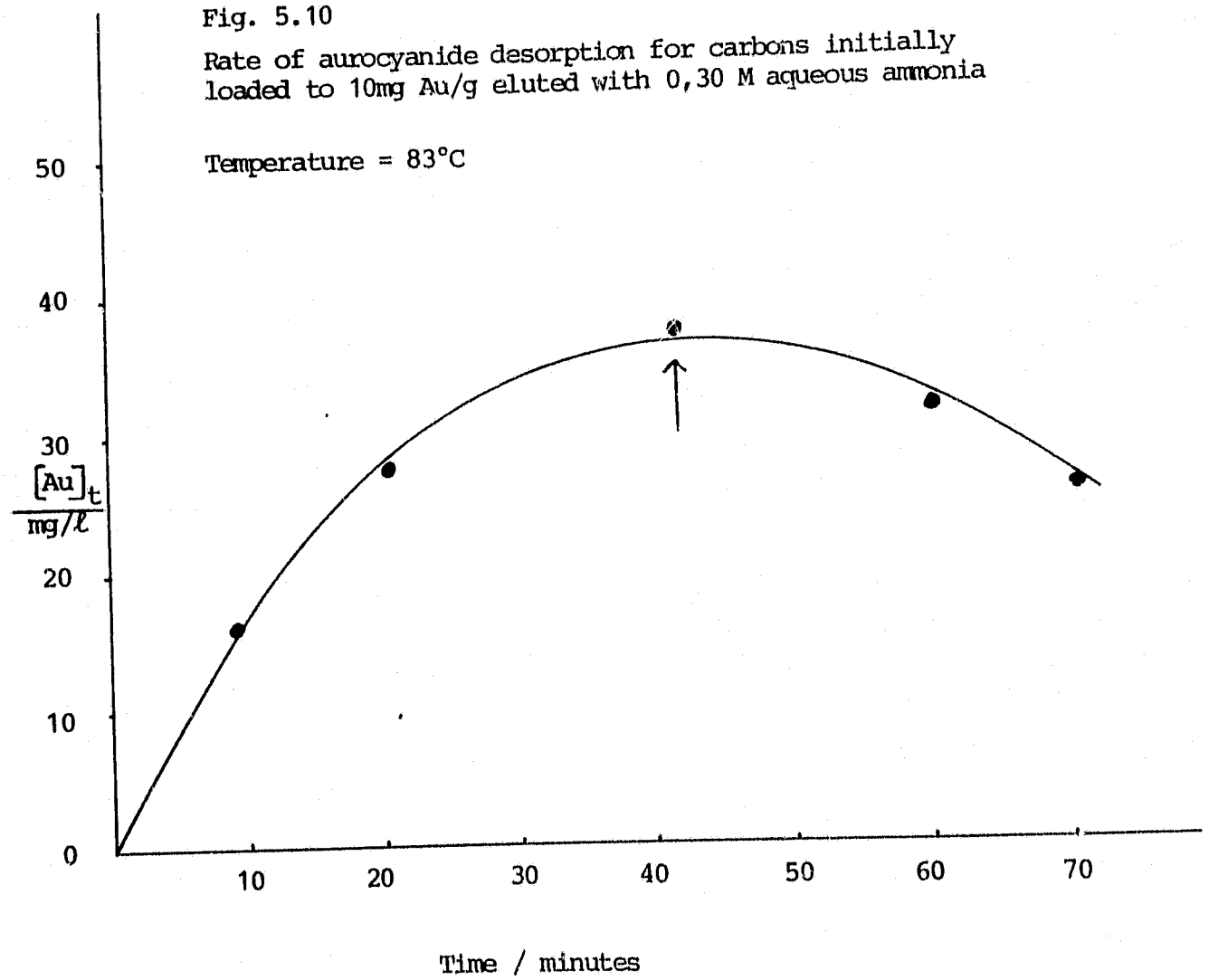

Fig.5.11

Effect of anion on distribution of aurocyanide

Graph of ℓnK_D versus 1/T
for NaOH and NaCN medium

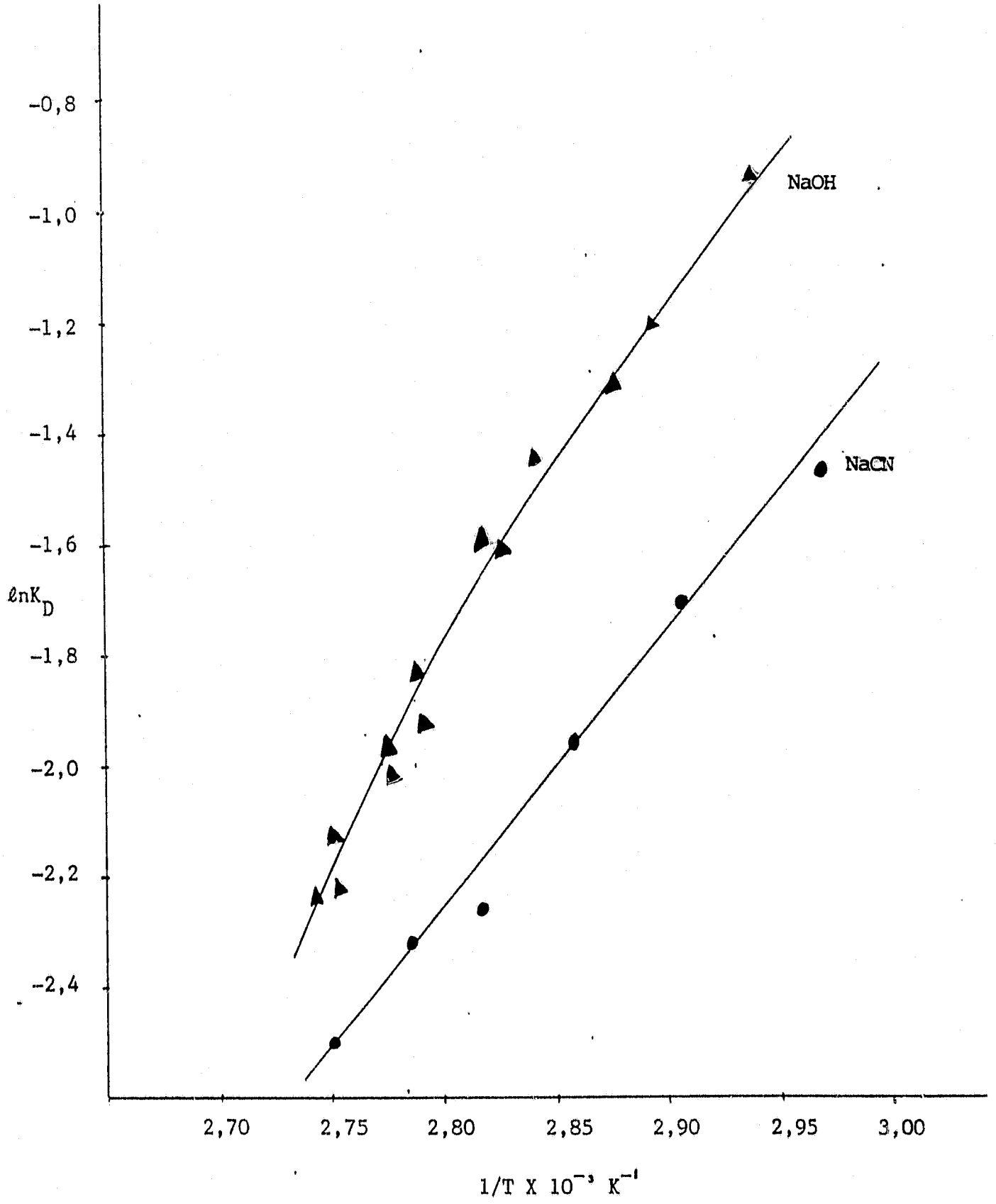

The specific anion of the desorption medium present in large excess disturbs the equilibrium as reflected by the distribution coefficents shown in Table(5.3).

Table 5.3 Effect of anions on the distibution of aurocyanide

Anion (as Na^+ salt)	ℓnK_D T=90°C
OH^-	-2,23
CN^-	-2,55
SH^-	v. small

The distribution of aurocyanide between the two phases is shifted towards the aqueous phase (i.e. desorption) with increasing size and polarizability of anion.
Note however that little aurocyanide desorption was effected using 0,30 M NaCℓ or de-ionized water alone.
Table (5.4) shows the heat of adsorption for the distribution of aurocyanide between the two phases and various media at constant ionic strength (I = 0,30M).

Table 5.4 Effect of anion on the heat of adsorption of aurocyanide by activated carbon

Anion (as Na^+ salt)	ΔH $kJmol^{-1}$
OH^-	-49,88
CN^-	-40,90
SH^-	-30*

*Estimated since the formation of polysulfides increases with time, which also shifts the equilibrium.

The heat of adsorption of aurocyanide in hydroxide medium is initially constant at higher surface coverages, but increases with increasing temperature. This increase is possibly due to increasing site energy at lower surface coverage. The magnitude of the heat of adsorption suggests that the interaction between the aurocyanide species and the carbon surface involves chemisorption or a more specific interaction.[84]

In cyanide medium, the heat of adsorption is constant over the whole temperature range investigated. The magnitude similarly suggests that chemisorption occurs between the carbon surface and the aurocyanide ion-pair. The cyanide medium competes more effectivly than hydroxide medium for the carbon surface, as reflected by the heat of adsorption for the two systems. However, at prolonged elevated temperatures, the cyanide anion decomposes to form ammonium ions which may complicate this system, since this introduces additional cations to the medium.

The effect of hydrosulfide (SH^-) on the system was examined. However, equilibrium was not attained due to the polymerization of SH^- ions to polysulfides of varying chain length. The initially colourless solution on contact with activated carbon, rapidly yellowed with time and temperature to form the polymeric species which possibly displaces the adsorbed gold. On contact with oxidants such as H_2O_2 , the hydrosulfide solution rapidly yellows to produce a similar visible and ultra-violet spectrum as that obtained on contact with activated carbon, proving that an oxidative mechanism prevailes.

Page 106 omitted in the pagination.

5.5 Factors effecting the equilibrium distribution of argentocyanide

Fig. (5.12) shows a plot of the appearance of silver as $Ag(CN)_2^-$ in solution with time for the elution of carbon containing 10mg Ag/g using 0,30 M KOH at various temperatures.

As in the aurocyanide system, the rate of approach to equilibrium obeys first order kinetics and tends to an equilibrium after approximately 120 minutes. The desorbed silver was assumed to be $Ag(CN)_2^-$ as this species has no U.V. spectrum.[60] Fig. (5.13) shows a plot of the distribution coefficient versus the cationic radius of the specific cation used in the desorption medium. The resulting n-curve is found to be flatter than that for the aurocyanide system and is probably due to the lower polarizability of this species. This is borne out by the lower heat of adsorption relative to the gold system as shown in Table (5.3). Fig. (5.14) shows the Van't Hoff plot for the various cations investigated.

Table 5.5

Heats of adsorption for argentocyanide onto activated carbon in hydroxide medium

Cation as OH^- salts	ΔH $kJmol^{-1}$
Na^+	-32,26
Li^+	-34,72
K^+	-35,72

Fig. 5.12

Rate of argentocyanide desorption for carbon initially loaded to 10mg Ag/g eluted with 0,30 M KOH

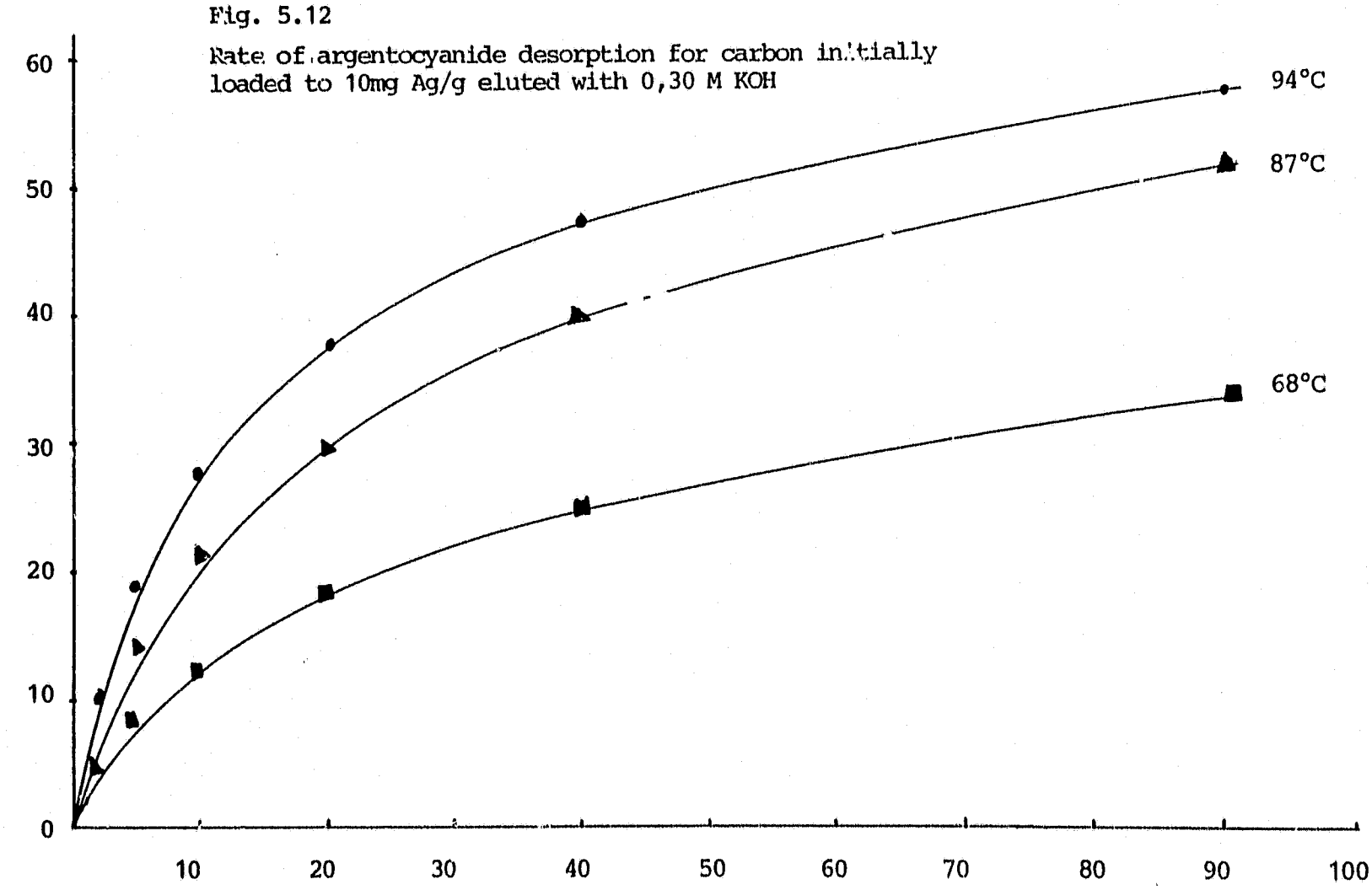

Plot of % elution versus cationic radius for the desorption of argentocyanide in hydroxide eluent

Fig. 5.13

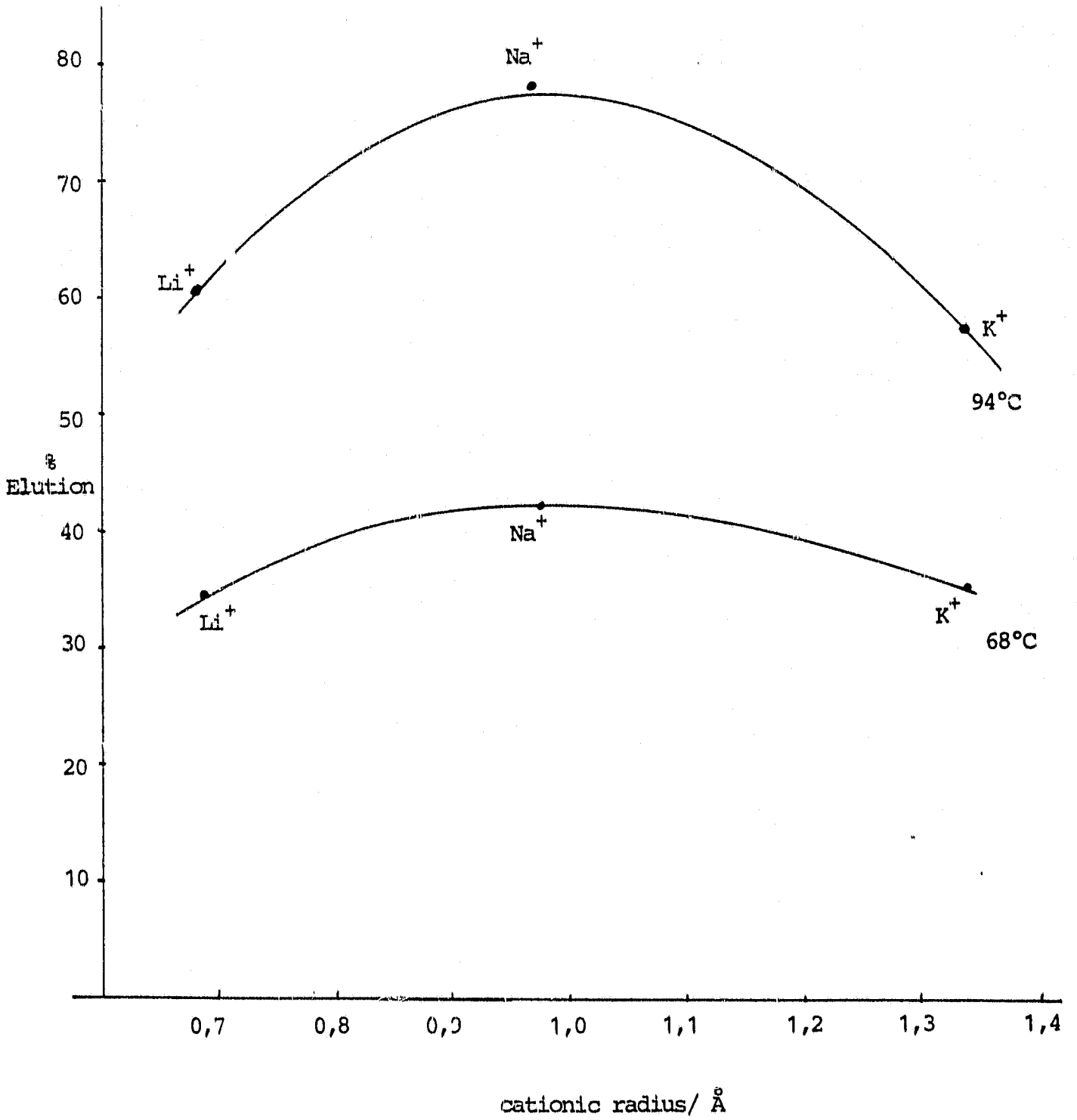

Fig. 5.14 Effect of various hydroxide media on distribution of argentocyanide

Graph of ℓnK_D versus 1/T

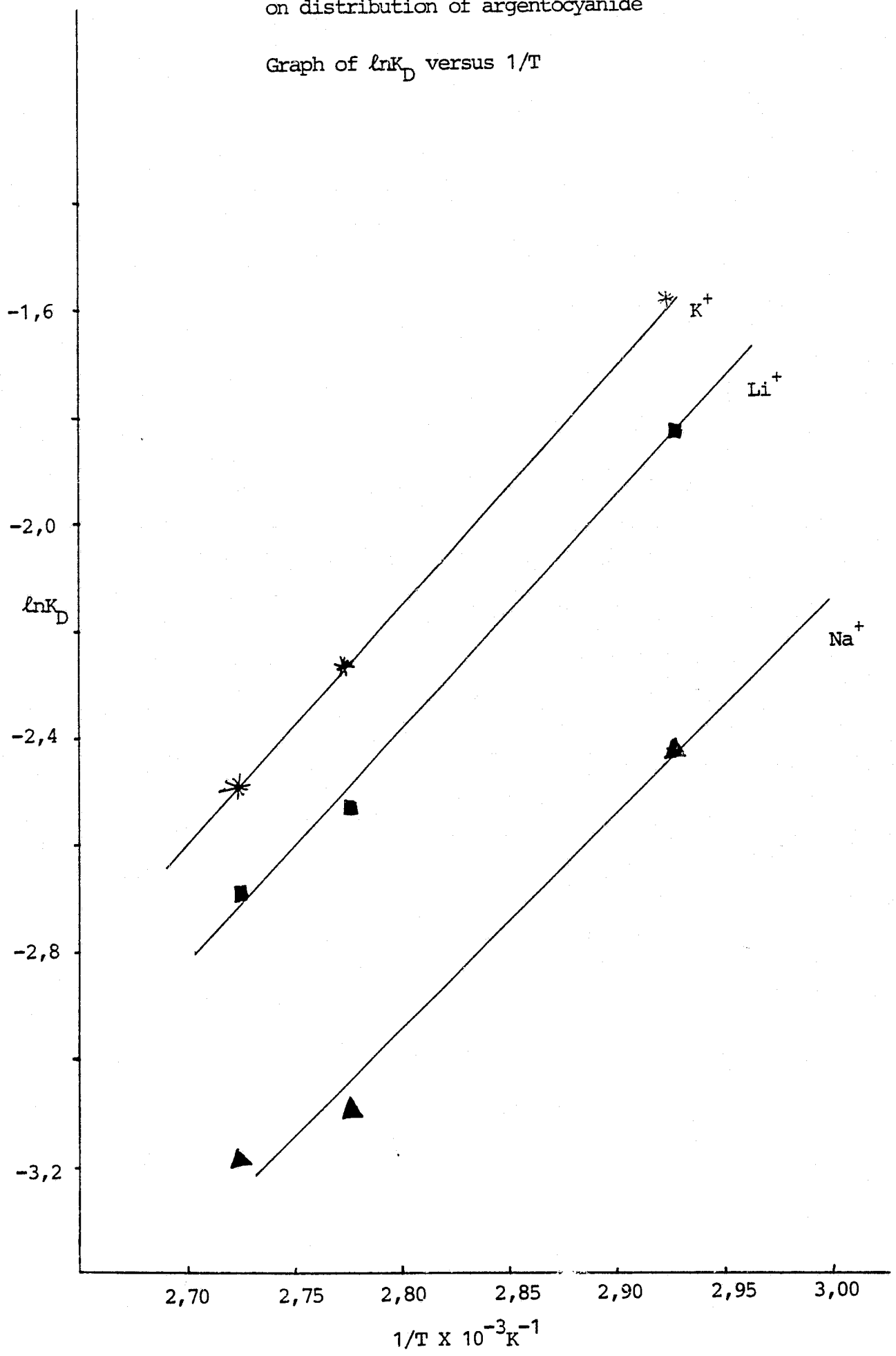

5.6 Summary and conclusions

Aurocyanide loaded carbons on contact with hydroxide at elevated temperatures undergo desorption whereby the rate of approach to equilibrium is influenced by the cation of the medium. For hydroxide medium, the rate of desorption is given by the series:

$$Na^+ > K^+ > Li^+$$

The specific cation ordering observed shows a trend of increasing rate with decreasing polarizability of cation, which is expected as the stength of the interaction between the specific ion-pair and the carbon surface also follows this trend.

The activation energy for the desorption process suggests that the interaction between the ion-pair and the carbon surface involves a truly chemical mechanism as their values are higher than that required for a diffusion controlled mechanism. The frequency factor A for the desorption also suggests that a caging effect occurs as the polarity of the cation increases. Thus the number of successful collisions necessary for the desorption of the ion-pair increases with increasing polarizability of the cation. The rate of approach to equilibrium shows no effects due to the cation initially loaded. This is expected as the large excess of cation in the desorption medium is expected to drive the cation exchange mechanism proposed by Davidson.[35,37] The local equilibrium at the carbon surface is expected to be fully reversable and exchange of cations is probably fast due to the short life-time of the ion-pair.

The desorption process achieves equilibrium after about 100 minutes reaction time. The cation in the medium again shows two trends for the distribution of aurocyanide between the two phases due to the formation of two kinds of ion-pair species.

In hydroxide medium the heat of adsorption suggests that the process involves a chemisorbed species on the carbon surface. This equilibrium is a reversable one. However

effects due to surface coverage are found, which is expected as the site energy decreases with increasing surface coverage.[38-40]

Other anions similarly influence the equilibrium distribution of aurocyanide between the two phases. The heat of adsorption for various anions investigated suggests that both size and polarizability are important factors. This must be due to competition for adsorption as the heat of adsorption for aurocyanide varies with the type of anion in solution. At elevated temperatures the distribution of aurocyanide is shifted towards the aqueous phase as the specific anion increases in size and polarizability.

In order to effect the desorption of the aurocyanide ion-pair, elevated temperatures are a necessary but not a sufficient condition, and the process requires concentrated basic medium. The solubility of the aurocyanide species may also have a role as it increases strongly with temperature. The hydroxide ion is known to be the strongest base that can exist in water, although in the environment of carbon, the solvent cannot be thought of as bulk water. Activated carbon contains about 3 percent (M/M) oxygen which is concentrated as edge groups and imparts polarity to the surface* This probably lowers the dielectric constant of the medium within carbon. Much evidence for the adsorption of ion-pairs has been proposed in the literature and transfer from aqueous to carbon phase must involve a neutral species to preserve charge neutrality.

Once the competing ion-pair is adsorbed, the aurocyanide ion-pair may be either displaced by the large concentration excess or caused to ionize. Anions of small size and localized charge are expected to increase in basicity because the solvent medium within carbon has a reduced or depleted ability to hydrogen bond and are less solvated than in aqueous medium. The formation of ion-pairs for lower valency-type ions is also favoured by elevated temperatures and low dielectric solution.[50,52]

* The concentration of oxygen may be of the order of 3-4 M within the carbon pore structure.

Highly basic media of aqueous alkali metal hydroxides have acidity functions (H_-) which increases in the order of KOH < NaOH < LiOH. This is due to the formation of ion-pairs at higher concentration.[76-78] The weakest base of the series is LiOH.

In aqueous solution weak acids would be expected to give the alkali salt of the conjugate base which may exist at either an ion-pair or as free ions as shown by equation (5.5)

$$RH + MOH \rightleftharpoons R\,M + H_2O$$
$$\Updownarrow$$
$$R^- + M^+ \qquad (5.5)$$

Association reactions become important at lower dielectric strength for oxygenated media. Within the carbon the following equilibrium may be relevant -

$$\overline{MAu(CN)_2 + MOH} \rightleftharpoons M^+_{aq} + OH^-_{aq}$$
$$\Updownarrow$$
$$\overline{MAu(CN)_2 + OH^- + M^+} \rightleftharpoons \overline{Au(CN)_2^- + MOH + M^+} \rightleftharpoons Au(CN)^-_{2aq} + M^+_{aq}$$

Thus the more ionized the competing anion, the more the equilibrium is shifted to the right hand side (i.e. desorption). The larger and more hydrophobic the competing anion in the environment of carbon, the larger the basicity, thus the greater the extent of ionization. This is reflected by the following series for increasing desorption -

$$Cl^- < OH^- < CN^- < SH^-$$

Some further evidence has been found for the ionization mechanism in that when $KAu(CN)_2$ salts are dissolved in concentrated $LiCl$ solution a visible yellow colour develops with time. When $KAu(CN)_2$ salts are dissolved in LiOH salts no yellow colour develops and similarly when $LiAu(CN)_2$ salts are dissolved in LiOH the colour is lost instantaneously. This suggests that both Cl^- and OH^- ions compete with $Au(CN)_2^-$ for coordination to Li^+. Keeping the anion constant and varying the cation, u-curves are obtained (Fig. (5.8)) which reflects the trend for increasing adsorption as the ion-pair increases in size and therefore hydrophobicity. Small cations similarly cause enhanced adsorption of aurocyanide and must reflect the increasing polarizability of the ion-pair due to the Lewis acidity of the cation.

Thus the adsorbed state involves equilibrium between the ion-pair, the cation and the competing anion. Temperature is also an important parameter whereby the distribution is shifted towards the aqueous phase with increasing temperature. This probably involves increasing basicity of the anion with temperature as the water becomes more structured with increasing temperature.[46] At elevated temperatures the increase in the solubility of the ion-pair probably has a role. However high temperature is a necessary but not sufficient condition to cause the desorption of aurocyanide. The basic medium is required to shift the equilibrium for effective desorption of aurocyanide.

6 Activated carbon

Introduction

The adsorptive properties of activated carbon have been known for centuries. Utilization of these properties have varied from a simple adsorber of gas molecules for air conditioning systems to an adsorber of organic molecules for water purification and more recently in extractive hydrometallurgy.

Activated carbon is a generic term for a group of carbonaceous substances which cannot be characterized by structural formula nor by chemical analysis. Properties associated with activated carbon include a carbon backbone or matrix, areas of microcrystalline carbon, oxygen containing surface groups, extensive porosity, and a large surface area (300-1200 m^2/g).

Numerous starting materials as well as variations in the processes of manufacture give rise to many forms of "active carbon", e.g. carbon black, channel black, furnace black and coke. Reaction conditions such as temperature of activation, reducing or oxidizing environments and reaction time imparts a variety of properties to the resulting products. Details of the manufacture have not been published by the industry and so the activation of carbon remains largely as a black art.

In general the carbon backbone is associated with an extensively porous hydrophobic surface. Regions of the matrix contain oxygen functionalities which impart a hydrophilic character.

6.1 Synthesis of aurocyanide adsorbing activated carbon

Pyrolysis of coconut char between temperatures of 200 - 1000°C under a steam atmosphere was conducted establish factors which influence aurocyanide adsorption capacity. An empirical approach was adopted in which the effects of temperature of activation, the burn-off or mass loss and the effect of steam was investigated with respect to aurocyanide adsorption. The nature of the surface functionalities of the samples generated was investigated via Fourier transform infrared spectroscopy (FTIR).

6.2 Results and discussion

i) Influence of activation temperature on aurocyanide adsorption

Fig. (6.1) shows the effect of the equilibrium activation temperature on the percentage of aurocyanide adsorption under steam and nitrogen atmosphere respectively. The adsorption of aurocyanide increases slightly under nitrogen with increasing temperature, whereas under steam activation a five fold increase in aurocyanide adsorption is observed. Activation in a steam atmosphere results in a large increase in the aurocyanide adsorption between 600 - 900°C after which a slight decrease in capacity is observed. This effect has also been reported by Gross and Scott.[30]

Fig. (6.2) shows the influence of activation temperature on the adsorption of aurocyanide as a function of surface coverage (steam activation). The data has been plotted according to the Temkin isotherm, where it can be seen that as the activation temperature increases a point of inflection is observed.

A change in slope is observed for carbons activated above 750°C where the large mass loss or burn-off begins. The variation of site energy predicted by the Temkin model is linear and the change in slope shows that at least two modes of adsorption are present. The slope of the initial region of adsorption is larger than that of carbons with higher gold loadings, which must be due to specific and non-specific modes of adsorption.

The specific region of adsorption was further investigated with respect to its formation with increasing activation temperature. Fig. (6.3) shows the Van't Hoff plot for the logarithm of the slope k of the Temkin plot versus the inverse of the equilibrium activation temperature. The resulting plot is linear and has a positive heat of formation of +45 $kJmol^{-1}$, which suggests that the formation of specific adsorption sites involves an endothermic reaction.

Fig.6.1

Graph of % Au adsorbed vs temperature of activation

● = steam/N_2 atmosphere

▲ = N_2 atmosphere

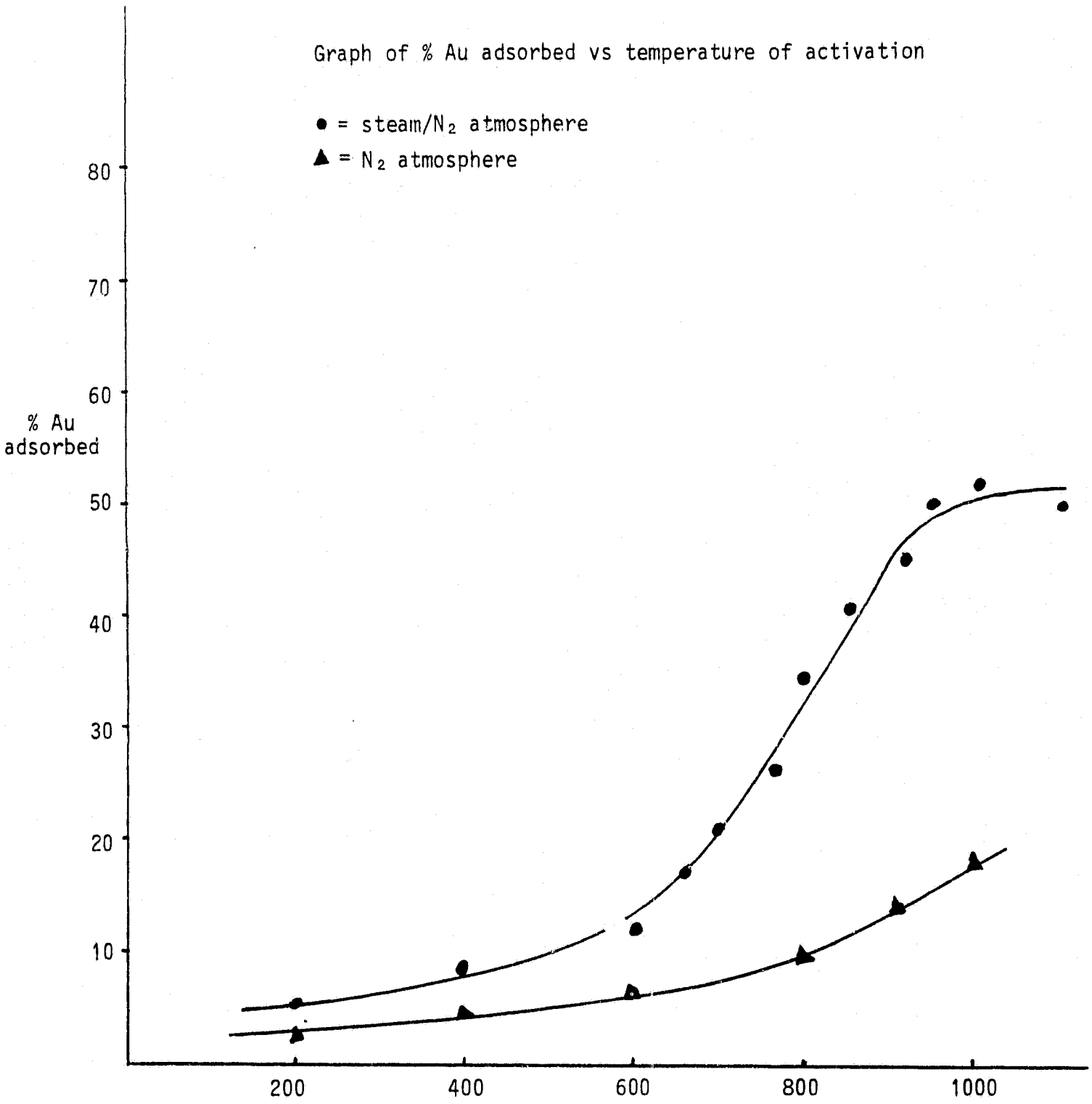

Fig.6.2

Temkin isotherms for carbons
activated at various temperatures
under steam atmosphere
Adsorption in I = 0,30 NaCℓ

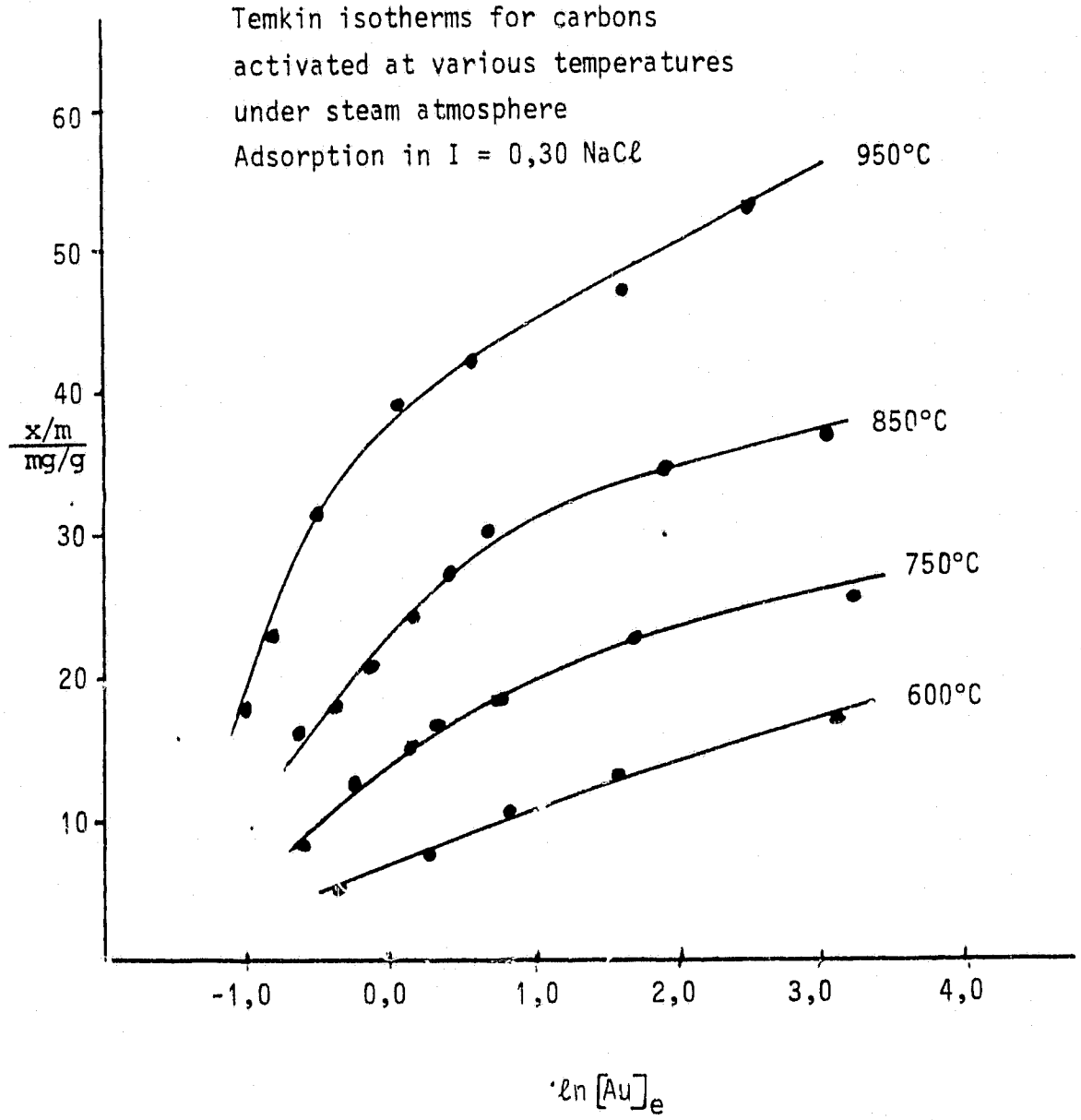

Fig 6.3

Graph of strength of adsorption parameter k versus activation temperature

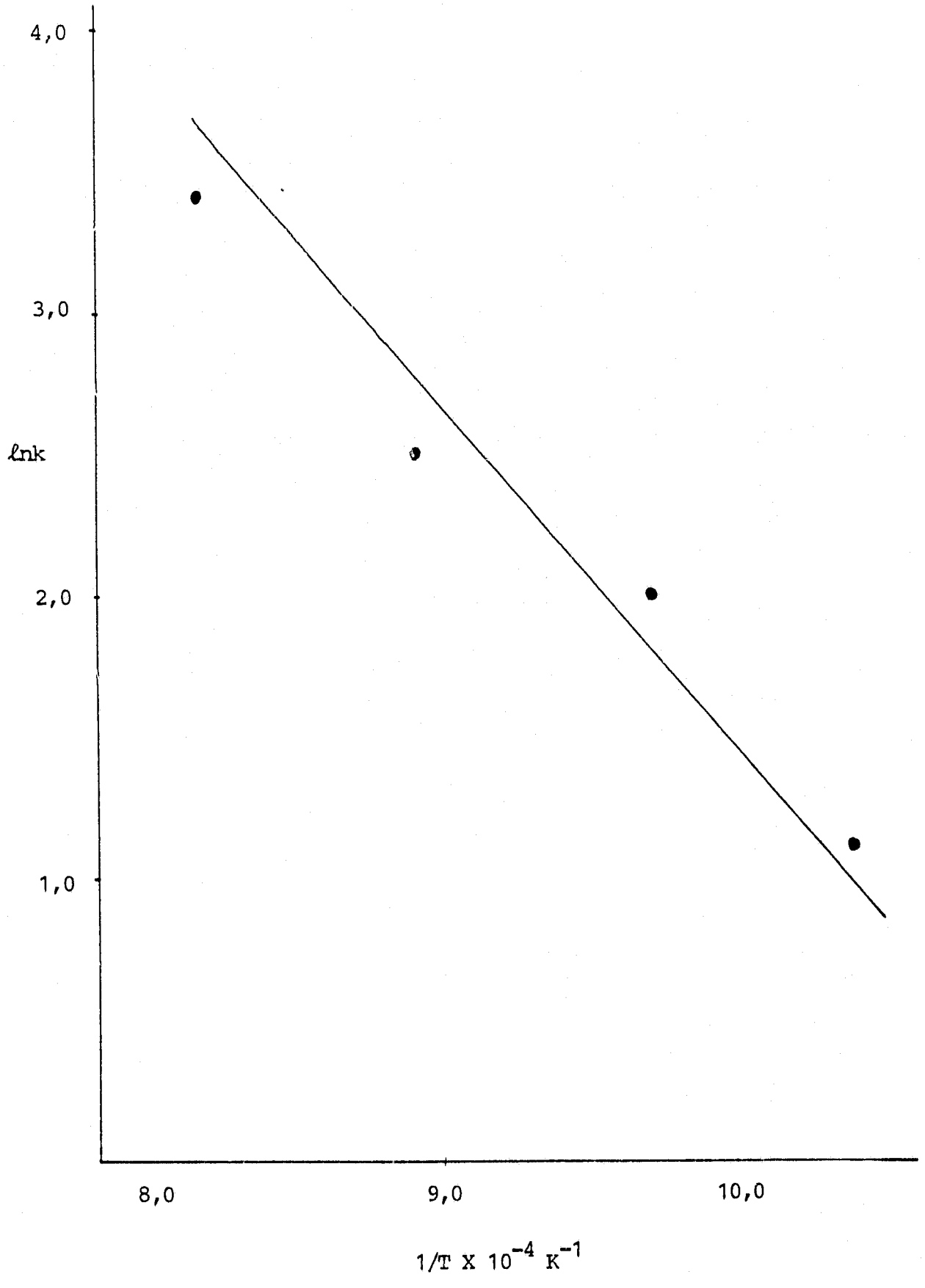

ii) Influence of burn-off on aurocyanide adsorption

Fig. (6.4) shows a plot of the percentage burn-off for steam activated coconut char versus the equilibrium activation temperature. A gradual mass loss of up to 35 percent is observed for activation temperatures below 800°C. This must be due to development of surface area and pore volume by the preferential oxidation of the more accessible carbon matrix. As the temperature increases a dramatic mass loss is observed above 850°C which is exponential in nature. This must be due to direct oxidation of the carbon matrix.

The relationship between burn-off and aurocyanide adsorption is shown in Fig. (6.5) where a plot of percentage gold adsorbed versus the percentage burn-off is shown. The relationship is approximately linear up to burn-offs of 35 percent, after which carbon matrix is lost without a proportionate increase in aurocyanide adsorption.

The relationship between burn-off and temperature is further shown in Fig. (6.6) as a van't Hoff plot. A reasonable linear region is observed between 600 - 850°C and has an enthalpy of about 48 $kJmol^{-1}$ of carbon. The decrease in the slope at higher temperatures is probably due to a change in the surface reaction.* This may involve a change from a rate limiting reaction to a diffusion limited one.

* Oxidation is essentially a rate process.

Fig 6.4

Graph of % burn off vs activation temperature for coconut char in steam atmosphere

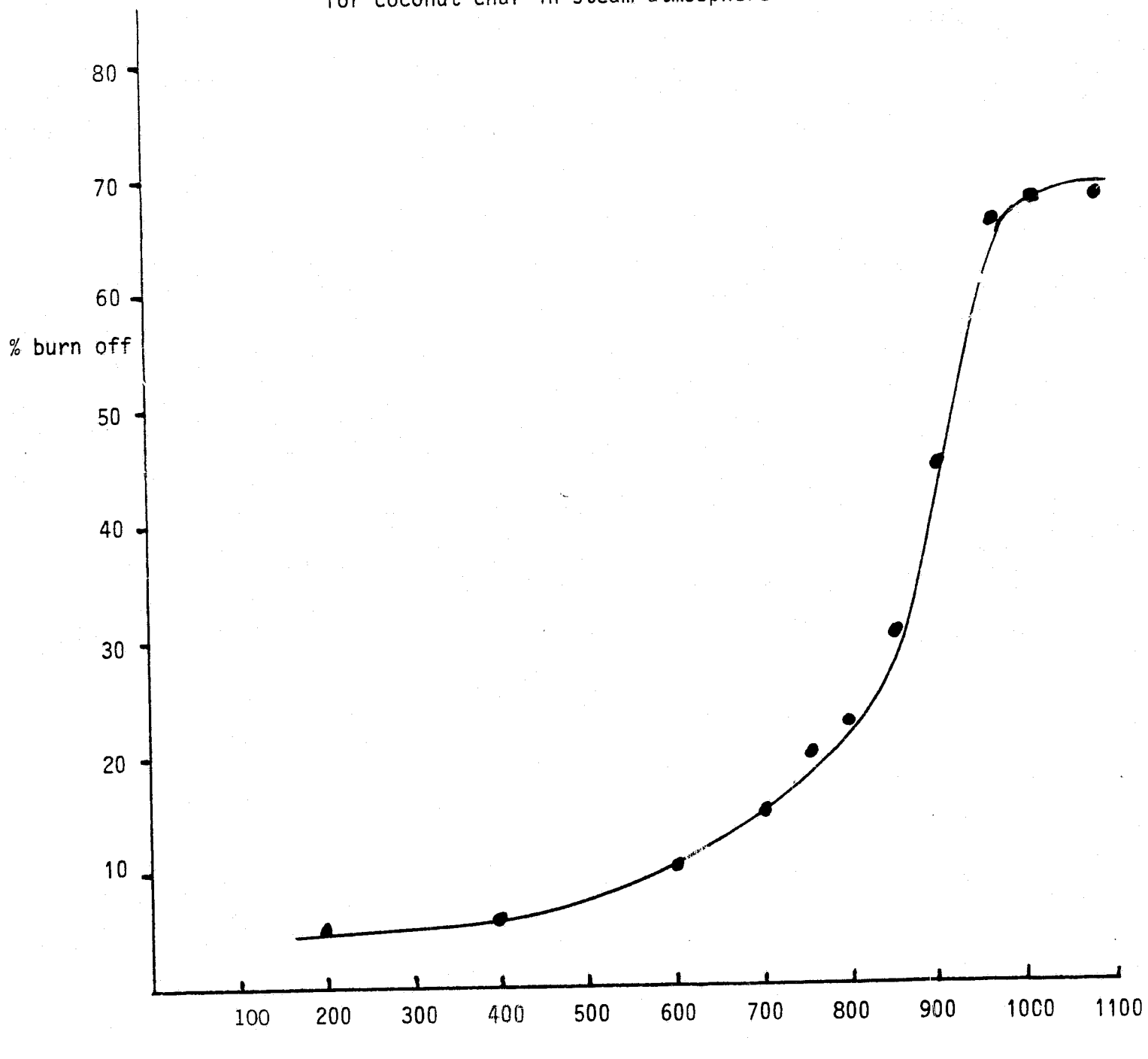

Fig 6.5

Graph of % Au adsorbed vs % burn off
for steam activated carbons

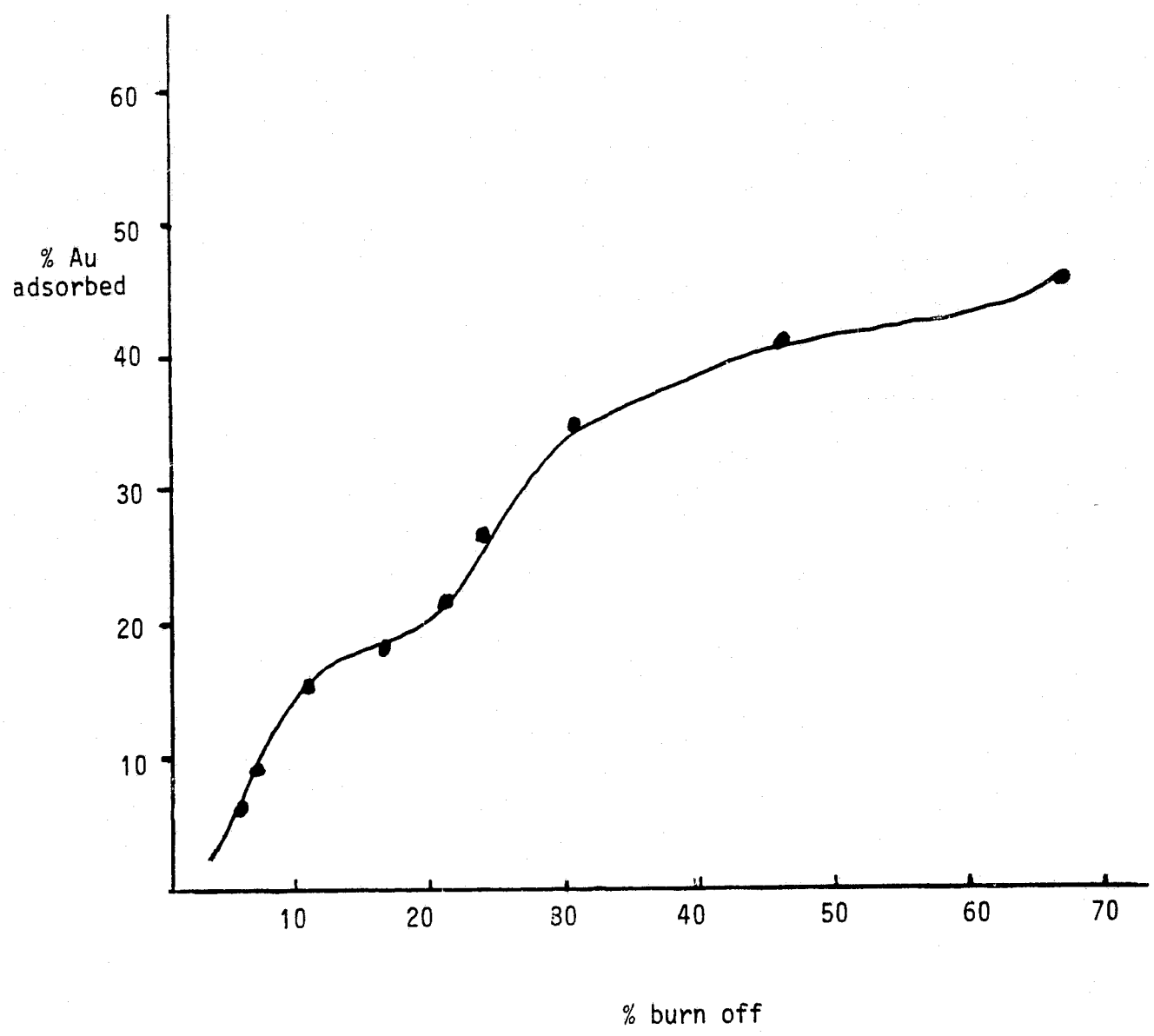

Fig. 6.6

Effect of Temperature on Mass loss
Graph of ℓn(% mass loss) versus 1/T

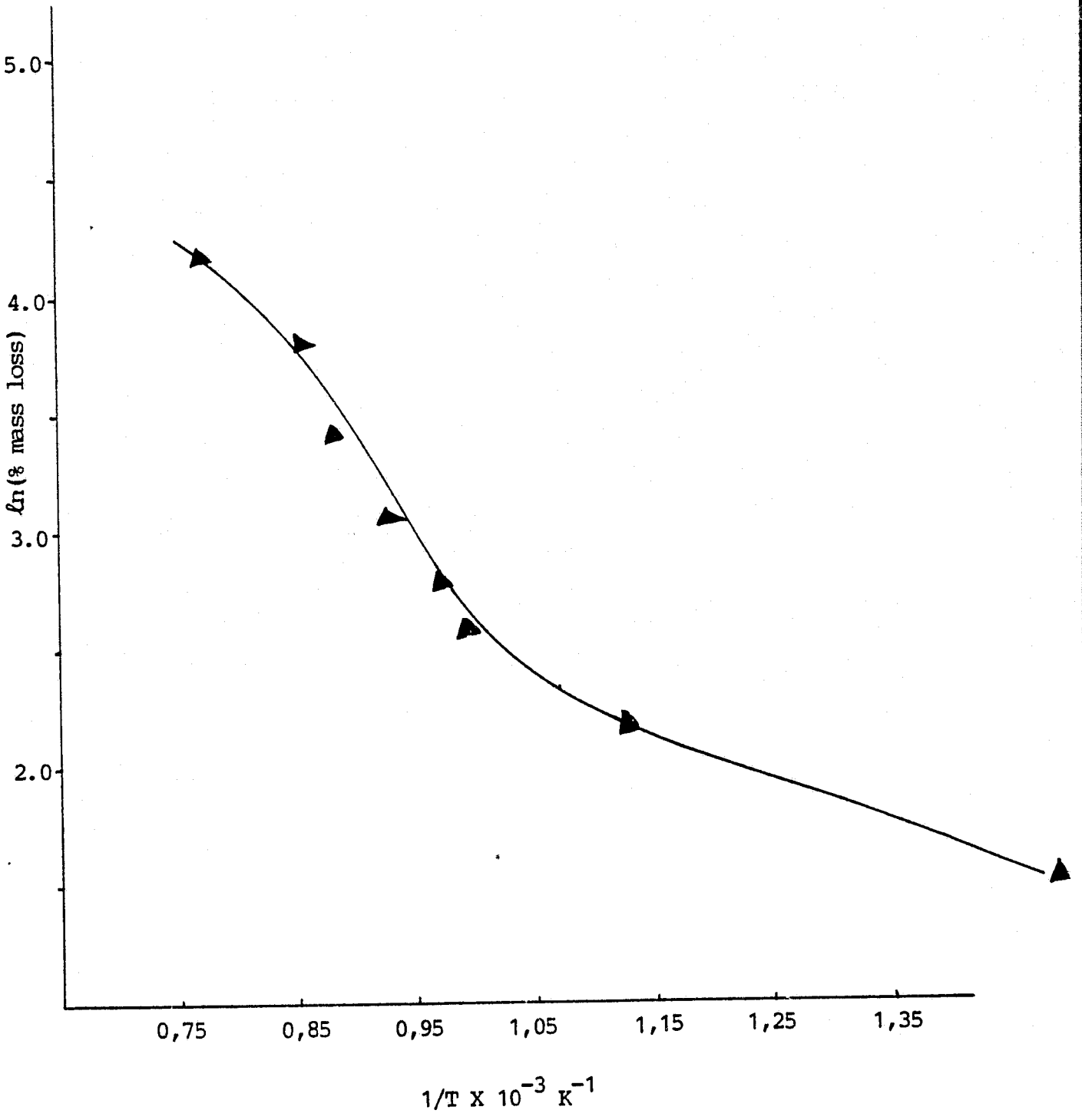

6.3 Characterization of surface functionalities on activated carbon via Fourier transform infrared spectroscopy

The characterization of surface functional groups on activated carbon, pyrolysed resins, chars and coals has been extensively investigated via spectroscopic techniques.[66-69,85] The surface groups on such products depend largely on the origin of starting material and method of manufacture(Table 6.3).

Products activated in steam or oxygen below 700°C generally contain a variety of oxygen functional groups.[3] These groups amongst others appear to involve carbonyl and carboxyl groups. Thermal decomposition studies on such products by Puri[82] have shown that such groups mainly evolve CO_2 gas. Carbons activated above 700°C under similar conditions in general appear to involve singly bound oxygen and may involve phenoxy and ether groups as these groups on thermal decomposition are removed as CO gas[82].

The literature on carbons with proven aurocyanide capacity reveal no spectroscopic studies of such products. In this study the coconut shell products obtained under vigorously controlled conditions were examined via FTIR spectroscopy. Various other chars and commercial products with proven aurocyanide capacity were also examined for similarities and differences.

Results and discussion

Fourier transform infrared spectra of the coconut shell steam activated products generated between temperatures of 700 - 1000°C are summarized in Fig. (6.7). Only five bands were found between the range 4000 to 400 cm^{-1} and in general relatively few significant trends can be distinguished. The five bands and their assignments are shown in Table (6.1)

Table 6.1

Assignment and characterization of observed bands for coconut shells activated by steam between temperatures of 700 to 1000°C

Wave No.	Assignment[83]	Characterization
2917 (vs)	methylene group	$-CH_2-$
2858 (vs)	" "	$-CH_2-O-$
1083 (m)	ether group	$-CH_2-O-CH_2-$
799 (s)	—	C-H
1556 (s)	aromatic	-C=C-

No bands in the range 1600cm^{-1} were observed which effectively rules out carbonyl functional groups such as ketones, aldehydes and esters. The alcohol functionality can be ruled out since no bands characteristic of ν(OH) were found in the range 3640 - 3610cm^{-1}. The band at 3450cm^{-1} has been assigned to water and not an alcohol since the spectrum of spectroscopic graphite also contains this band which confirms the assignment (see Fig. (6.12)).

The only possibility which remains is the ether functionality which has been postulated on a number of occasions.[3] The table below gives a list of some typical ether bands for various organic molecules.

Table 6.2

Ether bands ν(C-O) for some typical ether type organic molecules[83]

Ether groups	ν(C-O) / cm^{-1}
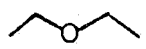 Diethylether	1145
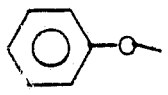 Anisole	1242
 Ethylene oxide	1270
 Oxacyclobutene	1010

Ether groups	ν(C-O) cm^{-1}
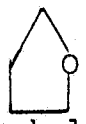 Tetrahydrofuran	1174
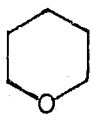 Pyran	1099
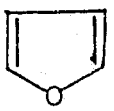 Furan	1170
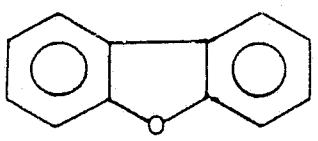 Diphenylene oxide	1198

Examination of the intramolecular factors affecting the ν(C-O) band in ethers shows that unsaturation increases with frequency; however no correlation is found with ring strain. The ν(C-O) frequency for the steam activated carbon approximates that for the highly strained oxycyclobutene and the pyran moiety. These molecules are saturated and are the most probable assignment[70] for the oxygen functionality of activated carbon. The carbon oxygen functionality is probably an ether type linkage between saturated carbon atoms ($-CH_2-O-CH_2-$).

Activation in steam causes an increase in this type of ether group since this band is absent from the spectrum of char. The band seems to increase in intensity with burn-off, at 1000°C the ν(C-O) band is very prominent where approximately 70 percent burn-off is achieved.

The band at 2917 cm^{-1} is due to methylene groups and seems to increase in intensity with activation temperature and burn-off. The band at 2858 cm^{-1} may be assigned to a methylene group whose frequency is shifted to higher energy by a moiety such as $-CH_2-O-$. The band at 1556 cm^{-1} has been assigned to an aromatic group frequency ν(C=C). The band at 800 cm^{-1} may be due to out of the plane bending for the C-H group (i.e. γ(CH)).

The FTIR spectrum of LeCarbon G210 AS (Fig. (6.9)) is very similar to that of steam activated carbon, this is not surprising since both products are coconut shell based. The spectrum of Norit R2020 and KOP carbon have a variety of bands which are similar to the above products, although there are some notable differences. These products are both coal based extruded carbons and may contain impurities due to the origin of coal and binding material. Fig. (6.11) shows the spectrum for a coke sample with proven aurocyanide adsorption. This product also has the band at 1090 cm^{-1}. However, the high energy band shifts to 600 cm^{-1}. As the method of preparation is not known no conclusions can be drawn.

The above limited range of carbons examined suggests the formation of an ether type of surface funtionality. If we consider that these groups exist exclusivly at the microcrystallite edges, it is possible that a reasonably large local concentration of such groups may constitute a site or a point of attachment. As approximately 90 percent of the surface consists of micropores of diameter <20 Å, an oxygen layer over a few carbon atoms with in the pore, might yeild a polar surface of approximately 2-4 M oxygen. The polarity of such groups may be further enhanced as the excess charge of the microcrystallite may be distributed to the surface by such groups.

The figure below shows a somewhat idealized model of such a surface.

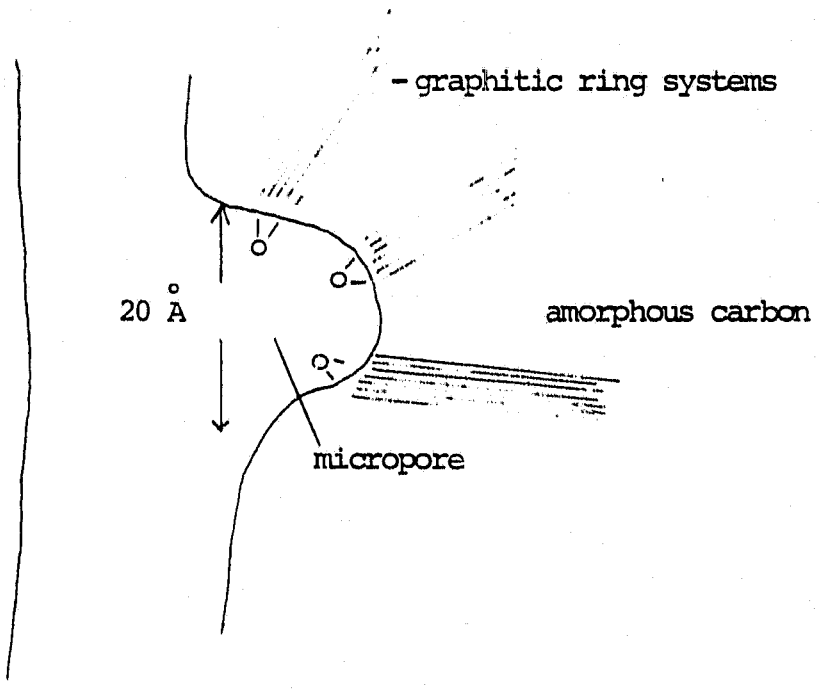

The volume of such a micropore, assuming a semi-spherical (r= 10 Å) configuration can be calculated to be of the order of 2000 $Å^3$.

Fig. 6.7

Steam activated coconut char

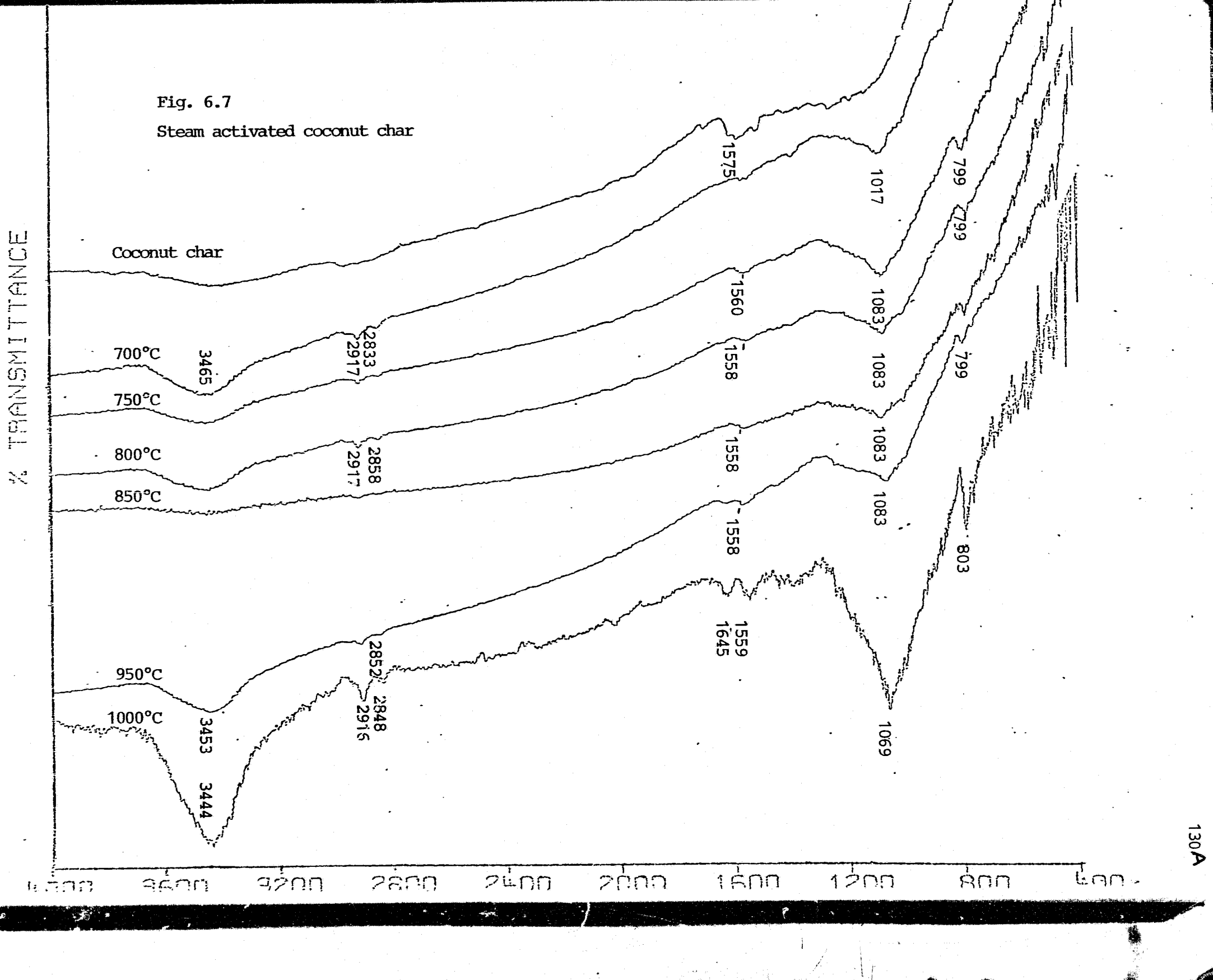

Fig. 6.8
KOP Activated carbon

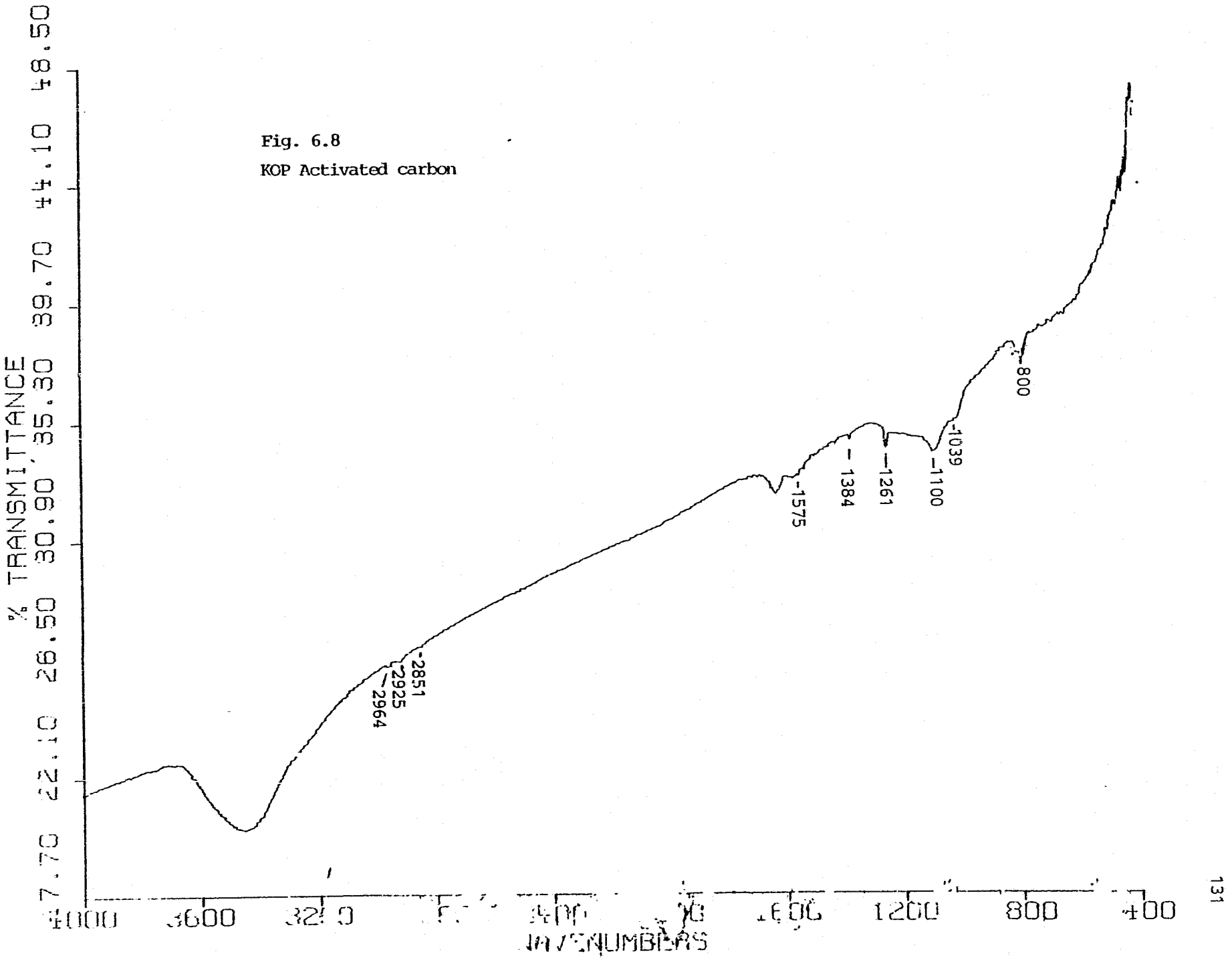

Fig. 6.9

LeCarbon Activated carbon

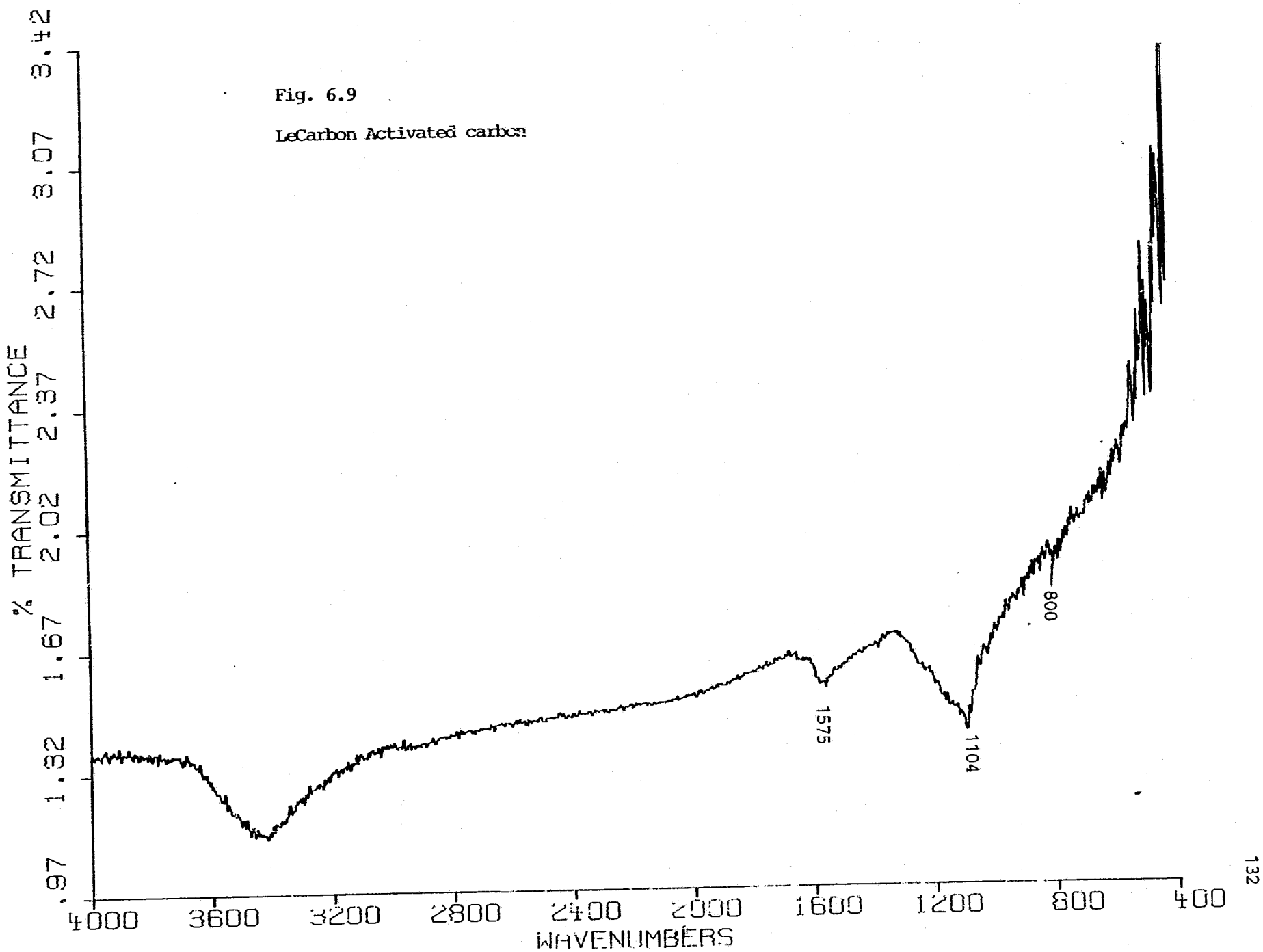

Fig. 6.10
Coconut char

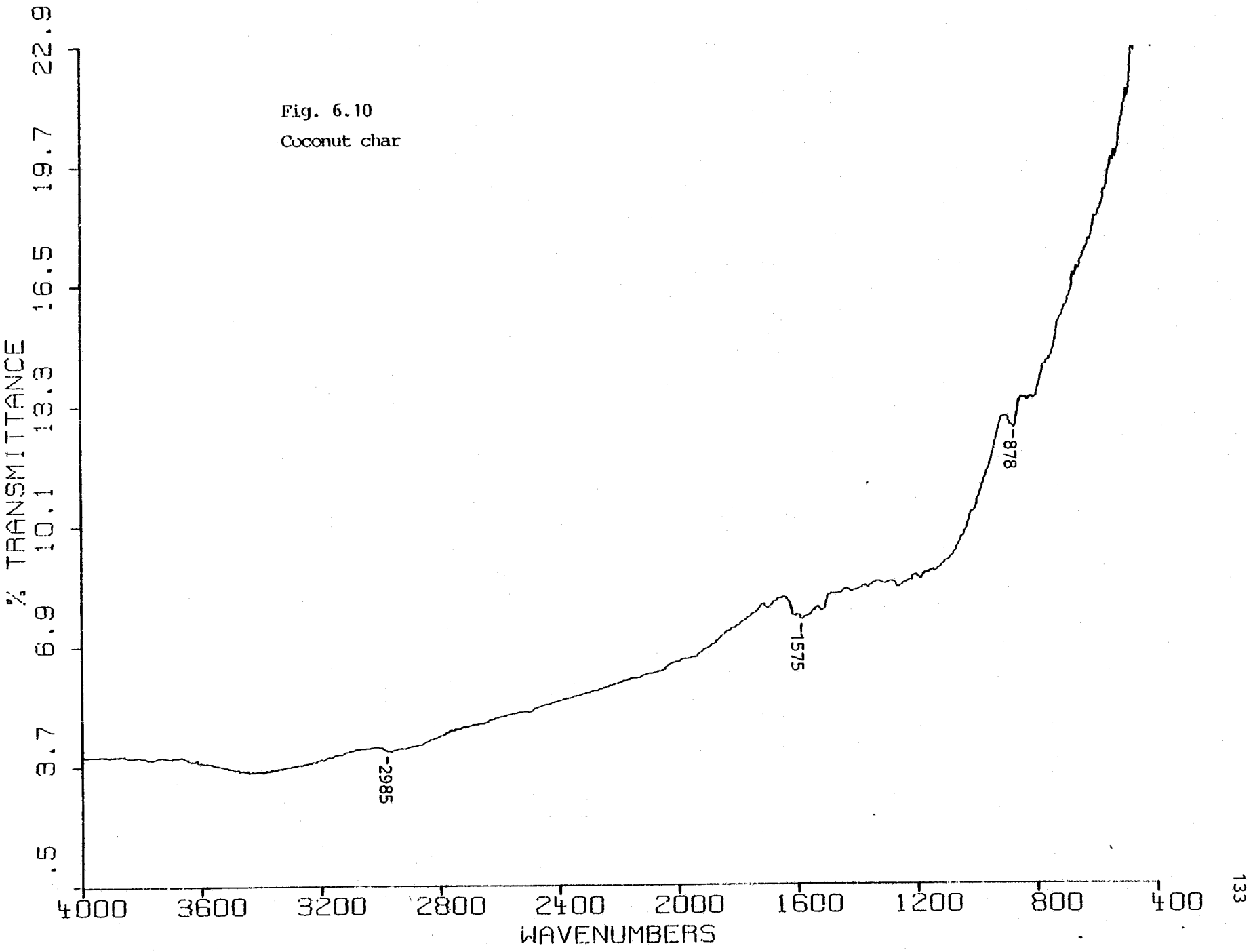

Fig. 6.11
Coke sample

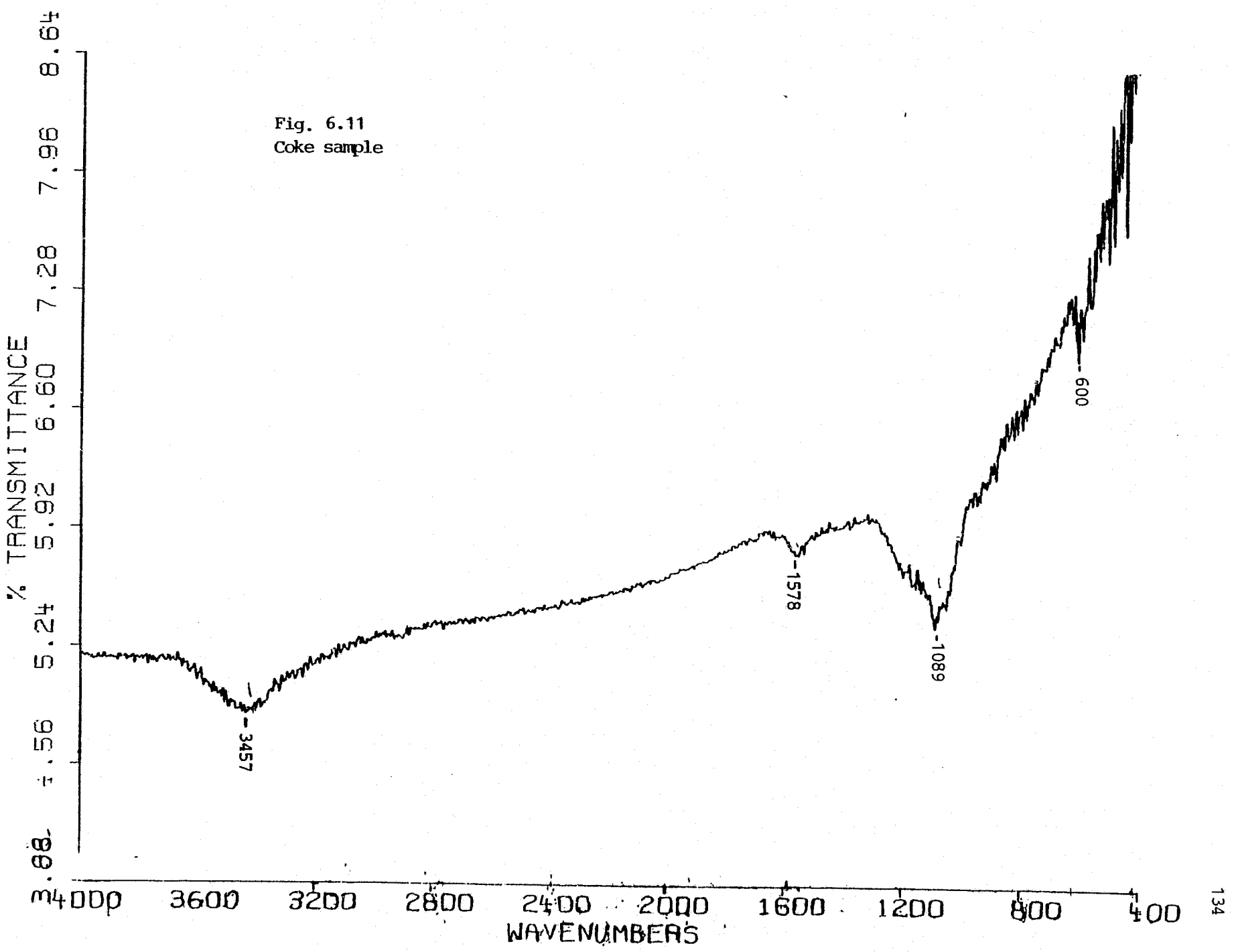

Fig. 6.12
Spectroscopic Graphite

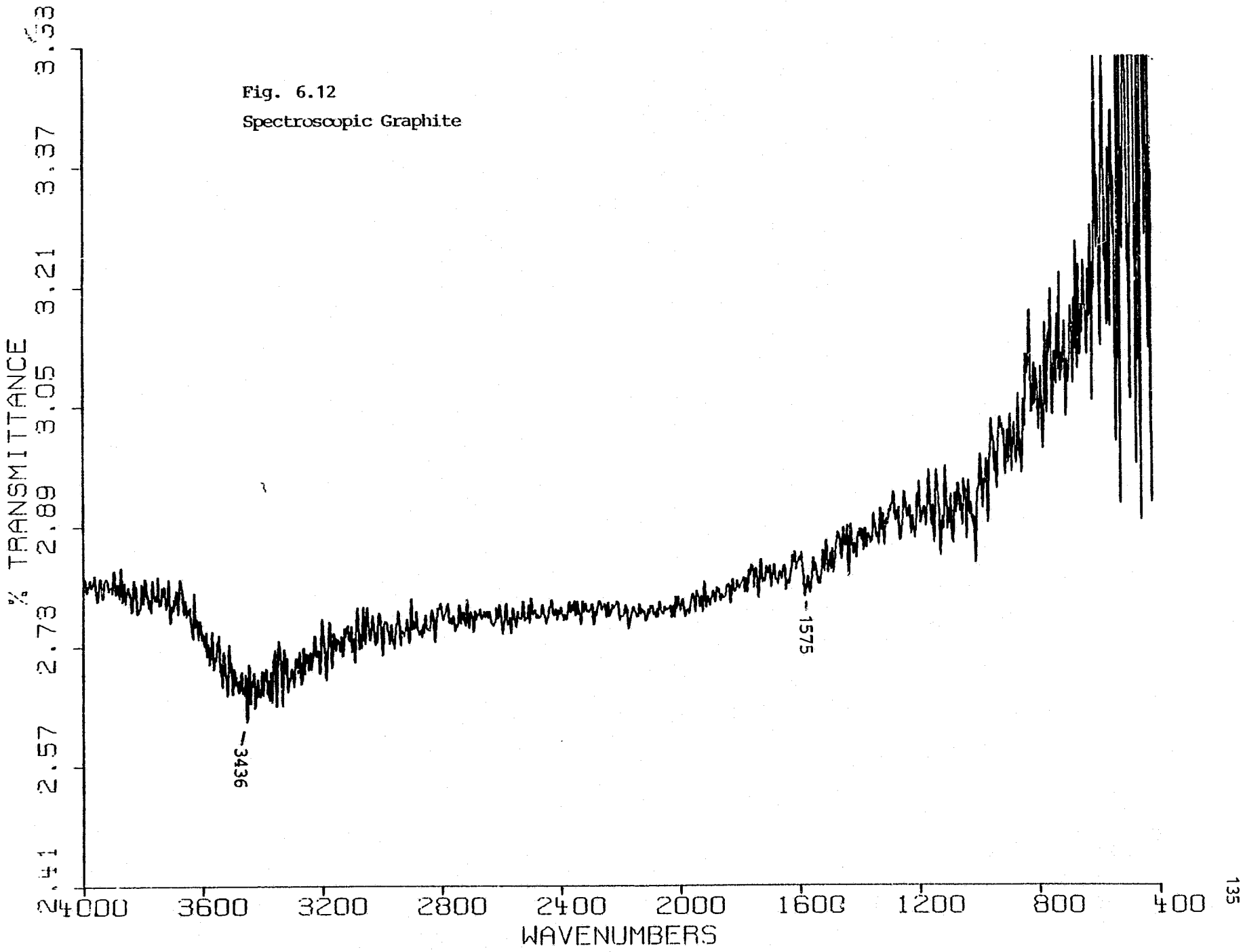

Table 6.3 Main bands appearing in IR spectra for various activated carbons, chars and coal

KOP	Norit R2020	LeCarbon G 210 AS	Typical coal[85]	Oxidized coal[85]	Pyrolysed PFA[67]
3440	3460	3440	3300	3440	
2964			2960		
2926	2918	-	2921	2926	
2857	2854	-	2860	2850	
				1765	1700
1640	-	-		1695	
			1610	1610	1600
1579	1580	1590			
			1480		
1384	-	-			1380
1230	1242	-			1280
				1200	
1103	-	-		1120	1180
1040	1095	1050	1050	1050	1080
803	304	800	-	-	-

PFA = polyfurfuryl alcohol

Wave number = cm^{-1}

6.4 Summary and conclusions

The empirical approach adopted in the study showed that the formation of aurocyanide adsorption characteristics by carbon are related to the temperature of activation, the burn-off or pyrolysis and the steam atmosphere. The pyrolysis of char under steam induces an eight fold increase in aurocyanide adsorption whereas in nitrogen atmosphere only small increases were observed. Activation under steam between 600 - 900°C results in a large increase in aurocyanide adsorption which is accompanied by large mass loss or burn-off. This increased mass loss is not observed under inert nitrogen atmosphere and must be due to the direct reaction with steam. The direct oxidation of carbon results in a mass loss by the formation of gaseous CO_2 via the formation of carbon-oxygen surface intermediates. The formation of "CO" type surface groups between 600 -850°C may be represented by the following equation[3]-

$$C + H_2O \longrightarrow CO_{ads} + H_2 \qquad (6.1)$$

A large concentration of CO type groups probably results on the surface since the desorption of CO_{ads} is rate controlling.[3]

At temperatures above 700°C the formation of CO_2 becomes increasingly favourable according to the following reaction which is essentially the water gas shift equilibrium[84]-

$$CO + H_2O \longrightarrow CO_2 + H_2 \qquad (6.2)\ \Delta H = 206\ kJmol^{-1}$$

This results in an increased mass loss which is accompanied by the evolution of gas in this temperature range. (Fig. (6.4)). Heat must be continuously supplied for the reaction to proceed as the reaction is endothermic. At temperatures above 850°C, the large concentration of CO_2 within the pores of carbon may further react with the matrix according to equation

$$C + CO_2 \longrightarrow 2CO \qquad (6.3)$$

At this temperature reaction 6.2 simultaneously occurs with reaction 6.3 and the net result is the loss of carbon matrix in an exponential manner which is accompanied by the volumous evolution of gas.

The formation of surface functionalities such as alcohols appear to involve an exothermic reaction. For example the gas phase synthesis of methanol[84] can be written -

$$CO + 2H_2 \longrightarrow CH_2OH \qquad (6.4)$$

The carbon dioxide formed may also be used in this reaction. However, it is first reduced by hydrogen to carbon monoxide which then reacts as above. The reaction is exothermic ($\Delta H = -91$ kJmol^{-1}) and the equilibrium methanol concentration decreases with increasing temperature. This probably explains the absence of the hydroxyl functionality from the spectra of high temperature steam activated carbon.

The identity of the surface groups was characterized via FTIR where activation in steam above 700°C results in the appearance of methylene groups as well as a carbon-oxygen band at $\sim$ 1080 cm^{-1}. These bands must be due to the reaction of steam with the carbon

surface since both are absent in the spectrum of char. Characterization by elimination of oxygen functionalities such as hydroxyl and carboxyl groups by their absence and the position of the observed bands suggests that an ether type group exists on the carbon surface. The presence and position of methylene groups suggest that the ether linkage is saturated and not aromatic in nature.

The absence of methylene groups in the spectra of LeCarbon and KOP carbons suggest that the formation of specific types of oxide groups may be dependent on reaction conditions since fast flow rates of steam may inhibit the accumulation of hydrogen within the pore. Alternatively, activation using CO_2 and CO may be responsible[3]. In all cases the carbons investigated have the ether type group and seem to be associated with high temperature steam activation.

The pyrolysis of carbon under nitrogen displays little capacity to adsorb aurocyanide. Under steam pyrolysis however a large capacity is induced between 600 - 950°C which is associated with a large mass loss. Fig.(6.5) shows an approximately linear relationship between the mass loss and the percentage gold adsorption. Thus the direct oxidation of carbon probably has a role in inducing aurocyanide capacity. In the previous section it was shown that a specific type of interaction between the adsorbed aurocyanide and the carbon matrix occurs at low surface coverages. The aurocyanide adsorption can be modelled by the Temkin isotherm, where the strength of interaction between aurocyanide and the carbon surface is given by slope k. It was observed that as the temperature of activation increased, the slope of the initial region of the Temkin isotherm also increased showing that the strength of

interaction between the aurocyanide and the carbon increases with increasing temperature of activation.

The Van't Hoff plot of the strength of interaction parameter k versus the activation temperature results in a linear relationship and yields an enthalpy of +45 $kJmol^{-1}$. Thus the formation of aurocyanide capacity involves an endothermic reaction between carbon and steam and the reaction proceeds ($\Delta G \leqslant 0$) above temperatures of 450°C where the burn-off is first observed to occur.

Activation of carbon above temperatures of 500°C simultaneously causes graphitization of the structure, while between 600-800°C the resistivity of carbon decreases.[14] This is thought to be due to ring closure. The single covalent C-C bond interacts with the non-localized ($2p_x$) orbitals of the planar carbon. This extra bonding gives the graphitic structure high thermal stability and π-electrons which gives rise to magnetic and electrical properties.

The formation of oxygen containing groups on the surface appears to involve reaction with the edge groups of such graphitized regions.[3] Loosely stacked layers of such microcrystalline carbon give rise to surfaces or localized regions which are reasonably polar. The formation of such a surface give activated carbon its hydrophilic character and is the most probable area for the adsorption of the more polar types of adsorbates.

The adsorption of many organic compounds at low concentration has been proposed by Weber and van Vliet[24,21] to involve an interaction of a more specific nature.

Aromatic compounds such as phenols are thought to accept charge from the carbon into their delocalized π systems to form donor/acceptor complexes. Substituted groups on aromatic compounds also influence the interaction. The more electron withdrawing the substituted group, the more electron density can be accepted into the aromatic ring which results in an even stronger donor/acceptor bond and therefore a higher relative adsorption is observed. This is demonstrated by the order of adsorption reported by Gupta and De[3] for various substituted aromatic compounds, the trend of increasing adsorption is given by the series -

$$\phi - NH_2 > \phi - OH > \phi - CO_2 \qquad \phi = \text{⬡}$$

This type of charge transfer from the carbon to the adsorbed aurocyanide has in fact been observed by Adams[41] particularly at low surface coverages. McDougall et al[24] using XPS on aurocyanide loaded carbons have similarly observed an apparent reduction in the oxidation state of the gold atom.

This charge transfer together with the polar surface, would suggest that the ion-pair with the more electron acceptor cation would induce a stronger interaction with the carbon surface.

7. The mechanism of aurocyanide adsorption by activated carbon-summary of conclusions

Although many different mechanisms for the adsorption of aurocyanide by activated carbon have been proposed, many of these can now be discarded. These include complete reduction to gold metal, partial reduction or degradation, adsorption into the electrical double layer on the surface, and ion-exchange with positively charged carbonium ion.

The mechanism of adsorption involves the adsorption/extraction of the ion-pair species $[M^{n+}]\ [Au(CN)_2^-]_n$ by activated carbon.

The adsorption by activated carbon of many organic an inorganic substances can be understood in terms of the interaction between the solvent, adsorbate and the adsorbant. This gives rise to a whole range of interactions whereby attractive interactions between solvent-adsorbent and adsorbate-adsorbent enhance the extent of adsorption whereas interactions between adsorbate-solvent and solvent-adsorbent discourages the adsorption.

The interaction between adsorbate and solvent has a marked effect on adsorption. In aqueous phase adsorption, water is quite polar and is able to hydrogen bond intermolecularly as well as the adsorbate and the adsorbant. Hydrophilic interactions are the result of a net repulsion between water and the non-polar regions of the adsorbant surface and the non-polar parts of the adsorbate.

Thus the non-polar regions of the adsorbant surface and the non-polar adsorbates are dispelled from the water phase which results in the accumulation of adsorbate at the solid-liquid interface. This hydrophobic effect has been recognized and is the basis of Traube's rule which states -

> "The adsorption of organic substances onto activated carbon from aqueous solution increases strongly and regularly as we ascend the homologous series."

Activated carbon may be considered to be a large but porous matrix which supports domains of hydrophobic and hydrophilic surface. The basal plane areas of activated carbon graphitic plates are hydrophobic and are expected to support hydrophobic and dispersion type forces. Weber and van Vliet[21] have shown that for various activated carbons and polymeric adsorbants, the extraction behaviour at high organic concentrations are similar. This may be ascribed to adsorption onto similar "sites" or surfaces where the hydrophobicity is the main consideration. At low concentration of organics however, the distribution coefficient for activated carbon is many orders of magnitude higher. This has been proposed to involve a more "specific" interaction between the organic and the carbon surface (chemisorption, hydrogen bonding and electrostatic).

The microcrystallite edges are reasonably polar due to the large concentration of oxygen-containing functional groups and are the most probable areas for the adsorption of the more polar adsorbates. These areas have been proposed to form the basis of the specific adsorption interactions between the organics and the carbon surface. The interaction between the adsorbate and the carbon may be enhanced by charge transfer from the delocalized π-electron system of carbon to form a donor/acceptor complex on the surface. Electron withdrawing groups on the adsorbed species may further enhance this type of effect.

The trend for the adsorption of aurocyanide shows that the presence of cations enhances the adsorption. This indicates that the mechanism involves the formation of ion-pair species at the carbon surface. Similarly, the extraction of many anions and cations by activated carbon reported in the literature can be now understood to involve the extraction of neutral ion-pair/acid-base/neutral molecules. Such large neutral species are then probably adsorbed onto the surface, and the hydrophobic effect results in their accumulation at the solid-liquid interface.

The trend for the adsorption of aurocyanide shows effects due to specific cations. The trend for increasing extraction with increasing size of cation can be understood in terms of increasing hydrophobicity with increasing size. The adsorption of the ion-pair with the more polarizable cations, in addition to the large hydrophobicity due to the size of the aurocyanide anion, must involve an additional interaction with the carbon surface whereby the charge-transfer mechanism enhances the donor/acceptor complex on the surface.

Much evidence for the polarizability of the aurocyanide anion has been found in U.V.[60,61] and Mossbauer[87] spectroscopy. The observed order of polarizability of linear metallocyanides is expected since, as we decend the group (Cu → Au), the effective nuclear charge decreases, whereby electrons are less effectively held. The aurocyanide species undergoes additional polarization due to metal to ligand charge transfer whereby the d-orbital electrons are delocalized into Au-C σ bonding as well as in π-donor and π-acceptor bonding with the CN^- ligand. IR/Raman spectroscopy of aurocyanide salts further demonstrates the extent of delocalization across the aurocyanide ligand where the Au-C σ bond as well as the cyanides carbon-nitrogen bond are both caused to strengthen or weaken as determined by the polarizability of the cation. This type of acid/base interaction is covalent, particularly with the more polarizable cations such as the Li^+ species, where the yellow colour is due to outer sphere charge transfer. The withdrawal of electron density from the aurocyanide effectively renders the gold atom positive and is expected to enhance the adsorption by activated carbon.

The molar solubility of the aurocyanide species shows that it varies according to the cation present in solution. Examination of the aqueous chemistry of this system gives insight into the thermodynamics of hydration for this species.

Solutes are usually classified with respect to their charges e.g. cations, anions and neutral species. Their interaction with water has been classified as hydrophobic and hydrophilic. In general hydrophilic solutes or structure breakers interact more strongly with water than do the molecules intramolecularly. These solutes are more readily soluble and give rise to hydration layers which are structurally different from those of bulk water. Hydrophobic or structure making[45,46] solutes are sparingly soluble in water since intermolecular forces between water and the solute are weaker than hydrogen bonding between water molecules themselves. The dissolution of such solutes causes a positive change in entropy. The solute molecules or ions are placed in holes in the water structure, which are adaptable to the requirement of the solute molecules for free rotation.

The distribution of aurocyanide between solid and aqueous phase at saturation, gives rise to the formation of ion-pairs, where the assocation constant K_{oss}, depends on the nature of the cation and the form of the resulting ion-pair. Examination of the trends results in a U-curve when the molar solubility versus cationic radius is plotted.

Models[51] for the variation of K_{oss} with cationic size predict a linear relationship with Z^2/r^+. However, within a series of related cations, their degree of hydration is also expected to have a role[81]. In addition to this, it has been often suggested, that the size and shape of the hydrated anion might be of more importance. The other model used to

predict ion-pair formation is due to Bjerrum and Fuoss. This model is based on electrostatic considerations and predicts that the ion with the smallest hydrated radius will be most expected to ion-pair. These two models both require a knowledge of hydrated radii which are not well established and the observed cation trends for the aurocyanide adsorption does not follow their predictions. The trend shows that the energetics of hydration can account for the observed aqueous solubilities by considering their effect on the structure of water. Ion-pairs will form so that they least disrupt the water structure and so maximize their free energy. In addition, reduction in the number of ions in solution, and the neutralization of charge results in an entropy change that favours the ion-pair formation. For large weakly polarized species, the forces between the ion-pair and the water are weakly dispersive and give rise to a hydrophobic hydration. The formation of such ion-pairs explains the solubility trend for the series $Cs^+ > K^+ > Na^+$.

Small polarizable cations however are strongly hydrated and lewis acid/base ion-pairs result due to the large enthalpy of hydration of the Lewis acid. The resulting ion-pair is also probably stabilized by the weak covalent charge transfer interaction. The solubility trend $Li^+ > Na^+$ is explained by such considerations and presumably the cation H^+ would also be expected to follow this trend.

In aqueous solution the ion-pair may be solvent separated or a contact ion-pair. The hydrophobic ion-pairs are probably solvent separated as are the Lewis acid/base types of ion-pairs. However some evidence exists that the highly polarizable Li^+ species may partially displace solvating water molecules by its strong interaction with aurocyanide.

Thus, to summarize, for very large ions or neutral species which are weakly polarized, a hydrophobic hydration occurs in polar water. The reduction in the number of ions in solution and the neutralization of charge results in an entropy change favouring the formation of ion-pairs. The forces between the water and the ion-pair are weak dispersion forces and these types of ions are "water-structure enforced" ion-pairs.[45,41] The formation of such a poorly hydrated ion-pair thus becomes increasingly compatible with the carbon phase, and, it undergoes extraction due to the ease of dehydration.

Examination of various reports in the literature concerning extraction or adsorption of aurocyanide can be explained by ion-pair considerations.

Trioctylamine[88] (Alamine) has been used as an extractant for metallocyanides. The order of extraction is given by the series -

$$Au(CN)_2^- > Ag(CN)_2^- > Cu(CN)_2^- > Zn(CN)_4^{2-} > Fe(CN)_6^{4-}$$

The order of extraction increases with increasing size and decreases with increasing charge.

Extraction of $HAu(CN)_2$ has been reported[89], where the distribution into various organic solvents increases with the order -

$$Cl^- < NO_3^- < HSO_4^-$$

This trend is explained by increasing competition with increasing size, and therefore polarizability. Interestingly enough, the selectivity displayed by foam fractionation[55] is given by -

$$Au(CN)_4^- > Hg(CN)_4^{2-} > Cd(CN)_4^{2-} > Zn(CN)_4^{2-}$$

This trend can be explained by the large size of $Au(CN)_4^-$ and its low charge. The interference displayed by competing anions has the following trend -

$$NO_3^- \sim Br^- \sim CN^- > Cl^- > SO_4^{2-}$$

The interference caused by the anion is greatest when the charge to radius ratio is small (i.e. it is polarizable).

Anion exchange resins such as IRA 400 show a large selectivity for aurocyanide adsorption. Burstall[53] and Avestone[54] have shown that large poorly hydrated anions such as ClO_4^- and $Ag(CN)_2^-$ effectively compete for adsorption, whereas the small hydrated F^- ion shows little competition. The hydration enthalpies of the anions closely follow the selectivity trends and are due to the form of the anion, the polymer supported cation, and the nature of the resulting ion-pair. The large ability to adsorb aurocyanide has also been ascribed[6] to the polarizability of the

anion as well as its linear shape. The selectivity coefficient for adsorption also follows the trend described by molar refraction (proportional to polarizability)[45], and a linear relationship is found for the plot of selectivity coefficient versus ionic refraction. The large selectivity is probably due to a mixture of these effects[6]. The large poorly hydrated monovalent anions will form ion-pairs, where the nature of the cation, the anion and the resulting ion-pair determine the degree of hydrophobicity. The observed trends also show that the polarizability also influences the anion/cation complex, the species with a low charge to radius ratio being preferred.

Returning to the adsorption of aurocyanide by activated carbon, the distribution ratio is decreased by the presence of various anions. The trend for increasing depression follows that of increasing size and polarizability thus these anions effectively compete for both carbon surface and cation in the aqueous phase.

Activated carbon surface also has an important role where the heat of adsorption at low surface coverages suggests the formation of a chemisorptive bond between the aurocyanide ion-pair and the carbon surface. The charge transfer mechanism probably stabilizes the adsorption of the neutral species, although as this type of surface is finite, any additional adsorbate undergoes degradation. X-ray diffractometry was used to determine if any AuCN was present. No evidence of this species was found for carbons loaded up to 80mg Au/g in the presence of various cations and even acid.

A mixture of finely ground carbon and the appropriate weight of AuCN readily yielded the characteristic AuCN diffraction pattern. Elution of aurocyanide loaded carbons showed that below loadings of about 40mg Au/g the adsorbate was fully eluted using hydroxide. Examination of the adsorbed species using U.V. spectroscopy showed the gold to be the aurocyanide species. This confirms the adsorption of the aurocyanide species below loadings of 40mg Au/g. However as the loading is increased the fraction remaining on carbon after desorption of the aurocyanide species probably involves gold metal. The X-ray diffraction result together with the failure to remove adsorbed gold with aqueous ammonia supports this result.

Examination of aurocyanide loaded carbons in the specific adsorption region shows that simple equilibrium effects are operative. The desorption of aurocyanide is affected by both the cation and the anion in the eluent phase at elevated temperatures. The equilibrium may be shifted by either increasing or decreasing the temperature.

At constant temperature the desorption of aurocyanide using hydroxide eluent follows first order kinetics where the polarizability of the cation of the medium influences the rate of desorption. This is expected since the polarizability of the cation determines the ion-pair/carbon interaction. The desorption of aurocyanide shows no effects due to the initially loaded cation, which is expected due to the large concentration excess of cations in the eluent phase.

The solubility of the aurocyanide species probably also has a role as it increases strongly with increasing temperature. However, in deionized water, no desorption is observed even at higher temperatures. Adsorption of the competing anion possibly as an ion-pair species probably displaces the aurocyanide ion-pair. However, some evidence has been found for an ionization mechanism.

The adsorption site of activated carbon possibly involves the micropore structure since this accounts for more than 90 percent of the so called surface. These pores have molecular dimensions that approximate semi-spheres with diameters of less than 20 Å. These pores are the result of etching or burn-off and might have a concentration of 2-4 M oxygen within the cavity. The configuration of oxygen groups in the pore cavity might be similar to that of a class of macrocycles called crown ethers[91]. In fact Pedersen[92] has shown that the complex dicyclohexyl-18-crown-6 is capable of forming a stable complex with aurocyanide as a salt or ion-pair.

The polar surface of the pore together with the excess charge from the graphitic structure.thus might constitute an adsorption site in activated carbon.

Appendix 1

1A Bonding in aurocyanide and other metallocyanides

Marked differences in the complexity of linear dicyano complexes in the region 200 - 300 nm have been noted.[60,61] The spectrum of $Au(CN)_2^-$ is most complex and is characterized by a number of high energy transitions. The spectra of $Ag(CN)_2^-$ and $Cu(CN)_2^-$ are less complex whereas the spectrum of $Hg(CN)_2$ is notably empty.

For the aurocyanide complex these transitions have been characterized[61] as LaPorte allowed metal to ligand (M→L) charge transfer (Au 5d $\longrightarrow$ * CN^-). These transitions are best described by spin-orbital effects which give rise to excited state energy splittings which allows for spin forbidden transitions. This results in an effective charge reduction on the Au atom -

$$N \equiv C - Au - C \equiv N \quad (\delta^- \leftarrow \delta^+ \rightarrow \delta^-)$$

The aurocyanide complex is further polarized by reduction of charge involving the utilization of 6s and 6p orbitals which penetrate the 5d orbitals.[87] According to Jones[63] good support for M - L back donation involving d orbitals is found by comparing the integrated intensity of the antisymmetric $\nu(CN)$ for a variety of cyanide complexes. The intensity of the band for aurocyanide is higher than for the species $Hg(CN)_2$ which confirms this result.

Coupling constants are proportional to the square of the effective charge on the central metal. For various linear metallocyanides the following trend has been reported[60,61] -

$$Au(CN)_2^- \gg Ag(CN)_2^- > Cu(CN)_2^- > Hg(CN)_2$$

Appendix 1

1A Bonding in aurocyanide and other metallocyanides

Marked differences in the complexity of linear dicyano complexes in the region 200 - 300 nm have been noted.[60,61] The spectrum of $Au(CN)_2^-$ is most complex and is characterized by a number of high energy transitions. The spectra of $Ag(CN)_2^-$ and $Cu(CN)_2^-$ are less complex whereas the spectrum of $Hg(CN)_2$ is notably empty.

For the aurocyanide complex these transitions have been characterized[61] as LaPorte allowed metal to ligand (M→L) charge transfer (Au 5d $\longrightarrow$ * CN^-). These transitions are best described by spin-orbital effects which give rise to excited state energy splittings which allows for spin forbidden transitions. This results in an effective charge reduction on the Au atom -

$$N \equiv C - Au - C \equiv N \quad (\delta^- \; \delta^+ \; \delta^-)$$

The aurocyanide complex is further polarized by reduction of charge involving the utilization of 6s and 6p orbitals which penetrate the 5d orbitals.[87] According to Jones[63] good support for M - L back donation involving d orbitals is found by comparing the integrated intensity of the antisymmetric $\nu(CN)$ for a variety of cyanide complexes. The intensity of the band for aurocyanide is higher than for the species $Hg(CN)_2$ which confirms this result.

Coupling constants are proportional to the square of the effective charge on the central metal. For various linear metallocyanides the following trend has been reported[60,61] -

$$Au(CN)_2^- \gg Ag(CN)_2^- > Cu(CN)_2^- > Hg(CN)_2$$

This is expected as the effect of the nuclear charge is shielded as one descends the group IB (Cu → Ag → Au).

The bonding mechanism of the aurocyanide anion thus involves d-orbital participation in Au - C σ bonding and both π-donor and π-acceptor bonding with the cyanide ligand.

Nakimoto has shown that for various metallocyanide complexes, relative group trends can be understood in terms of the frequency change for the fundamental band $\nu(C\equiv N)$.

a) Effect of electronegativity

$$Ni(CN)_4^{-2} < Pd(CN)_4^{-2} < Pt(CN)_4^{-2}$$

$\frac{\nu(C\equiv N)}{cm^{-1}}$	2128	2143	2150

The Ni(II) complex has the lowest electronegativity and so the σ donation is the smallest which is reflected in the lowest $\nu(CN)$ for the series.

b) Effect of oxidation state

$$V(CN)_6^{-5} < V(CN)_6^{-4} < V(CN)_6^{-3}$$

$\frac{\nu(C\equiv N)}{cm^{-1}}$	1910	2065	2077

The highest oxidation states are associated with good σ bonding which is reflected by the higher $\nu(CN)$ frequency.

c) Effect of coordination number

	$Ag(CN)_4^{3-}$	<	$Ag(CN)_3^{2-}$	<	$Ag(CN)_2^{1-}$
$\frac{\nu(C\equiv N)}{cm^{-1}}$	2092		2105		2135

An increase in the coordination number results in a decrease of positive charge on the metal which weakens the bonding. This is reflected in the decrease of the $\nu(C\equiv N)$ band.

d) Effect of cation

No specific study has been reported for metallocyanide complexes although cation effects have been reported for alkali earth complexes of sulphates.

e) Group Ib metallocyanides

	$Cu(CN)_2^-$	<	$Ag(CN)_2^-$	<	$Au(CN)_2^-$
$\frac{\nu(C\equiv N)}{cm^{-1}}$	2125		2135		2140

This shows that Au(I) has the highest electronegativity since the $\nu(C\equiv N)$ bond is the highest for the series.

f) Effect of oxidation state

	$KAu(CN)_2$	<	$KAu(CN)_4$
$\frac{\nu(C\equiv N)}{cm^{-1}}$	2140		2189

This shows that Au(III) has a stronger σ bond than the Au(I) complex which has also been shown by Jones.[63]

Complete vibrational assignments of the aqueous aurocyanide ion and polycrystalline alkali metal salts has been reported.[56] Assignments have been made on the basis of $D_{\infty h}$ symmetry for the aurocyanide salts of group IA cations :

$$M^{+}Au(CN)_2^{-} : \quad M^{+} = \{K^{+},\ Na^{+},\ Li^{+} \text{ and } NH_4^{+}\}$$

complexes such as $TlAu(CN)_2$ and $AgAu(CN)_2$ have been assigned on the basis of C_2 and C_{∞} symmetry respectively.

Correlations between the $\nu(C{\equiv}N)$ and the $\nu(Au\text{-}C)$ band with the cation in spectra of polycrystalline salts were noted and is the subject of this study. The study was expanded to include strong base resins, complexes of $MAu(CN)_2$(2,2-bipyridyl)[71] as well as various Au(III) cyno complexes.

Results and discussions

A) Polycrystalline aurocyanide salts

The effect of cation on the frequencies $\nu(C{\equiv}N)$ and $\nu(Au\text{-}C)$ for the aurocyanide species is shown in Figs. (A1) and (A2) . A reasonable correlation is obtained for both the symmetric and antisymmetric bands when plotted against the cationic radius. (see Table A1) The observed trend reflects the Lewis acidity for the cation which is given by the series -

$$Li^{+} > Na^{+} > K^{+} > Cs^{+}$$

A plot of the frequencies $\nu(C{\equiv}N)$ and $\nu(Au\text{-}C)$ for the aurocyanide species for various group IA cations

Fig. A1 Graph of $\nu(C\equiv N)$ for $MAu(CN)_2$ versus cationic radius

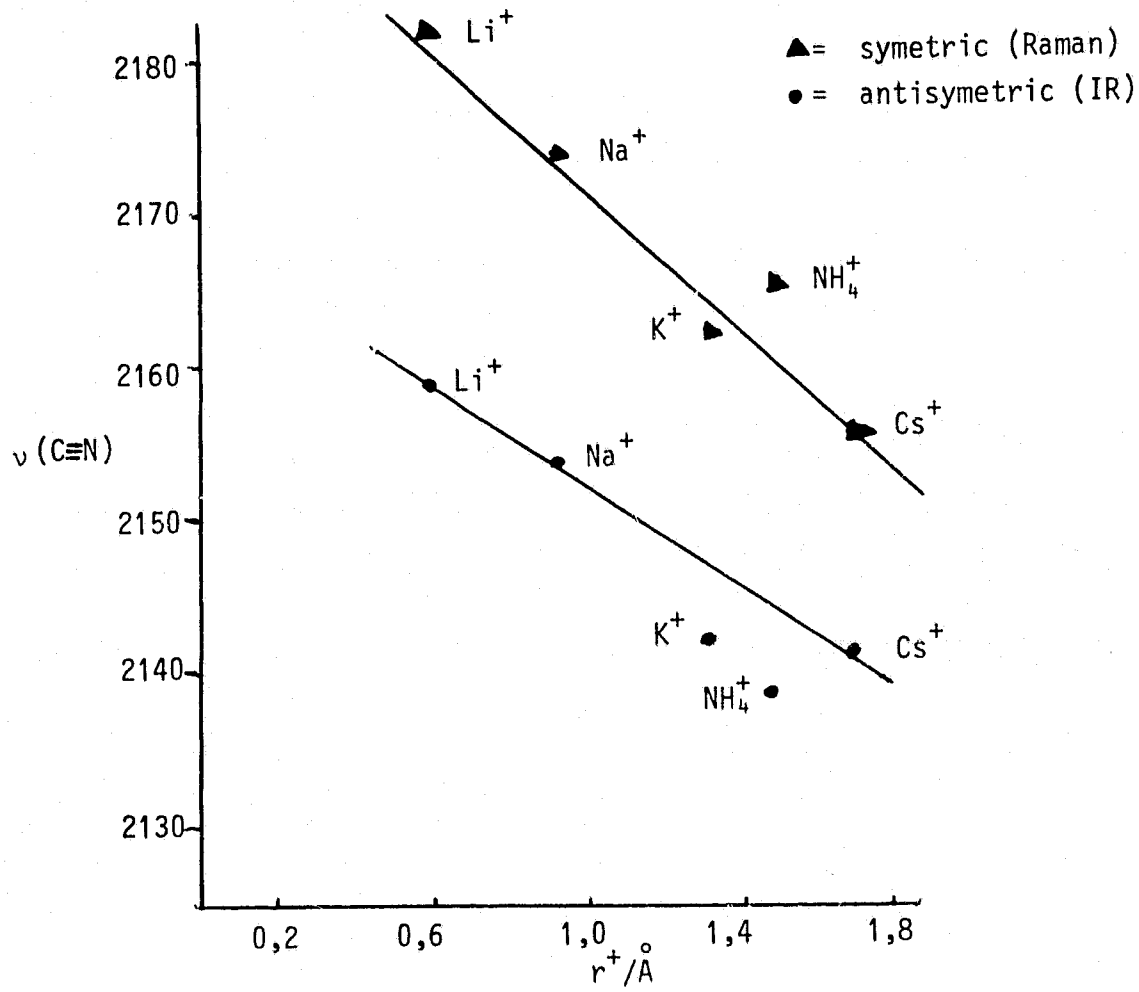

Fig. A2 Graph of $\nu(Au-C)$ for $MAu(CN)_2$ versus cationic radius

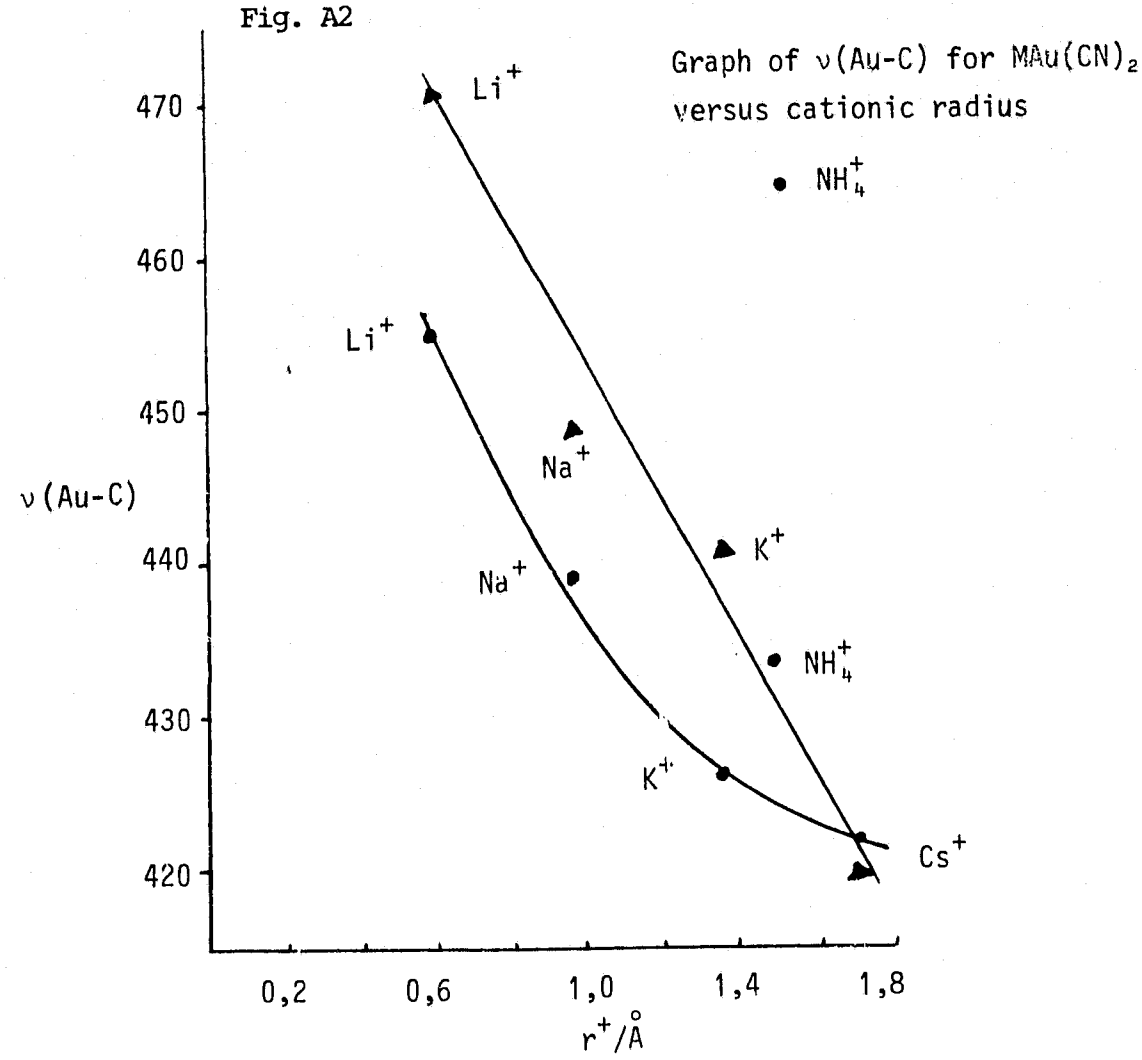

is shown in Fig. (A3). Both these fundamental bands increase in frequency with increasing acceptor strength of Lewis acid. This shows that the bonding is delocalized and the aurocyanide thus effectively participates in Au-C σ bonding as well as both π-donor and π-acceptor bonding with the cyanide ligand.

The Li^+ ion being a polar cation withdraws electron density from the aurocyanide ion, which causes further charge reduction in the central gold atom. The charge transfer is probably effected through the lone pairs of electrons on the nitrogen atom of the cyanide ligand :

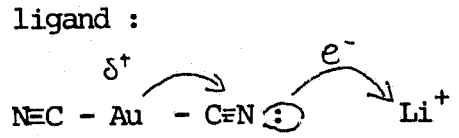

The complex $AgAu(CN)_2$ similarly interacts covalently as its fundamental symmetric and antisymmetric bands also follow the correlation. (Fig. (A3)).

A plot of ν(Au-C) versus the bending mode ν_6 is shown in Fig. (A4), the plot shows the effect of reduced mass. The complex $TlAu(CN)_2$ is known to have a weak Tl···Au bond and is T-shaped, consequently the bending mode for this complex has the lowest energy.

The complexes $LiAu(CN)_2$ and $[Be][Au(CN)_2]_2$ both have a characteristic yellow colour. This is due to a low energy transition between the polarized aurocyanide and these polar cations. The polymer $(AuCN)_p$ also has a yellow colour, this is due to extensive delocalization of electrons along the chain, which also involves a weak N···Au interaction.

Fig. A3 Graph of $\nu(C\equiv N)$ versus $\nu(Au-C)$ for $MAu(CN)_2$

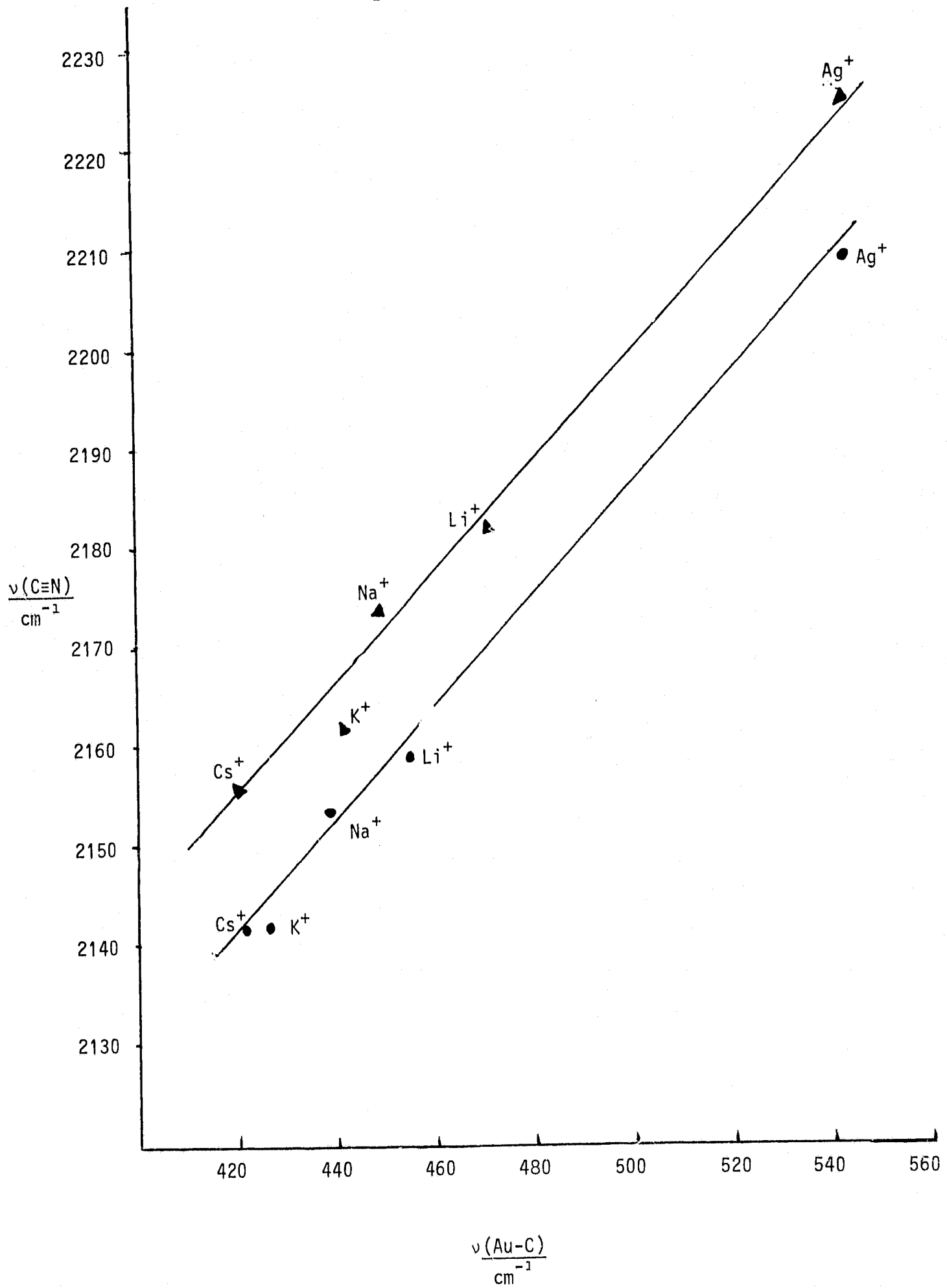

Fig. A4
Graph of ν(Au-C) vs ν_6(bending mode)
for $MAu(CN)_2$ salts.

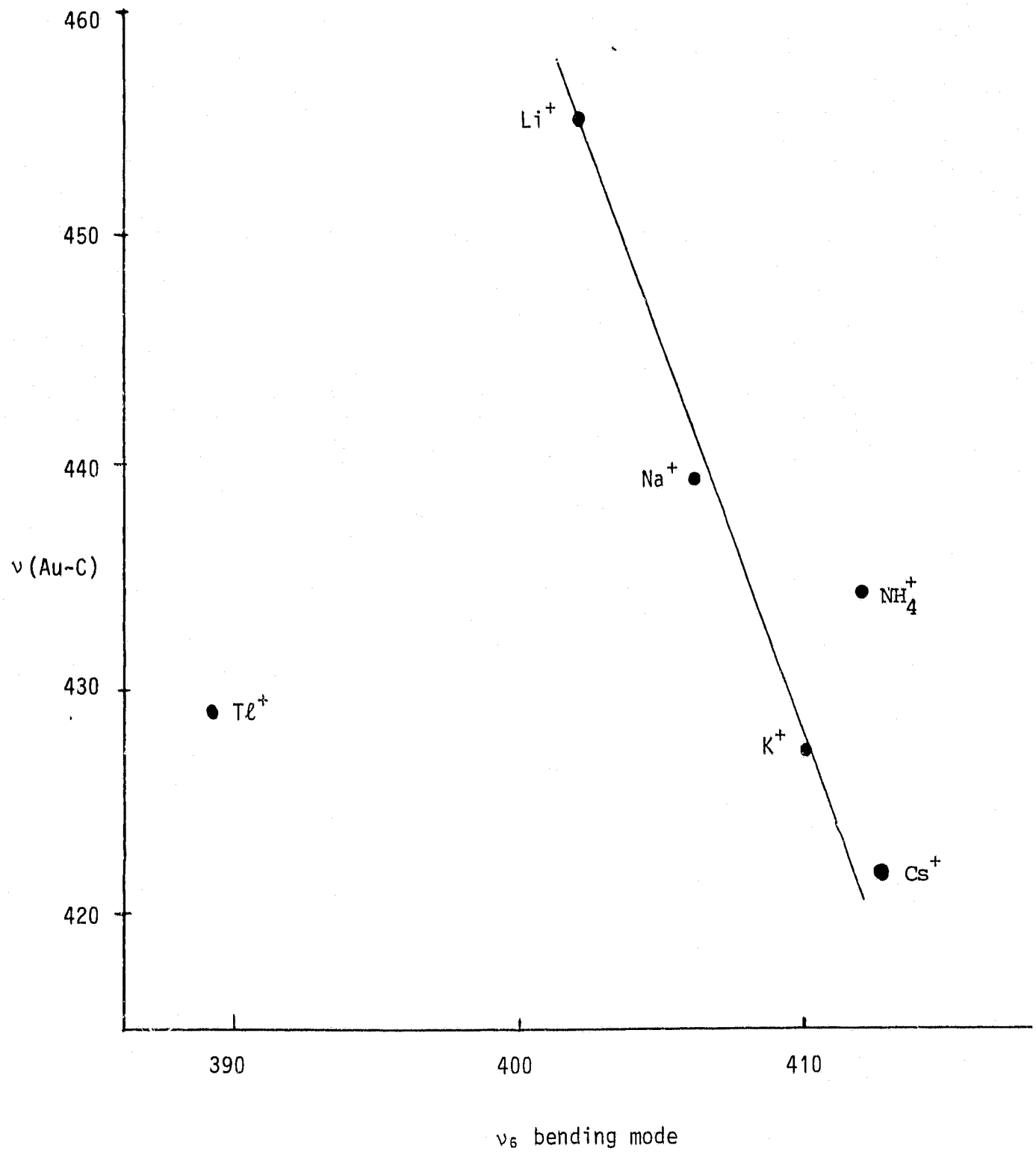

Table A 1 Infrared and Raman frequencies for various aurocyanide complexes

Complex	Infrared (C≡N) cm^{-1}	Infrared (Au-C) cm^{-1}	Ref.	Raman (C≡N) cm^{-1}	Raman (Au-C) cm^{-1}	Ref.
H^+	2142	427	59	-	-	
Li^+	2159	455	*	2182	471	*
Na^+	2154	439	*	2174	449	59
K^+	2142	426	*	2162	442	59
Cs^+	2159	455	*	2156	420	*
NH_4^+	2134	434	*	2161	465	59
Bu_4N^+	2140	427	*			
$T\ell^+$	2125 2134 2143	429	*	2145 2147 2153	453	
Ag^+	2209	542	*	2225	542	59
Be^{2+}	2165	-	*			
Ca^{2+}	2162 2142	465	*			
Zn^{2+}	2196 2156	420	*			
$M[Au(CN)_2(2,2'bipyridyl)]$ $M = Li^+, K^+, Na^+, Cs^+$	2140	not visible	*			
Resins						
IRA 400	2142	426	*			
Dow XF-4149	2142	427	*			

*= This work

Fig. A5
Photo Acoustic spectrum of $(AuCN)_p$

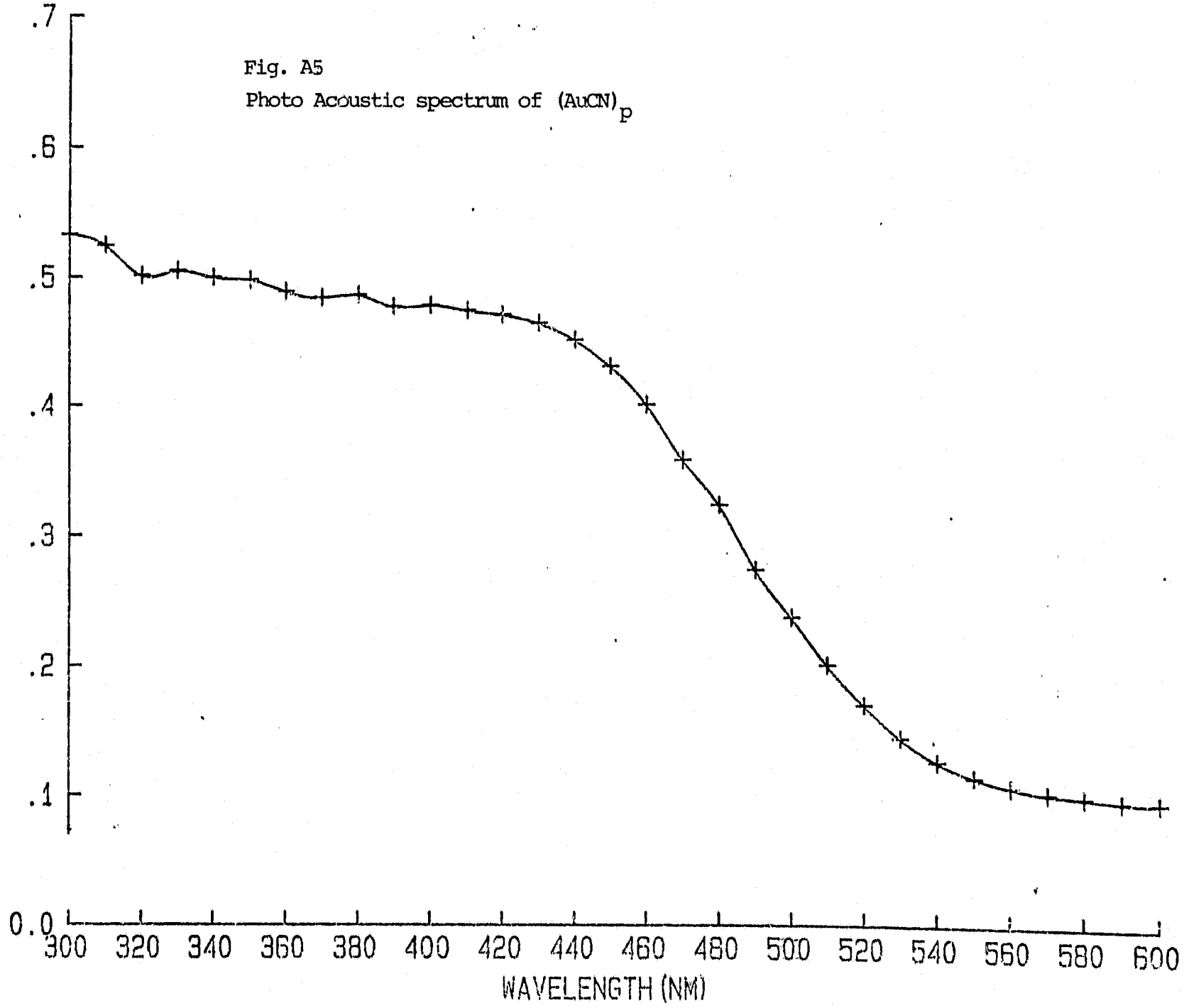

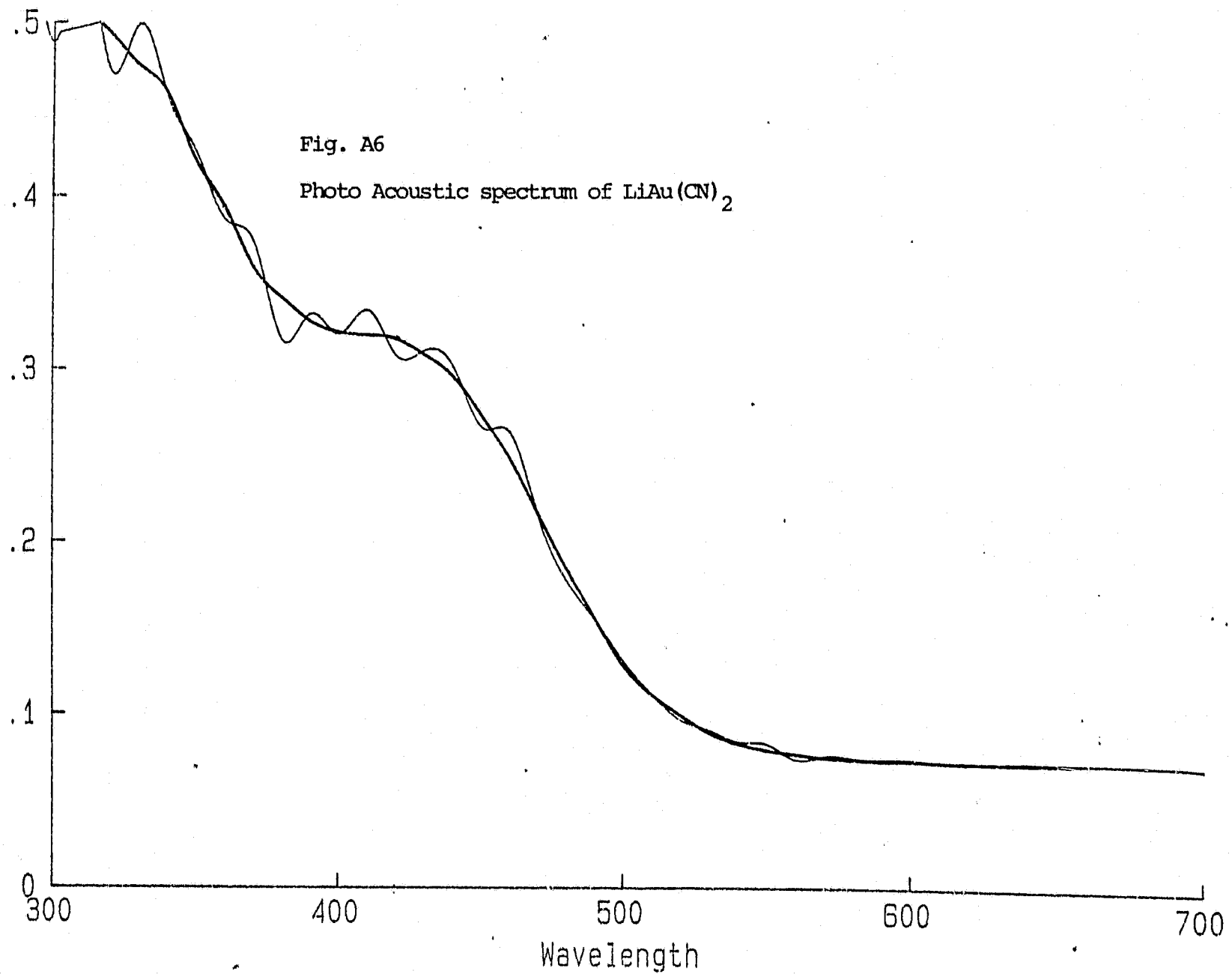

Fig. A6

Photo Acoustic spectrum of $LiAu(CN)_2$

The Photo acoustic spectra (PAS) of the solid compounds $LiAu(CN)_2$ and $(AuCN)_p$ are shown in Figs. (A5) and (A6). The visible transition for $LiAu(CN)_2$ is found at 420 nm (lemon-yellow) whereas the transition for $(AuCN)_p$ is found at slightly lower energy at 430 nm (yellow). The complex $[Zn][Au(CN)_2]_2$ was also found to have a yellow colour and is again due to the covalent interaction between the polarized aurocyanide and the strong Lewis acidity of the cation.

B) Polycrystalline salts of $M[Au(CN)_2(2,2'\text{-bipyridyl})]$

A recent crystallographic[71] study proved that there is no direct bond between the aurocyanide anion and the bipyridine moiety (bpy) as previously assumed. It was shown that the alkali metal M^+ was coordinated by seven N atoms, 3 from bpy and 4 from the CN groups as shown below -

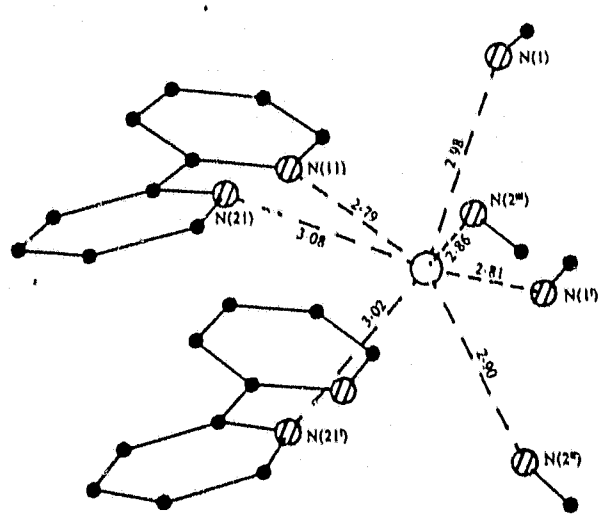

Fig. (A7) Coordination of the K^+ ion in complex $K\,Au(CN)_2(2,2'\text{-bipyridyl})$ after reference 71.

Various alkali metal complexes were synthesized according to reference (71). The I.R. spectra of these compounds showed no frequency variation with the specific cation in the region 2500 - 2000 cm^{-1}.

C Ammonium complexes of aurocyanide

The inductive effects of the substituted group on the ammonium cation were investigated to observe effects on the frequency of the aurocyanide bands. Two resins were investigated, IRA 400 which has the group $-N(CH_3)_4^+$ and Dow XF 4149 which has the group 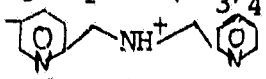 (bipicolylamine). These may be thought of as immobile ammonium cations. Polycrystalline salts of $NH_4Au(CN)_2$ and $NBu_4Au(CN)_2$ were also examined. In all four cases only a single $\nu(C{\equiv}N)$ at 2140 cm^{-1} was observed which suggests that the bonding with the aurocyanide anion is weakly polarized.

D Au(III) complexes

The aurocyanide anion can undergo oxidative addition reactions[62] with basic ligands to form d^8 square planer trans products. The complex is shown schematically in Fig. (A8). The reaction is summarized below -

$$Au(CN)_2^- + 2X^- \longrightarrow Au(CN)_2X_2^- \qquad X = \{Cl^-, Br^-, I^- \text{ and } CN^-\}$$

A plot of $\nu(C{\equiv}N)$ versus $\nu(Au-C)$ for the various complexes yields a good correlation and is shown in Fig. (A9). These spectra were obtained in aqueous solution and effectively shows the basicity of the ligand trans to the cyanide ligand.

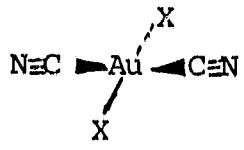

Fig. A8

The increase in the σ donor properties of the ligands ($Cl^- < Br^- < I^-$) trans to the cyanide causes a weakening of the Au-C and C≡N bond. This is expected since an increase in the electron density on the gold atom would tend to repel the cyanide ligands. The observed lengthening of the cyanide bands is the same as that of the σ donor properties i.e. $Cl^- < Br^- < I^-$. The complex $Au(CN)_4^-$ does not fit the correlation because the cyanide ligand acts as a π-acceptor as well as a σ-donor. This tends to greatly stabilize the complex and so the fundamental bands have a much higher frequency.

Available data[65] for the complex $Hg(CN)_2X_2^-$ shows similar trends and a plot of ν(C≡N) versus ν(Hg-C) is shown in Fig. (A10). The linear correlation indicates that the complex $Hg(CN)_2X_2^-$ has a trans configuration. The trend also shows a weakening of the Hg-C and the C≡N band as the σ-donor strength increases. The cyanide complex $Hg(CN)_4^{2-}$ fits the correlation and indicates that its σ-donor properties dominate the small π-acceptor contribution of the cyanide ligands.

Fig. A9 Graph of $\nu(C\equiv N)$ vs. $\nu(Au-C)$ for $[K][Au(CN)_2X_2]$

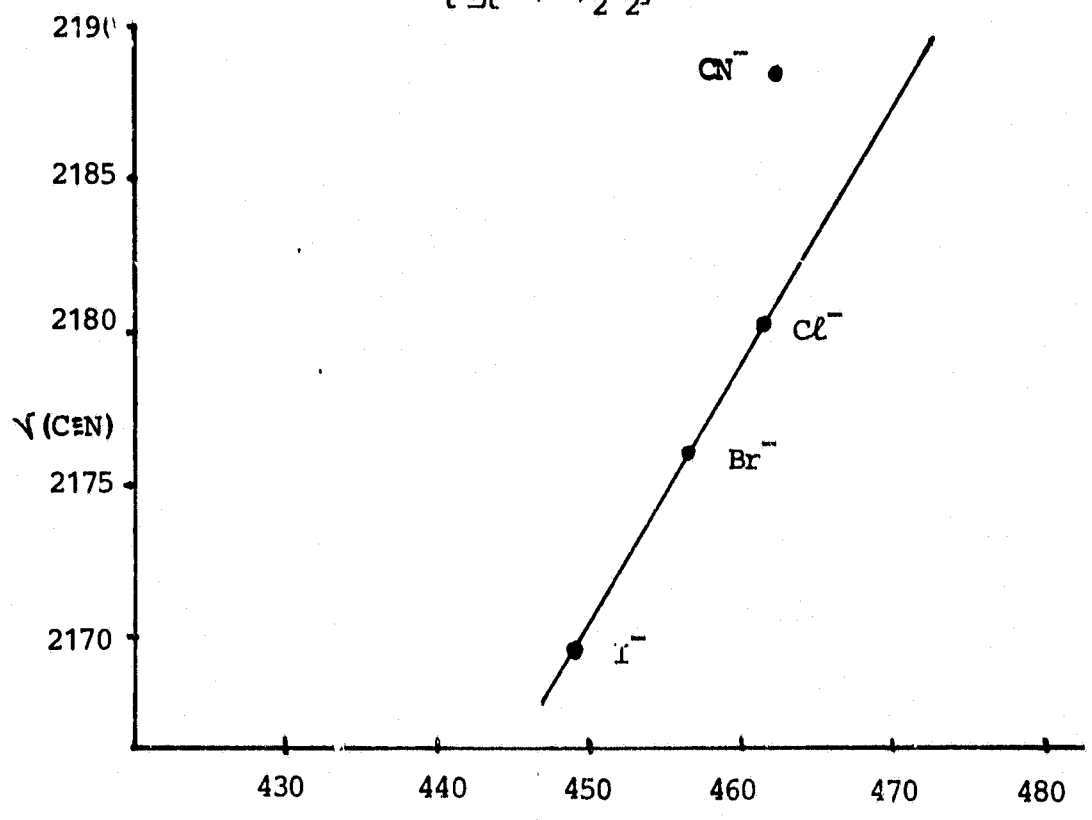

Fig. A10 Graph of $\nu(C\equiv N)$ vs. $\nu(Hg-C)$ for $[Hg(CN)_2X_2]^{-}$

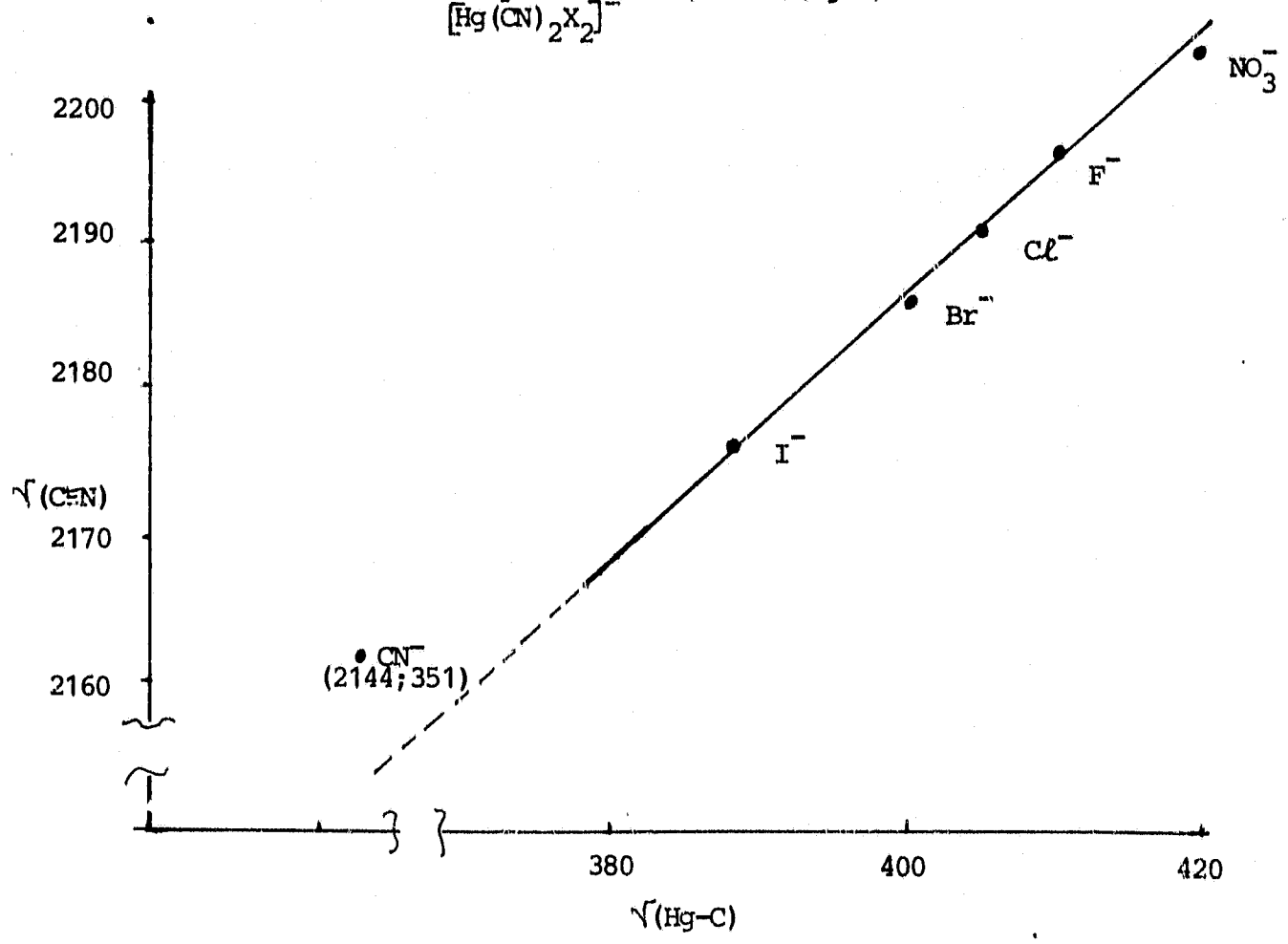

2A Association constants for aqueous aurocyanide

The aqueous chemistry of aurocyanide has been investigated via polarized Raman and infrared spectroscopy[56]. Saturated solutions of Na^+ and K^+ aurocyanide complexes display no spectral shifts or new bands which can be ascribed to the specific cation. The aqueous reaction can be written as -

$$M^+OH_2 + Au(CN)_2^- \rightleftharpoons M(OH_2)Au(CN)_2 \rightleftharpoons MAu(CN)_2$$

which represents the solvent separated and the contact ion-pair respectively. The absence of any changes in the spectra suggests that if ion-pair formation does occur, then for salts of Na^+ and K^+ a solvent separated complex is formed.

A similar result was concluded for the complex formation of $Fe(CN)_6^{3-}$ with group IA cations where no changes in the fundamental bands was observed.[6]

The Raman spectrum[58] of aqueous $LiAu(CN)_2$ displays weak bands at 412 cm^{-1} and 304 cm^{-1}. The ratio of intensity of these bands was found to be directly proportional to the concentration of $Au(CN)_2^-$ and Li^+ ions. This is proof of the association between Li^+ and the aurocyanide anion. The formation of a dimer has been considered, e.g. -

$$2Au(CN)_2^- \rightleftharpoons Au_2(CN)_4^{2-} \qquad \text{or} \quad Au(CN)_{2\,n}^- \quad n \geqslant 2$$

However, since no evidence of a higher coordinated Au(I) complex exists, this reaction is considered unlikely. A similar association with Li^+ cations

and the linear $Ag(CN)_2^-$ anion has been reported. Spectral changes were observed when $LiCl$ and $LiClO_4$ salts were added to 1 M $Ag(CN)_2^-$ solutions.

The molar solubility of $LiAu(CN)_2$ is about an order of magnitude greater than that of the large hydrophobic ion-pairs. The enhanced solubility of $LiAu(CN)_2$ is due to the large enthalpy of hydration of the Li^+ cation and is covalent interaction with the aurocyanide anion which gives rise to ion-pair formation.

The small polarizable Lewis acid strongly interacts with water and distributes its charge over a large volume resulting in a strongly hydrated aquo ion. The weakly hydrated aurocyanide ion is an electron donor which undergoes metal to ligand charge (M→L) transfer which results in a concentration of negative charge on the nitrogen atom of the cyanide ligand. The interaction between these two ions gives rise to the characteristic lemon-yellow colour observed in aqueous solutions and is due to outersphere charge transfer between the Li^+ and the aurocyanide anion. This probably results in an additional stabilization of the ion-pair.

The Li^+ cation may remain hydrated when the ion-pair is formed due to the large enthalpy of hydration, this is shown below -

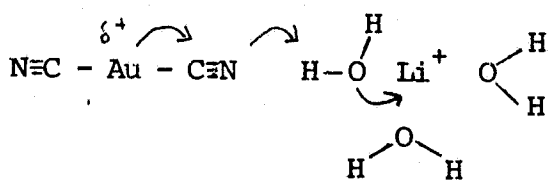

The charge transfer could be effected via the water molecule bound to the Li^+ cation. The yellow colour persists even in dilute solutions ($\sim 10^{-3}$ M) and gives rise to speculation that the hydration sphere of the Li^+ may be partly displaced on ion-pair formation. One reason for this is that $LiAu(CN)_2$ salts are known to be anhydrous, as are other aurocyanide salts. Additional evidence for this mechanism was found when $BeCl_2$ salts were added to a solution ($\sim 0{,}3$ M) of $KAu(CN)_2$. Initially a clear colourless solution was obtained which developed into a lemon-yellow colour after three months. The Be^{2+} ion is more strongly hydrated than the Li^+ species and the rate of substitution of the hydration sphere is known to be kinetically very slow.[89] These facts give credance to the hypothesis of partial dehydration on ion-pair formation.

The yellow colour of $LiAu(CN)_2$ solutions give rise to a small band with a low extinction coefficient at 370 nm. This band is thought to be due to charge transfer between the ligand and the solvated Lewis acid. For a transition to give rise to a visible colour an energy separation of 14000-28000cm^{-1} must exist between the HOMO and the LUMO orbitals. In general metal to ligand charge transfer bands are weaker than the ligand to metal type of transfer with intensities rarely exceeding 10 $\ell mol/cm^2$. Ion-pair formation in transition metals will have little effect on the d-d splittings because of the large energy separation of M^+ and X^-, small effects are due to forbidden d-d transitions which are a function of the polarization of the cation by the anion.

This system was studied by preparing aqueous solutions of $LiAu(CN)_2$ of varying concentrations in deionized water. The adsorbance of the resulting spectrum

at 370 nm was measured using a Beckman DU 7 single beam spectrophotometer. The adsorbance was found to be independent of changes in intensity with respect to time which effectively rules out any polymerization. A typical spectrum is shown in Fig. (A11) . The extinction coefficient for the low energy OSCT band was determined from the slope of the Beers law relationship at the more concentrated region where the association was assumed to be essentially complete.[72] Once the extinction coefficient for the ion-pair was known then it became possible to determine the degree of association in the more dilute solutions.

The ion-pair formation constant K_{oss} is defined as -

$$K_{oss} = \frac{[\text{ion-pair}]}{[[\text{Cation}] - [\text{ion-pair}]]\,[[\text{anion}] - [\text{ion-pair}]]}$$

The calculation of K_{oss} is summarized in Table (A2) and gives rise to an average association constant of -

$$K_{oss} = 375 \pm 56 \quad M^{-1}$$

Table A2

Adsorbance at 370 nm versus concentration of $LiAu(CN)_2$ salts

$\overset{+}{Li} = Au(CN)_2^-$	Absorbance	Ion-pair	%IP	K_{oss}
M X 10^{-3}	at 370 nm	X 10^{-3}		M^{-1}
3,91	0,0245	2,147	54,91	-
7,81	0,0471	4,129	52,75	304,72
9,77	0,0567	4,967	50,83	423,51
11,72	0,0721	6,319	53,91	401,77
15,63	0,0974	8,536	54,61	310,58
19,54	0,1405	12,314	63,01	374,22
22,00	0,1701	14,908	67,76	436,42

Mean $K_{oss} = 375 \pm 56\ M^{-1}$

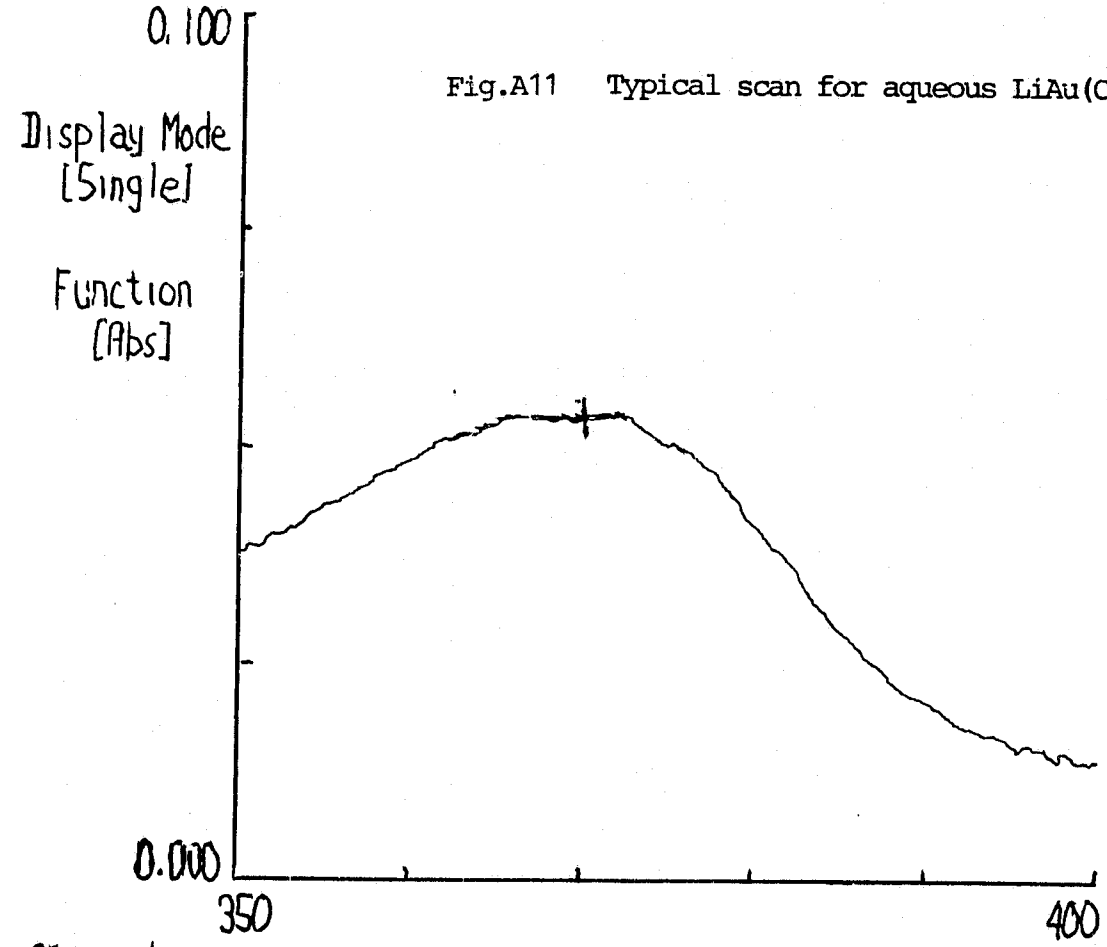

Fig.A11 Typical scan for aqueous $LiAu(CN)_2$

Appendix 2

Effect of Ionic Strength on Aurocyanide Adsorption

Additive	$[Au]_i$	I	$[Au]_e$
	mg/ℓ	M	mg/ℓ
NaCℓ	298,4	0,500	41,31
		0,250	41,00
		0,125	42,37
		0,063	43,50
	315,7	0,400	43,05
		0,200	42,97
		0,100	44,87
		0,050	46,13
	325,5	0,300	45,32
		0,150	45,73
		0,075	47,15
		0,038	48,61
NaOH	278,7	0,500	56,73
		0,250	54,93
		0,125	52,74
		0,063	48,66
	321,4	0,400	64,79
		0,200	63,55
		0,100	58,14
		0,050	55,82
	301,4	0,300	60,01
		0,150	56,25
		0,075	53,45
		0,038	51,33

Additive	$[Au]_i$	I	$[Au]_i$
	mg/ℓ	M	mg/ℓ
NaCℓ	307,8	0,500	82,65
		0,250	79,99
		0,125	73,34
		0,063	61,87
	298,4	0,400	78,05
		0,200	79,11
		0,100	66,41
		0,050	55,79
	284,7	0,300	76,61
		0,150	70,83
		0,075	58,07
		0,0375	50,45

Effect of Cations and Anions on
Aurocyanide Adsorption by Carbon

t=96hr	$\frac{[Au]_i}{ppm}$	$[Au]_e$/ppm			
Additive I=0,30 M		$C\ell^-$	OH^-	CN^-	SH^-
Na^+	274,3	37,50	55,00	73,23	210,0
K^+	293,0	36,81	53,70	61,99	-
Li^+	325,7	38,32	53,05	56,70	-
Cs^+	277,4	32,95	-	-	-
H^+	283,4	27,44	-	-	-
No Additive (as K^+ salt)	303,8	46,3			

Effect of Additives on Equilibrium

System	T	$[Au]_i$	$[Au]_e$
	C°	mg/ℓ	mg/ℓ
(KCℓ/KOH)			
	91,5	99	44,26
	84,3		30,66
	79,5		27,51
	89,0	100	37,98
	87,9		36,03
	77,4		25,33
	74,0	110	24,08
(NaCℓ/KOH)			
	73,9	100	23,82
	80,0		28,91
	78,7		26,90
	88,5		40,19
	84,0	101	31,95
	92,3		42,96
	72,3		22,00
	76,5	110	25,58

Effect of Additives on Equilibrium

System	T	$[Au]_i$	$[Au]_e$
	C°	mg/ℓ	mg/ℓ
(NaCℓ/NaOH)			
	90,0	101	49,14
	88,0		44,32
	82,5		34,04
	79,0		30,95
	73,1	100	26,03
	92,0		53,50
	87,9		42,87
	86,5	99	41,15
	75,0		27,43
	68,1		20,47
	90,0		45,79
	76,6		25,84
(No Additives/NaOH)			
	91,2	102	49,97
	85,4		40,01
	81,3		34,5

Effect of Additives on Equilibrium

System	T	$[Au]_i$	$[Au]_e$
	C°	mg/ℓ	mg/ℓ
(NaCℓ/NaOH)			
	90,0	101	49,14
	88,0		44,32
	82,ɔ		34,04
	79,0		30,95
	73,1	100	26,03
	92,0		53,50
	87,9		42,87
	86,5	99	41,15
	75,0		27,43
	68,1		20,47
	90,0		45,79
	76,6		25,84
(No Additives/NaOH)			
	91,2	102	49,97
	85,4		40,01
	81,3		34,5

Surface coverage at constant ionic strenth (I=0,30 M)

Additive

	NaCℓ		KCℓ		LiCℓ	
No.	Carbon Loading mgAu/g	Gold in Solution ppm	Carbon Loading mgAu/g	Gold in Solution ppm	Carbon Loading mgAu/g	Gold in Solution ppm
1	2,949	0,513	0,976	—		
2	4,944	0,556	4,976	0,691	4,943	0,573
3	9,935	0,642	9,976	0,691	9,939	0,616
4	19,916	0,836	19,761	0,697	19,930	0,701
5	29,868	1,332	29,889	1,112	39,825	1,464
6	39,734	2,668	39,817	1,826	59,517	4,834
7	49,501	4,975	49,694	3,056	78,626	13,745
8	59,039	9,588	59,441	5,595	106,68	34,610
9	76,798	31,970	77,877	21,227		
10	92,324	76,792	94,207	57,934		
11						
12						

Surface coverage at constant ionic strenth (I=0,30 M)

Additive	CsCl		$CaCl_2$	
No.	Carbon Loading mgAu/g	Gold in Solution ppm	Carbon Loading mgAu/g	Gold in Solution ppm
1	0,895	1,050	0,874	1,257
2	4,895	1,050	4,874	1,136
3	9,989	1,090	9,870	1,299
4	19,882	1,180	19,862	1,383
5	39,825	1,740	39,824	1,758
6	59,442	5,575	59,582	4,177
7	77,808	20,920	78,836	11,643
8	94,920	42,520	90,472	25,282
9				
10				
11				
12				

Surface coverage at constant ionic strenth (I=0,30 M)

Additive	NaOH		KOH		LiOH	
No.	Carbon Loading mgAu/g	Gold in Solution ppm	Carbon Loading mgAu/g	Gold in Solution ppm	Carbon Loading mgAu/g	Gold in Solution ppm
1	0,998	0,232	0,923	0,077	0,198	0,980
2	2,997	0,335	4,988	0,300	0,390	4,961
3	4,996	0,437	9,347	0,653	0,774	9,923
4	9,990	0,999	19,770	2,299	0,966	13,903
5	19,970	2,969	29,457	5,425	2,238	19,776
6	24,995	5,066	38,980	10,198	9,000	38,543
7	29,929	7,084	48,231	17,687	13,510	48,699
8	34,990	10,129	56,344	36,562	30,013	61,999
9	39,867	13,274	67,909	120,906	80,171	7?,983
10	49,353	64,721				
11						
12						

Surface coverage at constant ionic strenth (I=0,30 M)

Additive	NaCN		KCN		LiCN	
No.	Carbon Loading mgAu/g	Gold in Solution ppm	Carbon Loading mgAu/g	Gold in Solution ppm	Carbon Loading mgAu/g	Gold in Solution ppm
1	0,547	4,622	3,810	0,619	0,708	2,920
2	4,055	5,766	4,048	4,595	2,649	3,515
3	8,191	6,842	4,603	9,540	4,651	3,489
4	14,154	9,488	6,865	19,314	19,602	3,981
5	20,086	13,464	10,753	28,925	39,396	6,050
6	27,113	20,086	17,696	38,230	58,252	17,482
7	38,475	44,791	42,857	45,714	69,578	104,220
8	49,403	99,484	51,982	54,862	77,820	221,720
9	54,598	245,420	100,783	69,922		
10			142,045	85,796		
11						
12						

Desorption of aurocyanide loaded carbons using sodium hydroxide followed by aqueous ammonia at 90°C in columns

Adsorption medium	Initial loading	%gold desorbed with hydroxide	%gold desorbed with ammonia	Mass balance*
	mg Au/g			mg Au/g
NaCℓ	9,98	94,69	3,71	9,73
	19,91	97,29	5,17	20,53
	29,35	91,99	5,38	29,11
	47,35	81,88	4,52	47,28
	64,38	66,71	5,41	64,92
CaCℓ	9,99	92,31	3,60	9,75
	19,95	95,72	2,56	19,78
	29,95	90,37	1,90	29,84
	49,12	82,30	1,81	48,81
	57,95	73,61	2,12	58,98
HCℓ	10,00	74,49	3,70	10,06
	30,00	42,10	3,43	28,39
	49,99	33,09	3,16	48,23
	69,98	35,01	4,49	66,93

*= sum of fractions of eluand plus ashed carbon

Adsorption of $[Ca][Au(CN)_2]_2$ by activated carbon in de-ionized water

$[Au]_e$	[carbon loading]	$[Ca^{2+}]_e$	[carbon loading]
mg /ℓ	mmol /ℓ	mg /ℓ	mmol /ℓ
0,0	$5,03 \times 10^{-3}$	-	-
0,0	$2,51 \times 10^{-2}$	3,52	$4,30 \times 10^{-3}$
0,0	$5,03 \times 10^{-2}$	6,01	$1,12 \times 10^{-2}$
0,0	$1,00 \times 10^{-1}$	12,03	$2,23 \times 10^{-2}$
0,50	$1,51 \times 10^{-1}$	18,88	$3,14 \times 10^{-2}$
1,81	$2,00 \times 10^{-1}$	22,02	$4,92 \times 10^{-2}$
4,34	$2,49 \times 10^{-1}$	25,56	$6,70 \times 10^{-2}$
15,05	$2,94 \times 10^{-1}$	25,56	$9,32 \times 10^{-2}$
53,29	$3,76 \times 10^{-1}$	30,18	$1,33 \times 10^{-1}$
124,24	$4,40 \times 10^{-1}$	23,51	$2,02 \times 10^{-1}$

Arrhenius plot

System	lnk	1/T, $K^{-1} \times 10^{-3}$	
(No additives/NaOH)			R = 0,9391
	-2,849	2,825	α = 1,5739
	-2,946	2,860	b = -1573,64
	-2,762	2,747	E_a = 13,08 $kJmol^{-1}$
	-2,807	2,790	= 4,82 s^{-1}
(NaCl)/NaOH)			
	-2,752	2,755	R = 0,9094
	-2,793	2,770	α = 2,4373
	-2,833	2,813	b = -1883,03
	* -2,816	2,739	E_a = 15,65 $kJmol^{-1}$
	-3,019	2,890	A = 11,44 s^{-1}
	-2,795	2,805	
	-2,808	2,771	
	-2,929	2,841	
	* -2,900	2,874	
	* -2,807	2,755	
(NaCl/KOH)			
	-3,080	2,861	R = 0,9370
	-3,081	2,882	α = 3,2145
	-2,985	2,833	b = -2189,22
	-2,967	2,843	E_a = 18,13 $kJmol^{-1}$
	-2,853	2,766	A = 24,89 s^{-1}
	* -2,867	2,801	
	* -2,852	2,739	
	-3,142	2,896	

Arrhenius plot

System	ℓnk	1/T $K^{-1}X10^{-3}$	
(KCℓ)/(KOH)			
	-2,845	2,744	R = 0,9488
	-2,937	2,801	∝ = 2,1541
	-2,964	2,837	b = -1828,37
	* -2.831	2,762	E_a= 15,21 $kJmol^{-1}$
	-2,884	2,770	A = 8,88 s^{-1}
	-3,068	2,857	
	-3,096	2,882	
(NaCℓ)/(LiOH)			
	-3,226	2,841	R = 0,9816
	-3,042	2,785	∝= 4,1753
	-3,135	2,813	b = -2594,42
	* -3,070	2,740	E_a= 21,57 $kJmol^{-1}$
	-2,962	2,755	A = 65,06 s^{-1}
	-3,225	2,857	
	-3,325	2,896	
(LiCℓ)/(LiOH)			
	-3,054	2,747	R = 0,9730
	-3,290	2,847	∝= 3,0962
	-3,138	2,798	b=-2234,90
	-3,190	2,821	E_a= 18,18 $kJmol^{-1}$
	-3,013	2,732	A = 22,11 s^{-1}
	-3,032	2,773	

Effect of Additives on Equilibrium

System	T	$[Au]_i$	$[Au]_e$
	C°	mg/ℓ	mg/ℓ
(LiCℓ/LiOH)			
	91,0	100	35,84
	78,2		20,18
	81,5		22,57
	93,0		41,70
	87,6	101	28,13
(NaCℓ/LiOH)			
	86,1	102	30,54
	92,0		42,05
	90,1		36,30
	82,5*	110	28,24
	77,0		22,94
	72,3		21,16
(CsOH/CsOH)			
	90,2	99,8	37,3
	86,6		35,0
	81,3		26,6
	84,7		29,3
	77,8		2[illegible],9

Effect of temperature on rate of auricyanide desorption

Temperature = 91,0°C
$[Carbon]_i$ = 10 mg/g
I_L = 0,30M LiCℓ
I_E = 0,30M LiOH

Data pt.	Time min	[Au] mg/g	ℓnQ
1.	0	0,00	3,5835
2.	6	9,135	3,2908
3.	10	13,68	3,1056
4.	26	22,00	2,6391
5.	30	27,30	2,1632
6.	40	29,31	1,9003
7.	60	33,87	0,7547
8.	120	27,35	–

R = 1,0000
ℓnα = 3,5792
α = 35,84
slope = 0,0279
ℓn(slope) = -3,0538
$[Au]_e$ = 36,00

Temperature = 78,2°C
$[Carbon]_i$ = 10 mg/g
I_L = 0,30M LiCℓ
I_E = 0,30M LiOH

Data pt.	Time min	[Au] mg/g	ℓnQ
1.	0	0,00	3,0204
2.	5	3,60	3,6054
3.	10	7,00	2,6027
4.*	20	13,33	1,9687
5.	40	15,92	1,5215
6.	60	18,53	0,6760
7.	128	18,01	–
8.			

R = 0,9991
ℓnα = 3,0051
α = 20,18
slope = 0,0373
ℓn(slope) = -3,2901
$[Au]_e$ = 20,50

Effect of temperature on rate of aurocyanide desorption

Temperature = 84,4°C

$[Carbon]_t$ = 10 mg/g

I_L = 0,30 M LiCℓ

I_E = 0,30 M LiOH

Data pt.	Time min	[Au] mg/g	ℓnQ
1.	0	0,00	3,2189
2.	5	5,35	2,9778
3.	10	8,64	2,7951
4.	23	15,85	2,2135
5.	40	20,22	1,5640
6.	60	23,43	0,4479
7.	110	22,35	–
8.			

R = 0,9989

ℓnα = 3,2131

α = 24,86

slope = 0,0433

ℓn(slope) = −3,1385

$[Au]_e$ = 25,00

Temperature = 81,5°C

$[Carbon]_t$ = 10 mg/g

I_L = 0,30 M LiCℓ

I_E = 0,30 M LiOH

Data pt.	Time min	[Au] mg/g	ℓnQ
1.	0	0,00	3,1135
2.	5	4,24	2,9045
3.	22	12,99	2,2520
4.	40	18,36	1,4209
5.	60	20,55	0,6642
6.	110	21,87	–
7.			
8.			

R = 0,9989

ℓnα = 3,1171

α = 22,58

slope = 0,0412

ℓn(slope) = −3,1897

$[Au]_e$ = 22,50

Effect of temperature on rate of aurocyanide desorption

Temperature = 93,0°C
[Carbon]$_C$=10mg/g
I_L=0,30M LiCℓ
I_E=0,30M LiOH

Data pt.	Time min	[Au] mg/g	ℓnQ
1.	0	0,00	3,7377
2.	5	9,00	3,4965
3.	19	17,01	3,2184
4.	20	26,50	2,7406
5.	30	32,36	2,2669
6.	40	35,55	1,8635
7.	69	37,77	1,4404
8.	120	41,57	–

R= 0.9994
ℓnα= 3,7307
α= 41,71
slope = 0,0491
ℓn(slope) = -3,0133
$[Au]_e$ = 42,00

Temperature = 87,6°C
[Carbon]$_C$=10mg/g
I_L=0,30M LiCℓ
I_E=0,30M LiOH

Data pt.	Time min	[Au] mg/g	ℓnQ
1.	0	0,00	3,3322
2.	5	6,07	3,0879
3.	–	–	–
4.	20	17,00	2,3978
5.	40	23,95	1,3975
6.	60	26,00	0,6931
7.	120	27,09	–
8.			

R= 0,9996
ℓnα= 3,3371
α= 28,14
slope = 0,0482
ℓn(slope) = -3,0323
$[Au]_e$ = 28,00

Effect of temperature on rate of auricyanide desorption

Temperature = 79,0°C
[Carbon]$_t$=10mg/g
I_L=0,30M NaCℓ
I_E=0,30M LiOH

Data pt.	Time min	[Au] mg/g	ℓnQ
1.	0	0,00	3,2189
2.	5	4,54	3,0186
3.	10	8,43	2,8062
4.	30	17,10	2,0667
5.	60	22,72	0,8220
6.	100	24,35	–
7.			
8.			

R= 0,9995
ℓnα= 3,2204
α= 25,04
slope = 0,0397
ℓn(slope)= -3,2261
$[Au]_e$ = 25,00

Temperature = 86,1°C
[Carbon]$_t$=10mg/g
I_L=0,30M NaCℓ
I_E=0,30M LiOH

Data pt.	Time min	[Au] mg/g	ℓnQ
1.	0	0,00	3,4012
2.	5	6,63	3,1511
3.	10	10,64	2,9633
4.	40	25,08	1,5925
5.	60	28,35	0,4996
6.	100	29,05	
7.			
8.			

R=0,9981
ℓnα= 3,4190
α= 30,54
slope = 0,0477
ℓn(slope)= -3.0422
$[Au]_e$= 39,00

Effect of temperature on rate of aurocyanide desorption

Temperature = 82,5°C
$[Carbon]_t$=10mg/g
I_L=0,30M NaCℓ
I_E=0,30M LiOH

Data pt.	Time min	[Au] mg/g	ℓnQ
1.	0	0,00	3,3322
2.*	5	5,53	3,1122
3.	10	9,73	2,9050
4.	40	22,73	1,6630
5.	60	26,00	0,6926
6.	120	23,09	–
7.	180	19,96	
8.			

R= 0,9989
ℓnα= 3,3407
α= 28,24
slope = 0,0435
ℓn(slope) = -3,1354
$[Au]_e$ = 28,24

Temperature = 92,0°C
$[Carbon]_t$=10mg/g
I_L=0,30M NaCℓ
I_E=0,30M LiOH

Data pt.	Time min	[Au] mg/g	ℓnQ
1.	0	0,00	3,7495
2.	5	9,00	3,5115
3.	10	16,10	3,2733
4.	40	36,10	1,8552
5.	60	39,85	0,9734
6.	120	37,20	–
7.			
8.			

R= 0,9998
ℓnα= 3,7389
α= 42,05
slope = 0,0464
ℓn(slope) = -3,0704
$[Au]_e$ = 42,50

Effect of temperature on rate of aurocyanide desorption

Temperature = 90,0°C
[Carbon]$_t$=10mg/g
I_L=0,30M NaCℓ
I_E=0,30M LiOH

Data pt.	Time min	[Au] mg/g	ℓnQ
1.	0	0.00	3,5835
2.	5	8,03	3,3311
3.	10	14,50	3,0679
4.	40	30,94	1,6218
5.	60	34,38	0,4824
6.	125	35,37	–
7.			
8.			

R=1,0000
ℓnα= 3,5860
α= 36,09
slope = 0,0517
ℓn(slope) = -2,9618
$[Au]_e$ = 36,00

Temperature = 77,0°C
[Carbon]$_t$=10mg/g
I_L=0,30M NaCℓ
I_E=0,30M LiOH

Data pt.	Time min	[Au] mg/g	ℓnQ
1.	0	0,00	3,1355
2.	5	4,23	2,9320
3.	10	7,60	2,7344
4.	25	14,50	2,1397
5.	40	18,20	1,5680
6.	60	21,30	0,5283
7.	120	20,03	–
8.			

R = 1,0000
ℓnα= 3,1329
α= 22,94
slope = 0,0398
ℓn(slope) = -3,2246
$[Au]_e$ = 23,00

Effect of temperature on rate of aurocyanide desorption

Temperature = 72,3°C

$[Carbon]_t$ = 10 mg/g

I_L = 0,30M NaCℓ

I_E = 0,30M LiOH

Data pt.	Time min	[Au] mg/g	ℓnQ
1.	0	0,00	3,0445
2.	5	3,44	2,8657
3.	10	6,00	2,7081
4.	25	12,35	2,1571
5.	40	16,01	1,6068
6.	60	18,44	0,9400
7.	120	20,35	–
8.			

R = 0.9997

ℓnα = 3,0521

α = 21,16

slope = 0,0360

ℓn(slope) = -3,3246

$[Au]_e$ = 21,00

Effect of temperature on rate of aurocyanide desorption

Temperature = 89,°C
[Carbon]$_t$=10mg/g
I_L=0,30M KCℓ
I_E=0,30M KOH

Data pt.	Time min	[Au] mg/g	ℓnQ
1.	0	0,00	3,6376
2.	5	10,01	3,3318
3.	11	17,84	3,0039
4.	20	26,40	2,4507
5.	40	35,35	0,9742
6.	60	40,31	–
7.	120	36,96	–
8.			

R= 0,9995
ℓnα= 3,6371
α= 37,98
slope = 0,0590
ℓn(slope) = -2,8310
$[Au]_e$ = 38,00

Temperature = 88,1°C
[Carbon]$_t$=10mg/g
I_L=0,30M KCℓ
I_E=0,30M KOH

Data pt.	Time min	[Au] mg/g	ℓnQ
1.	0	0,00	3,5835
2.	5	9,05	3,2938
3.	10	15,53	3,0187
4.	20	23,77	2,5035
5.	40	32,18	1,3400
6.	60	35,03	-0,0336
7.	120	36,535	–
8.			

R= 0,9992
ℓnα= 3,5707
α= 35,54
slope = 0,0538
ℓn(slope) = -2,9224
$[Au]_e$ = 38,00

Effect of temperature on rate of auro-cyanide desorption

Temperature = 89,°C
[Carbon]$_t$=10mg/g
I_L=0,30M KCℓ
I_E=0,30M KOH

Data pt.	Time min	[Au] mg/g	ℓnQ
1.	0	0,00	3,6376
2.	5	10,01	3,3318
3.	11	17,84	3,0039
4.	20	26,40	2,4507
5.	40	35,35	0,9742
6.	60	40,31	–
7.	120	36,96	–
8.			

R= 0,9995
ℓnα= 3,6371
α= 37,98
slope = 0,0590
ℓn(slope) = -2,8310
$[Au]_e$ = 38,00

Temperature = 88,1°C
[Carbon]$_t$=10mg/g
I_L=0,30M KCℓ
I_E=0,30M KOH

Data pt.	Time min	[Au] mg/g	ℓnQ
1.	0	0,00	3,5835
2.	5	9,05	3,2938
3.	10	15,53	3,0187
4.	20	23,77	2,5035
5.	40	32,18	1,3400
6.	60	35,03	-0,0336
7.	120	36,535	–
8.			

R= 0,9992
ℓnα= 3,5707
α= 35,54
slope = 0,0538
ℓn(slope) = -2,9224
$[Au]_e$ = 38,00

Effect of temperature on rate of auro-cyanide desorption

Temperature = 77,0°C
[Carbon]$_t$=10 mg/g
I_L=0,30M KCℓ
I_E=0,30M KOH

Data pt.	Time min	[Au] mg/g	ℓnQ
1.	0	0,00	3,2387
2.	5	5,50	2,9956
3.	10	10,03	2,7388
4.	20	15,03	2,3484
5.	30	19,35	1,8161
6.	40	21,77	1,3156
7.	60	24,01	0,3961
8.	110	23,36	-

R= 0,9973
ℓnα= 3,2320
α= 25,33
slope = 0,0465
ℓn(slope) = -3,0682
$[Au]_e$ = 27,50

Temperature = 74,0°C
[Carbon]$_t$=10 mg/g
I_L=0,30M KCℓ
I_E=0,30M KOH

Data pt.	Time min	[Au] mg/g	ℓnQ
1.	0	0,00	3,1781
2.	5	4,93	2,9481
3.	10	8,53	2,7386
4.	20	15,03	2,3484
5.	30	19,35	1,8161
6.	40	21,77	1,3156
7.	60	24,01	0,3961
8.	110	23,36	-

R= 0,9997
ℓnα= 3,1814
α= 24,08
slope = 0,0452
ℓn(slope) = -3,0959
$[Au]_e$ = 24,00

Effect of temperature on rate of aurocyanide desorption

Temperature = 91,5°C
[Carbon]$_t$=10mg/g
I_L=0,30M KCℓ
I_E=0,30M KOH

Data pt.	Time min	[Au] mg/g	ℓnQ
1.	0	0,00	3,7910
2.	5	11,13	3,5015
3.	10	20,35	3,1633
4.	20	29,83	2,6717
5.	40	40,03	1,4514
6.	60	42,63	–
7.	130	38,35	–
8.			

R= 0,9999
ℓnα= 3,7900
α= 44,25
slope = 0,0581
ℓn(slope) = −2,8453
$[Au]_e$ = 44,30

Temperature = 84,3°C
[Carbon]$_t$=10mg/g
I_L=0,30M KCℓ
I_E=0,30M KOH

Data pt.	Time min	[Au] mg/g	ℓnQ
1.	0	0,00	3,4340
2.	5	7,60	3,1527
3.	10	13,10	2,8844
4.	20*	22,53	2,13464
5.	40	27,31	1,3054
6.	60	30,03	−0,0315
7.	110	35,55	–
8.			

R= 0,9999
ℓnα= 3,4230
α= 30,66
slope = 0,0530
ℓn(slope) = −2,9370
$[Au]_e$ = 31,00

Effect of temperature on rate of aurocyanide desorption

Temperature = 79,5°C

$[Carbon]_t$ = 10 mg/g

I_L = 0,30M KCℓ

I_E = 0,30M KOH

Data pt.	Time min	[Au] mg/g	ℓnQ
1.	0	0,00	3,3142
2.	5	6,17	3,0603
3.	10	11,31	2,7841
4.	22	18,51	2,1964
5.	40	24,03	1,2439
6.	60	26,08	0,3514
7.	110	27,03	–
8.			

R = 0,9998

ℓnα = 3,3145

α = 27,51

slope = 0,0516

ℓn(slope) = -2,9641

$[Au]_e$ = 27,50

Effect of temperature on rate of cyanide desorption

Temperature = 76,5°C
[Carbon]$_t$=10mg/g
I_L=0,30M NaCℓ
I_E=0,30M KOH

Data pt.	Time min	[Au] mg/g	ℓnQ
1.	0	0,00	3,2387
2.	5	6,51	2,9440
3.	10	8,63	2,8255
4.	25	16,68	2,1769
5.	40	21,64	1,3501
6.	100	24,50	–
7.	180	22,31	–
8.			

R= 0,9928
ℓnα= 3,2418
α= 25,58
slope = 0,0459
ℓn(slope)= -3,0803
$[Au]_e$ = 25,50

Temperature = 74,0°C
[Carbon]$_t$=10mg/g
I_L=0,30M KCℓ
I_E=0,30M KOH

Data pt.	Time min	[Au] mg/g	ℓnQ
1.	0	0,00	3,1781
2.	5	5,10	2,9390
3.	10	10,36	2,6132
4.	25	16,55	2,0083
5.	40	20,17	1,3423
6.	100	23,75	–
7.	180	20,21	–
8.			

R= 0,9998
ℓnα= 3,1705
α= 23,82
slope = 0,0459
ℓn(slope)= -3,0804
$[Au]_e$ = 24,00

Effect of temperature on rate of cyanide desorption

Temperature = 76,5°C
[Carbon]$_t$=10mg/g
I_L=0,30M NaCℓ
I_E=0,30M KOH

Data pt.	Time min	[Au] mg/g	ℓnQ
1.	0	0,00	3,2387
2.	5	6,51	2,9440
3.	10	8,63	2,8255
4.	25	16,68	2,1769
5.	40	21,64	1,3501
6.	100	24,50	-
7.	180	22,31	-
8.			

R= 0,9928
ℓnα= 3,2418
α= 25,58
slope = 0,0459
ℓn(slope)= -3,0803
$[Au]_e$ = 25,50

Temperature = 74,0°C
[Carbon]$_t$=10mg/g
I_L=0,30M KCℓ
I_E=0,30M KOH

Data pt.	Time min	[Au] mg/g	ℓnQ
1.	0	0,00	3,1781
2.	5	5,10	2,9390
3.	10	10,36	2,6132
4.	25	16,55	2,0083
5.	40	20,17	1,3423
6.	100	23,75	-
7.	180	20,21	-
8.			

R= 0,9998
ℓnα= 3,1705
α= 23,82
slope = 0,0459
ℓn(slope)= -3,0804
$[Au]_e$ = 24,00

Effect of temperature on rate of aurocyanide desorption

Temperature = 80,0°C
$[Carbon]_t$=10mg/g
I_L=0,30M NaCℓ
I_E=0,30M KOH

Data pt.	Time min	[Au] mg/g	ℓnQ
1.	0	0,00	3,3673
2.	5	6,52	3,1126
3.*	10	13,48	2,7422
4.	30	22,75	1,8321
5.	40	25,13	1,3545
6.	60	27,48	0,4167
7.	100	27,38	–
8.			

R = 0,999
ℓnα = 3,3642
α = 28,91
slope = 0,0505
ℓn(slope) = −2,9850
$[Au]_e$ = 29,00

Temperature = 78,7°C
$[Carbon]_t$=10mg/g
I_L=0,30M NaCℓ
I_E=0,30M KOH

Data pt.	Time min	[Au] mg/g	ℓnQ
1.	0	0,00	3,2958
2.	5	6,12	3,0386
3.	10	10,94	2,7765
4.	25	19,53	2,0112
5.	40	23,54	1,2119
6.	60	25,75	0,2207
7.	120	23,373	–
8.			

R = 0,9999
ℓnα = 3,2921
α = 26,90
slope = 0,0515
ℓn(slope) = −2,9670
$[Au]_e$ = 27,00

Effect of temperature on rate of aurocyanide desorption

Temperature = 88,5°C
[Carbon]$_t$=10mg/g
I_L=0,30M NaCℓ
I_E=0,30M KOH

Data pt.	Time min	[Au] mg/g	ℓnQ
1.	0	0,00	3,6889
2.	5	9,90	3,4045
3.	10	17,41	3,1175
4.	30	32,80	1,9737
5.	60	38,74	0,2271
6.	120	37,45	-
7.	180	33,48	-
8.			

R= 1,0000
ℓnα= 3,6936
α= 40,19
slope = 0,0577
ℓn(slope) = -2,8527
$[Au]_e$ = 40,00

Temperature = 84,0°C
[Carbon]$_t$=10mg/g
I_L=0,30M NaCℓ
I_E=0,30M KOH

Data pt.	Time min	[Au] mg/g	ℓnQ
1.	0	0,00	3,4812
2.	5	8,4	3,1611
3.	10	14,90	2,8389
4.	30	26,64	1,6790
5.	60	31,79	-1,5606
6.	120	32,41	-
7.			
8.			

R= 0,9993
ℓnα= 3,4642
α= 31,95
slope = 0,0569
ℓn(slope) = -2,8670
$[Au]_e$ = 32,50

Effect of temperature on rate of aurocyanide desorption

Temperature = 92°C
[Carbon]$_t$ = 10 mg/g
I_L = 0,30 M NaCℓ
I_E = 0,30 M KOH

Data pt.	Time min	[Au] mg/g	ℓnQ
1.	0	0,00	3,8918
2.	5	12,60	3,5945
3.	10	22,20	3,2882
4.	30	41,21	2,0522
5.	60	47,45	0,4415
6.	125	45,77	–
7.			
8.			

R = 0,9989
ℓnα = 3,8660
α = 47,75
slope = 0,0577
ℓn(slope) = -2,8519
$[Au]_e$ = 49,00

Temperature = 92,3°C
[Carbon]$_t$ = 10 mg/g
I_L = 0,30 M NaCℓ
I_E = 0,30 M KOH

Data pt.	Time min	[Au] mg/g	ℓnQ
1.	0	0,00	3,7612
2.	5	10,81	3,4719
3.	10	18,89	3,1828
4.	40	38,84	1,4255
5.	60	41,67	0,2874
6.	130	40,3	
7.			
8.			

R = 1,0000
ℓnα = 3,76
α = 42,96
slope = 0,0580
ℓn(slope) = -2,8469
$[Au]_e$ = 43,00

Effect of temperature on rate of aurocyanide desorption

Temperature = 72,3°C

$[Carbon]_o$ = 10 mg/g

I_L = 0,30M NaCℓ

I_E = 0,30M KOH

Data pt.	Time min	[Au] mg/g	ℓnQ
1.	0	0,00	3,0910
2.	5	4,35	2,8708
3.	10	7,83	2,6511
4.	30	15,84	1,8174
5.	62	20,50	0,4048
6.	110	20,49	–
7.	180	18,43	–
8.			

R = 0,9999

ℓnα = 3,0910

α = 22,00

slope = 0,0432

ℓn(slope) = -3,1422

$[Au]_e$ = 22,00

Effect of temperature on rate of auricyanide desorption

Temperature = 75,0°C
[Carbon]$_t$=10mg/g
I_L=0,30M NaCℓ
I_E=0,30M NaOH

Data pt.	Time min	[Au] mg/g	ℓnQ
1.	0	0,00	3,2958
2.	5	6,19	3,0352
3.	10	11,00	2,7723
4.	30	21,64	1,6790
5.	60	26,00	0,0000
6.	100	26,10	–
7.			
8.			

R= 0,9999
ℓnα= 3,3116
α= 27,43
slope = 0,0550
ℓn(slope) = -2,900
$[Au]_e$ = 27,00

Temperature = 90,0°C
[Carbon]$_t$=10mg/g
I_L=0,30M NaCℓ
I_E=0,30M NaOH

Data pt.	Time min	[Au] mg/g	ℓnQ
1.	0	0,00	3,8286
2.	5	12,21	3,5202
3.	10	21,06	3,2165
4.	30	38,50	2,0148
5.	60	43,35	0,9764
6.	120	46,01	–
7.			
8.			

R= 1,0000
ℓnα= 3,8241
α= 45,79
slope = 0,0604
ℓn(slope) = -2,8073
$[Au]_e$ = 46,00

Effect of temperature on rate of aurocyanide desorption

Temperature = 87,9°C

$[Carbon]_t$ = 10 mg/g

I_L = 0,30M NaCℓ

I_E = 0,30M NaOH

Data pt.	Time min	[Au] mg/g	ℓnQ
1.	0	0,00	3,7612
2.	6	13,15	3,3963
3.	10	19,60	3,1527
4.	30	36,01	1,9445
5.	60	41,85	0,1398
6.	120	42,00	
7.			
8.			

R = 1,0000

ℓnα = 3,7582

α = 42,87

slope = 0,0603

ℓn(slope) = −2,8078

$[Au]_e$ = 43.00

Temperature = 79,0°C

$[Carbon]_t$ = 10 mg/g

I_L = 0,30M NaCℓ

I_E = 0,30M NaOH

Data pt.	Time min	[Au] mg/g	ℓnQ
1.	0	0,00	3,4340
2.	5	7,30	3,1653
3.	10	12,83	2,8998
4.	30	24,80	1,8244
5.	60	29,74	0,2287
6.	130	28,51	–
7.			
8.			

R = 1,0000

ℓnα = 3,4324

α = 30,95

slope = 0,0535

ℓn(slope) = −2,9290

$[Au]_e$ = 31,00

Effect of temperature on rate of aurocyanide desorption

Temperature = 73,0°C
[Carbon]$_i$=10mg/g
I_L=0,30M NaCℓ
I_E=0,30M NaOH

Data pt.	Time min	[Au] mg/g	ℓnQ
1.	0	0,00	3,2581
2.	5	5,63	3,0141
3.	10	9,95	2,7755
4.	25	18,33	2,0373
5.	40	22,31	1,3062
6.	90	26,01	—
7.			
8.			

R= 1,0000
ℓnα= 3,2592
α= 26,03
slope = 0,0488
ℓn(slope) = -3,0193
$[Au]_e$ = 26,00

Temperature = 83,5°C
[Carbon]$_i$=10mg/g
I_L=0,30M NaCℓ
I_E=0,30M NaOH

Data pt.	Time min	[Au] mg/g	ℓnQ
1.	0	0,00	3,5835
2.	5	10,50	3,2385
3.	10	15,16	3,0367
4.	30	31,99	1,3893
5.	60	35,00	0,0000
6.	120	36,00	–
7.			
8.			

R= 0,9858
ℓnα= 3,5334ℓ
α= 34,24
slope = 0,0611
ℓn(slope) =-2,7945
$[Au]_e$ = 36,00

Effect of temperature on rate of auro-cyanide desorption

Temperature = 82,5°C
$[Carbon]_t$ = 10 mg/g
I_L = 0,30 M NaCℓ
I_E = 0,30 M NaOH

Data pt.	Time min	[Au] mg/g	ℓnQ
1.	0	0,00	3,5264
2.	5	8,52	3,2281
3.	10	14,93	2,9480
4.	25	26,20	2,0540
5.	40	31,40	0,9551
6.	100	30,50	
7.			
8.			

R = 0,9999
ℓnα = 3,5275
α = 34,04
slope = 0,0588
ℓn(slope) = −2,8329
$[Au]_e$ = 34,00

Temperature = 92,0°C
$[Carbon]_t$ = 10 mg/g
I_L = 0,30 M NaCℓ
I_E = 0,30 M NaOH

Data pt.	Time min	[Au] mg/g	ℓnQ
1.	0	0,00	3,9797
2.	5	14,28	3,6692
3.	10	25,07	3,3474
4.	30	45,65	2,0604
5.	60	52,00	0,4055
6.	100	49,70	
7.			
8.			

R = 0,9986
ℓnα = 3,9485
α = 51,86
slope = −0,0598
ℓn(slope) = −2,8166
$[Au]_e$ = 53,50

Effect of temperature on rate of auricyanide desorption

Temperature = 90,0°C
[Carbon]$_t$ = 10 mg/g
I_L = 0,30 M NaCℓ
I_E = 0,30 M NaOH

Data pt.	Time min	[Au] mg/g	ℓnQ
1.	0	0,00	3,8712
2.	5	13,02	3,5549
3.	10	22,51	3,2383
4.	30	40,81	1,9727
5.	60	46,92	0,0770
6.	120	47,938	-2,7806
7.			
8.			

R = 0,9997
ℓnα = 3,8949
α = 49,15
slope = -0,0638
ℓn(slope) = -2,7524
$[Au]_e$ = 48,00

Temperature = 88,0°C
[Carbon]$_t$ = 10 mg/g
I_L = 0,30 M NaCℓ
I_E = 0,30 M NaOH

Data pt.	Time min	[Au] mg/g	ℓnQ
1.	0	0,00	3,7495
2.	5	10,21	3,4748
3.	10	18,50	3,1780
4.	32	35,51	1,9445
5.	61	41,50	0,0000
6.	130	40,10	
7.			
8.			

R = 0,9981
ℓnα = 3,7916
α = 44,33
slope = -0,0612
ℓn(slope) = -2,7934
$[Au]_e$ = 42,50

Effect of temperature on rate of cyanide desorption

Temperature = 85,4°C

$[Carbon]_t$ = 10 mg/g

I_L = 0,30 M No Additeves

I_E = 0,30 M NaOH

Data pt.	Time min	[Au] mg/g	ℓnQ
1.	0	0,00	3,689
2.*	5	10,41	3,3878
3.	10	17,00	3,1361
4.	30	32,97	1,9523
5.	60	38,93	-0,0770
6.	130	40,01	
7.			
8.			

R = 0,9995

$\ell n\alpha$ = 1,3146

α = 3,7231

slope = 0,0.604

ℓn(slope) = -2,8070

$[Au]_e$ = 40,01

Temperature = 81,0°C

$[Carbon]_t$ = 10 mg/g

I_L = 0,30 M No Additives

I_E = 0,30 M NaOH

Data pt.	Time min	[Au] mg/g	ℓnQ
1.	0	0,00	3,5410
2.	5	9,01	3,2382
3.	10	14,94	2,9746
4.	20	23,72	2,3777
5.	60	33,40	0,0953
6.	130	35,40	
7.			
8.			

R = 0,9996

$\ell n\alpha$ = 1,2639

α = 3,5391

slope = 0,0579

ℓn(slope) = -2,8494

$[Au]_e$ = 34,50

Effect of temperature on rate of cyanocyanide desorption

Temperature=76,6°C

$[Carbon]_t$=10mg/g

I_L=0,30M No Additives

I_E=0,30M NaOH

Data pt.	Time min	[Au] mg/g	lnQ
1.	0	0,00	3,2519
2.	5	6,00	2,9877
3.	10,43	10,43	2,7350
4.	25	18,90	1,9373
5.	40	22,81	1,1086
6.	110		
7.			
8.			

R=0,999

$\ln\alpha$=1,798

α=3,254

slope =0,526

ln(slope) =-2,9457

$[Au]_e$ = 25,84

Temperature = 91,0°C

$[Carbon]_t$=10mg/g

I_L=0,30M No Additives

I_E=0,30M NaOH

Data pt.	Time min	[Au] mg/g	lnQ
1.	0	0,00	3,9110
2.	5	13,93	3,5853
3.	10	23,42	3,2791
4.	20	36,03	2,6354
5.	40	46,33	1,2932
6.	120	49,78	-
7.			
8.			

R= 0,9997

$\ln\alpha$= 3,9077

α=3,9077

slope =0,632

ln(slope) =-2,7615

$[Au]_e$ = 49,97

Effect of Temperature on Pyrolysis of Coconut Char

Atmosphere: N_2/Steam	
Equilibrum Temperature C°	Mass loss %
200	5
400	6
600	10
700	15
750	20
800	23
850	30
900	45
1000	68
1100	68

Atmosphere: N_2	
Equilibrum Temperature C°	Mass loss %
200	4
400	6
600	8
700	-
800	11
900	14
1000	17

Effect of Temperature of Activation on
Aurocyanide Adsorption

System	$[T_a]$ / C°	$[Au]_i$ / mg/ℓ	$[Au]_e$ / mg/ℓ	$[C]_e$ / mgAu/g	%
N_2	200	207	200	2,8	3,4
	400		197	4,0	4,8
	600		193	5,6	6,8
	700		191	6,4	7,7
	800		187	8,0	9,7
	900		179	11,2	13,5
	1000		168	15,6	18,8
N_2/steam	200	216	203	5,2	6,0
	400		197	7,6	8,8
	600		190	10,4	12,1
	650		179	14,8	17,1
	700		170	18,4	21,3
	750		159	22,8	26,4
	800		142	29,6	34,3
	850		127	35,6	41,2
	900	196	107	45,6	45,4
	950		98	39,2	50,0
	1000		91	42,0	53,6
	1100	207	104	41,2	49,8

Effect of Activation Temperature on
Equilibrum Aurocyanide Adsoption

Activation Temperature	$[Au]_i$	$[Au]_e$	[Carbon]
C°	mg/ℓ	mg/ℓ	mgAu/g
600	97,70	21,31	0,4393
		4,76	0,7149
		2,30	0,8950
		-	
		1,32	1,2436
		0,67	1,9680
750	98,40	25,27	0,2770
		5,64	0,4077
		2,08	0,5232
		1,46	0,5864
		1,23	0,6808
		0,78	0,7735
		0,52	1,2189
850	103,2	20,69	0,2133
		7,09	0,2747
		2,07	0,3340
		1,51	0,3744
		1,22	0,4128
		0,82	0,4835
		0,68	0,5536
		0,55	0,6071
950	102,6	12,31	0,1702
		4,95	0,2037
		1,73	0,2375
		1,02	0,2576
		0,61	0,3235
		0,45	0,4319
		0.36	0.5580

Appendix 3

References

1. Fleming, C.A. and Nicol, M.J. Alternative processes to filtration carbon-in-pulp and resin-in-pulp in the metallurgical industry. Hydrometallurgy 81, Proc. Soc. Chem. Ind. Symp., Manchester, 1981, V2, 1-17.

2. Zadra, J.B., Engel, A.K. and Heinen, H.J. A process for recovery of gold from activated carbon by leaching and electrolysis. USBM Reports of Investigations, 4843, 1952.

3. Mattson, J.S. and Mark, H.B., Activated Carbon, Marcel Dekker, New York 1971.

4. Garten, V.A. and Weiss, D.E., The Ion- and Electron-Exchange Properties of Activated Carbon in Relation to its Behaviour as a Catalyst and Adsorbent, Rev. Pure Appl. Chem., 7, 69-121 1957.

5. McDougall, G.J. and Hancock, R.D., Gold Complexes and Activated Carbon. A Literature Review, Gold Bull., 14, 138-153 1981

6. Finkelstein, N.P., The Chemistry of the Extraction of Gold. In: Adamson, R.J. (ed), Gold Metallurgy in South Africa, Chamber of Mines of South Africa, Johannesburg 1972 Chapter 10

7. Fleming, C.A., Some Aspects of the Chemistry of Carbon-in-pulp and Resin-in-pulp Processes, Murdoch University Seminar of the Chemistry of Activated Carbon and Gold, 12 June, 1982

8. Ruane, M. Comparison of the Zadra Anglo-American and organic proceeds for desorption of gold from Activated Carbon. ibid. 1982

9. Sigworth, E.A. and Smith, S.B. Adsorption of Inorganic Compounds by Activated Carbon, Water Research, June 386-391 1972

10. Gore, W.T., Charcoal Production and Properties, CSIR Special Report, Hout 262, August 1982

11. Hughes and Thomas, Nature 193, 4818, 839, 1962

12. Dubinin, V., On the Formation of Porous Structure in Carbon Activation. In: de Boer (ed.), Reactivity of Solids, Elsevier 1961

13. Wolff, W.F., A Model of Active Carbon, J.Phys.Chem 63:653 1959

14. Pinwick, H.T., Electronic Properties of Carbons and Graphites, Proc. 1st Conf. of Carbon, 1953, 3

15. Shafizadeh, F. and Sekiguchi, Y., Development of Aromaticity in Cellulosic Chars Carbon Vol. 24 No. 5, 511-516 1983

16. Warren, B.E., X-ray Study of the Graphitization of Carbon Black, Proc. 2nd Conf. on Carbon, 1955, 49

17. Henning, G.R., Proc. 5th Conf. Carbon, 1961 Vol. 1 pg. 143, Pergamon Press, Oxford, England 1962

18. Boehm, H.P., Chemical Identification of Surface Groups Advances in Catalysis, Vol.16 pg. 179-279 1966

19. Youssef, A.M., El-Shobaky, G.A. and El-Nabarawy, T.H. Adsorption Properties of Carbons in Relation to the Various Methods of Activation. Surface Technology 7, pg. 451-458, Elsevier Sequoia S.A. 1978

20. Weber, W.J. and van Vliet, B.M., Synthetic Adsorbents and Activated Carbons for Water Treatment: Overview and Experimental Comparisons, Research and Technology, 1981, 420-426;
Synthetic Adsorbents and Activated Carbons for Water Treatment: Statistical Analyses and Interpretations, ibid, 1981, 426-431

21. van Vliet, B.M.,Weber,W.J.(JR) and Hozumi,H. Modeling and Prediction of Specific Compound Adsorption by Activated Carbon and Synthetic Absorbents,Water Research,14,1719.1728 1980

22. Austin, J.M., Groenewald, T. and Spiro, M. Part 18, The Catalysis by Carbons of oxidation-reduction reactions J.C.S. Dalton, 6, pg. 854-859 1980

23. McDougall, G.J., The Mechanism of Adsorption of the Cyanide Complexes of Gold (I), Gold (III), Silver (I), Nickel (II) Copper (I) and Mercury (II) onto Activated Coconut-shell Carbon, National Institute for Metallurgy, S.A., Mineral and Process Chemistry Division, Technical Memorandum No. 14108, 1978

24. McDougall, G.J.,Hancock,R.D., Nicol M.J. Wellington, O.L. and Copperthwaite F.G. The Mechanism of the Adsorpton of Gold Cyanide on Activated Carbon, J.S.A.Inst. Min. Met., 80 334-356 1980

25. Bernardin , F.E., Cyanide detoxification using adsorption and catalytic oxidation on granular activated carbon, Journal WPCF Vol 45. No 2, 221-231 1973

26. Basolo F. and Pearson R.G. Mechanisms of Inorganic Reactions, A study of Metal Complexes in Solution, 2nd ed., Wiley 1967

27. Swift, H.E. and Douglas, B.E., The Racemization of Complex Ions on Activated Carbon. III. The Effect of Electrolytes on the Racemization of Tris(ethylenediamine) Cobalt (III) Chloride and Potassium Ethylenediaminetetraacetatocobaltate (III), J. Inorg. Nucl. Chem., 26, 601-607 1964

28. Millar - quoted in reference 3

29 Maartman,R.W. Rubnish,D.N.,Mellema,B.J. Baas,G.R., and Hoekstra, P.M. The Exclusion of Ions from the Region near the Surface of Activated Carbon, J. Coll. Interface SCI, 31:95 1969

30. Snoeyink, V.L. and Weber, W.T., Jr., Reaction of the Hydrated Proton with Active Carbon, Advances in Chemistry Series No. 79:112 (Washington D.C., American Chemical Society 1968)

31. Gross, J. and Scott, J.W., Precipitation of Gold and Silver from Cyanide Solution on Charcoal, U.S. Bureau of Mines, Washington D.C., Tech. Paper No. 378, 1927

32. McDougall, G.J. and Hancock, R.D., Activated Carbons and Gold - a Literature Survey, Minerals Sci. Engng., 12, 85-99 1980

33. Kuz'minykh, V.M., Tyurin, N.G., and Nikulova, A.A. J. of Appl. Chem. of the USSR, 42(9), 1886 (Sept., 1969)

34. Kuz'minykh, V.M., and Tyurin, N.G. Izv. Vyssh, Ucheb. Zaved., Tsvet Metall., 11, 65-70 1968

35. Davidson, R.J., The Mechanism of the Adsorption of Gold Cyanide on Activated Carbon, J. S. A. Inst. Min. Met., 75, 67-76 1974

36. Davidson, R.J. and Duncanson, D., The Elution of Gold from Activated Carbon Using Deionized Water, J. S. A. Inst. Min. Met., 77 254-261 1977

37. Davidson, R.J., Veronese, V., Further Studies on the Elution of Gold from Activated Carbon using water as the Eluant, J. S. A. Inst. Min. Met., 79, 437-445 1979

38. Cho, E. and Pitt, C.H., The Adsorption of Silver Cyanide on Activated Charcoal, Metall. Trans., 10B, 159-164

39. Cho,E.,Dixion,S.N.,Pitt,C.H. Kinetics and Thermodynamics of Silver Cyanide Adsorption on Activated Charcoal,Metall. Trans., 10B, 165-184 The Kinetics of Gold Cyanide Adsorption on Activated Charcoal,Metall,Trans. 10B, 185-189

40. Grobbelaar, E., M.Sc. Thesis, University of the Witwatersrand, Johannesburg 1983

41. Adams, M., M.Sc. Thesis, University of the Witwatersrand, Johannesburg 1983

42. Davidson, R.J. The Intensive Cyanidation of Gold-plant Gravity Concentrates. J. S. A. Inst. Min. Met., Jan. 1978

43. Muir, D.M., Recovery of Gold from Cyanide Solutions Using Activated Carbon: A Review, Murdoch University Seminar on the Chemistry of Activated Carbon and Gold, 12 June 1982

44. Groenewald, T., The Dissolution of Gold in Acidic Solutions of Thiourea, Hydrometallurgy, Vol. 3, pg. 277-290 1976

45. Marcus, Y., Introduction to Liquid State Chemistry, Wiley 1977

46. Gutman, V., The Donor-Acceptor Approach to Molecular Interactions, Plenum Press. 1978

47. Dr. Field - 2nd year tutorial.

48. Weast, R.C. (ed), CRC Handbook of Chemistry and Physics, 60th Edition, CRC 1979

49. Fleming, C.A., Personal communication.

50. Barrow, G.M., Physical Chemistry, 3rd Ed.
McGraw-Hill 1973

51. Nancollas, G.H., Ion Association in Aqueous
Solution, Quarterly Reviews No. 8
pg. 402-426 1957

52. Mayer, U., Solvent Effects on Ion-Pair
Equilibria, Coord. Chem. Rev., 21,
159-179 1976

53. Burstall,F.H.,Forrest,G.,Kember,S. and
Wells,R.A. Ion-Exchange Process for
Recovery of Gold from Cyanide Solution,
Ind. and Eng. Chem., 45., 1648-1658 1953

54. Aveston,J.,Everest,D.A. and Wells R.A.
Adsortion of Gold from Cyanide Solutions
by Anionic Resins, J. Chem. Soc.,45
1958, 231-239

55. Walkowiak, W. and Grieves, R.B., Foam
Fractionation of Cyanide Complex Anions
of Zn(II), Cd(II), Ag(II) and Au(III),
J. Inorg. Nucl, Chem., 38, 1351-1356

56. Chadwick, B.M. and Frankiss, S.G., Vibrational Spectra and Structures of Some Dicyanoaurate (I) Complexes, J. Mol. Struct., 31, 1-9 1976

57. Penneman, R.A. and Staritzky, E., Preparation and Properties of $LiAu(CN)_2$, $NaAu(CN)_2$, and the Double Compound $LiAu(CN)_2$, $KAu(CN)_2$, J. Inorg. Nucl. Chem., 7, 45-50 1958

58. Jones, C.H., Raman Spectra of the Linear Dicyanides, Spectrochim. Acta, 19, 1675-1681 1963

59. Penneman, R.A., Jones, L.H. Preparation and Some Properties of $HAu(CN)_2$, J. Am. Chem. Soc., 78, 62 1956

60. Mason, W.R., Electronic Structure and Spectra of Linear Dicyno Complexes, J. Am. Chem. Soc., 95, 3573-3581 1973

61. Mason, W.R., Metal to Ligand Charge-Transfer Spectra in Tetra-n-butylammonium Dicyanourate (I), J. Am. Chem. Soc., 98, 5182-5187 1976

62. Ford-Smith, M.H., Habeeb, J.J., and Rawsthorne, J.H. Kinetics and Thermodynamics of the oxidative-addition reactions of Iodine with Dicyanoaurate (I) Ion in Aqueous Solution. J. Chemical Soc., Dalton, pg. 2116-2120 1972

63. Jones, L.H., Assignment of MC Stretching and MCN Bending Frequencies in Metal Cyanide Complexes. Inorganic Chemistry Vol. 4, No. 10 1472-1473 1965

64. Pratt, J.M. and Thorp, R.G., CIS and Trans Effects in Cobalt (III) Complexes. Advances in Inorganic Chem. and Radio Chemistry No. 12, 385-389 1969

65. Cooney, R.P.J. and Hall, J.R., Raman study of complexing of Halide of Mercury (II) Cyanide in Aqueous Solution. J. Inorg. Nucl. Chem. Vol. 28, 1679-1682 1966

66. Friedel, R.A. and Hofer, L.J.E., Spectral Characterization of Activated Carbon, J. of Physical Chemistry, Vol. 74 No. 15 1970

67. Marsh, H., Surface Oxygen Complexes on Carbons from Atomic Oxygen: An Infrared (IRS), High-Energy Photoelectron Spectroscopic (XPS), and Thermal Stability Study, J. Coll. Int. Sci., 49, 368-382 1974

68. Mattson,J.S.,Lee,L.,Mack,H.B. and Weber, W.J. Surface Oxides of Activated Carbon: INter Internal Reflectance Spectroscopic Examination of Activated Sugar Carbons, J.Coll. Int Sci., 33, 284-293 1070

69. Painter, P.C. and Coleman, M.M., Fourier Transform Infrared Studies of Coal and Mineral Matter in Coal, Int. Lab., April 1980, 17-30

70. Henniker, C.J., Infrared Spectrometry of Industrial Polymers. Academic Press, pg. 160-164 1976

71. Jones,P.G., Clegs,W., Sheldrick,G.M., Potassium Dicyanoaurate (I)-2-2' Bipyridyl. Acta Cryst. B36, 160-162 1980

72. Curtis, J.C. and Meyer, T.J., Outer-sphere Charge-transfer in Mixed-metal Ion-pairs, Inor. Chem. 21, 1562-1571 1982

73. Vogel's Practical Organic Chemistry. 3rd Ed., Longman

74. Mantell, C.L., Industrial Carbon. Its Elemental, Adsorptive and Manufactured Forms, 2nd Ed., Van Nostrand 1946

75. Feldtman, W.R., The Precipitating Action of Carbon in contact with Auriferous Cyanide Solutions, Trans. Instn. Min. Metall., Vol. 24 pg. 329 (1914-1915)

76. Yagil, G. and Anbar, M., J. Am. Chem. Soc., 85, pg. 2376 1963

77. Jones, J.R., Trans. Faraday Soc., 64, pg. 440, 1968

78. Stewart, R., Q. Rep. Sulphur Chem., 3, pg. 99, 1968

79. Horváth, C. and Melander, W., Reversed-phase Chromatograph and the Hydrophobic Effect, International Laboratory, November/December, pg. 11-35 1978

80. Bernal and Fowler, J. Chem. Phys. Vol. 1, pg. 515, 1933

81. Williams. J. Phys. Chem. vol. 58, pg. 121 1954

82. Puri, B.R., Studies in Surface Chemistry of Carbon Black, Part I. High Temperature Evacuations, Carbon 1: 451 1964
Studies in Surface Chemistry of Carbon Black II Surface Acidity in Relation to Chemisorbed Oxygen, ibid 1:457 1964

83. Pecsok,R.L., Shields,L.D., Cairns,T., McWilliam,I.G., Modern Methods of Instrumental Analysis, 2nd Ed., Wiley 1976

84. Bond, G.C., Heterogeneous Catalysis Principles and Applications, Oxford University Press 1974

85. Painter P. G and Coleman M. Fourier transform infrared studies of coal and minerials in coal. International Laboratory,Vol 10, No 3 April 1980

86. Basolo F. and Pearson R.G. Mechanisms of Inorganic Reactions, A study of Metal Complexes in Solution, 2nd ed., Wiley 1967

87. Bartunik,H,D.,Polzl,W. Mossbauer,R.L. Resonance Spectroscopy of γ-Radiation on Au(I) and Au(III) Compounds Z. Physik 240, 1-16 (1970)

88. Ritcey,G.M. ,Solvent Extraction, Principles and Applications to Process Metallurgy, Part II Elsevier 1979

89. Zvyagintsev,O.E., The Distribution of Dicyanoauric (I) Acid in Aqueous Solutions and Certain Alcohols and Ketones, Russ. J . Inorg. Chem., 5, 59-63 (1960)
ibid, 5, 63-66 (1960)

89. Cotton, F.A. and Wilkinson,G, Advanced Inorganic Chemistry, Wiley,1972

90. Siedlewski, J. and Smigiel, W., Characteristics and determination methods of functional groups on the surface of activated charcoals Wiadomosci Chemiczne,Vol. 29, No 4, 241-253 1975

91. Melson, G.A. et al Coordination Chemistry of Macrocyclic Compounds, Plenum Press, 1979

92. Pedersen, C.J. Cyclic Polyethers and Their Complexes with Metal Salts J. Am. Chem. Soc. 86, 7017 : 1967